This is to certify that the

thesis entitled

THE RATE OF LIPID OXIDATION OF A PRODUCT MODEL SYSTEM PACKAGED IN ANTIOXIDANT IMPREGNATED LAMINATE FILM STRUCTURES

presented by

Youn Suk Lee

has been accepted towards fulfillment
of the requirements for

Master degree in **Packaging**

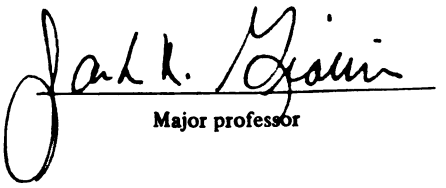

Major professor

Date **August 11, 1999**

THE RATE OF LIPID OXIDATION OF A PRODUCT MODEL SYSTEM PACKAGED IN ANTIOXIDANT IMPREGNATED LAMINATE FILM STRUCTURES

By

Youn Suk Lee

A THESIS

Submitted to
Michigan State University
in partial fulfillment of the requirements
for the degree of

MASTER OF SCIENCE

School of Packaging

1999

ABSTRACT

THE RATE OF LIPID OXIDATION OF A PRODUCT MODEL SYSTEM PACKAGED IN ANTIOXIDANT IMPREGNATED LAMINATE FILM STRUCTURES

By

Youn Suk Lee

A freeze-dried model food product system was developed as the source for the autoxidation of linoleic acid in storage stability studies. Moisture sorption isotherms for the model product were determined at 18, 28, 38°C. The sorption isotherms of the model product were fitted to the Halsey model. However, for the model product with low levels of linoleic acid, at 38°C, the Henderson model was found to give the best fit.

The effectiveness of an antioxidant impregnated film to retard autoxidation of a packaged model product containing linoleic acid, via the evaporation-sorption mechanism, was evaluated as a function of storage time and temperature. The rate of loss of BHT from the package film structure was found to be much higher than the rate of loss of α-tocopherol, at both storage conditions (23°C and 45°C, 50%RH).

The effectiveness of BHT and α-tocopherol impregnated laminated film pouches showed no significant different ($p<0.05$), due to the lack of lipid oxidation in the model food product, when stored at 23°C, as a function of the time. The BHT impregnated laminate pouch showed a notable effectiveness in retarding lipid oxidation of the model product at 45°C as a function of storage time. The control (non-antioxidants) and α-tocopherol impregnated laminate pouch structures showed no effect on retarding lipid oxidation of the model product during storage at 45°C.

ACKNOWLEDGMENTS

I would like to express my sincere thanks to my major professor, Dr. Jack Giacin, for his guidance and patience in preparing this thesis.

I would also like to express sincere appreciating to my committee member, Dr. Theron Downes and Dr. Gale Strasburg for serving on the guidance committee. I would like to acknowledge Dr. Jack Throck Watson and Dr. Douglas Gage for use of the GC/MS system at the Mass Spectrometer Laboratory in the Department of Biochemistry.

Special thanks should also be attribute to many friends at the School of Packaging for their support and assistance. This project was supported by the Center for Food and Pharmaceutical Packaging Research (CFPPR) at School of packaging.

Finally, I would like to express my deepest gratitude to my parents for their love, support and encouragement.

TABLE OF CONTENTS

LIST OF TABLES

LIST OF FIGURES

INTRODUCTION

Oxidation is a major limiting factor in the shelf life of lipid-containing food products. The first products of lipid oxidation are hydroperoxides, which are colorless, tasteless, and ordorless. Hydroperoxides, however, break down to low molecular weight compounds, which impart flavors and odors to food products, that are associated with rancidity. The secondary products of oxidation are free radicals, peroxides, epoxides, aldehydes, ketones, cyclic monomers, dimers, and polycyclic aromatic hydrocarbons; many of which are toxic (Bidlack, and Tappel, 1973).

Several factors can influence the rate of lipid oxidation. Jeon (1984) reported that factors such as light, relative humidity, temperature, and availability of oxygen affect the production of lipid oxidation products. Quast and Karel (1971) reported that lipid oxidation is likely the most common mechanism of oxygen uptake in fried foods, such as potato chips. For fried foods, the extent of oxidation of the frying oil also contributes to the product's oxidation.

Since oxygen first attacks food at the surface, impregnating packaging materials with an antioxidant has long been used to protect the product from oxidative rancidity and thus prolong shelf life (Laermer *et al.*, 1994). The proposed mechanism of antioxidant activity involves the following 3 step process: (i) antioxidant diffusion through the polymer bulk phase; (ii) evaporation of antioxidant from the surface of the packaging material; and (iii) subsequent antioxidant sorption onto the surface of the packaged product.

3,5-Di-Tert-Butyl-4-Hydroxy Toluene (BHT) has been used extensively for its antioxidant activity. The application of BHT for its antioxidant properties in foods has been suggested for use in a variety of products (Giese, 1996). Hoojjat *et al.* (1987) demonstrated the effectiveness of a BHT impregnated film to retard lipid oxidation of a packaged oatmeal cereal, through the migration of antioxidant from the package to the product via an evaporation/sorption mechanism. However, because of questions related to safety of the migratory BHT from high density polyethylene (HDPE) to foods and food simulants (Till *et al.*, 1982), there is some concern regarding its continuous use as an antioxidant in food packaging materials. As a result of these considerations, there has been a growing interest in using α-tocopherol (i.e. Vitamin E) as an alternative antioxidant for polymer processing.

Laermer and Nabholtz (1990), Laermer and Zambetti (1992), and Laermer *et al.* (1993) have recently shown that α-tocopherol, when used at low concentrations, such as 100 ppm (w/w), is an effective processing stabilizer for polyethylene and polypropylene. α-Tocopherol alone or in combination with synergistic additives such as tris(2,4-di-butylphenyl) phosphite compares favorably with, and in some cases is superior to, Irganox 1010 or 1076 as a color and melt flow stabilizer.

Further, Ho *et al.* (1994) have shown the effectiveness of α-tocopherol as an antioxidant for reducing the off-odor and off-taste from blow molded HDPE bottles, and Laermer *et al.* (1994) showed noticeable retention in flavor for a cereal product stored in an α-tocopherol impregnated package structure. Compared to BHT, α-tocopherol is a larger, less volatile molecule, and would be expected to migrate less rapidly from a packaging material into a food or food simulant.

The present study will therefore focus specifically on developing an accurate understanding of how the rate of lipid oxidation of a packaged product is affected by both the nature and level of antioxidant incorporated within the package structure and the temperature dependency of the oxidation process. Such knowledge is essential for estimating the keeping quality of a packaged product, where quality is associated with lipid oxidation.

The objectives of the study include:

1. Development of a freeze-dried product model using linoleic acid as the oxidizable substrate and characterization of the product equilibrium sorption isotherms as a function of temperature.

2. Evaluate the effectiveness of antioxidant impregnated film in preventing or retarding lipid oxidation of the packaged model substrate via the evaporation-sorption mechanism. The extent of fatty acid oxidation will be determined as a function of the nature and level of antioxidant and temperature, using hexanal as an index of oxidation. All oxidation studies will be carried out at constant water activity. The specific water activity level will be based on the products equilibrium sorption isotherm.

It is assumed that the results of these studies would enable better design and selection of packaging systems for controlled transfer of antioxidant, and the concomitant reduction in product lipid oxidation. The temperature studies should also improve our understanding of the effectiveness of direct addition of antioxidants in products.

REVIEW OF LITERLATURE

2-1. Lipid Oxidation in Food System

Oxidation of food products is a major factor in the development of off-flavors due to oxidative chemical changes of lipids. Lipids are one of the major constituents in many food systems. Most food products of plant and animal origin contain measurable levels of unsaturated fatty acids or lipids (Moran and Rajah, 1994). The main cause of lipid degradation involves oxidative and hydrolytic reactions. The oxidative reaction, referred to as autoxidation, can occur from progressive reactions with atmospheric oxygen to produce free radicals. Here, autoxidation is an autocatalytic reaction, where the rate of oxidation increases with reaction time. In such a case, the oxidation induction period or the initiation step is a slow process and then increases as the oxidation reaction progresses (Chan, 1987). These oxidative reactions induce unstable physical and chemical changes in the stored food product. Frankel (1991) described the autoxidative mechanism that leads to the formation of free radicals to produce off-flavors from polyunsaturated edible oils. The hydrolytic reactions occur by the reaction of lipase enzymes, which act on the triglyceride ester linkage, resulting in the hydrolysis of lipids. Controlling temperature conditions can minimize the oxidation and hydrolytic reactions associated with enzymatic activity.

The oxidation of lipids is catalyzed by the presence of light, trace metals, lipoxygenase enzymes, or the effect of heat to initiate the production of free radicals. The free radicals react with oxygen to yield the primary products of lipid hydroperoxides. Unsaturated

fatty acids are susceptible more specifically to oxygen attack leading to the free-radical mechanism. The hydroperoxides formed from the reaction of unsaturated fatty acids with oxygen are also catalyzed by the action of lipoxygenase (Jadhav, *et al.*, 1996).

Also, for the case of food systems with relatively low amounts of unsaturated fats, oxidative rancidity can still play a role as the main influence of deterioration of food quality during storage. The off-flavors arising in a food system with higher amounts of unsaturated fatty acids can be absorbed in the lipid, since most of the off-flavor compounds are lipophilic, volatile compounds (Roozen, *et al.*, 1994).

Fujii, *et al.*, (1995) studied the autoxidation of methyl linoleate in emulsions containing dextrin. As the concentration of the dextrin increased, the autoxidation of the methyl linoleate decreased. Roozen, *et al.*, (1994) observed that a model food system containing linoleic acid showed a large difference in the amount and composition of volatile oxidation products formed, depending upon the lipid concentration (low and high fatty acids), types of emulsified oils (oleic sunflower oil, triolein and stripped corn oil), and the presence of antioxidants (i.e., α-tocopherol).

The main concerns involving the oxidation of a stored food product occur due to the lipid oxidation, and are typically addressed by controlling the environmental conditions of product storage, which include: temperature, relative humidity, and light. The incorporation of antioxidants into food products also helps to extend the product shelf life, by retarding oxidation processes under normal storage conditions. The oxidative process in food systems containing unsaturated fatty acids can be retarded by adding antioxidants, either directly to the food products or by incorporating them into the packaging materials (Coulter, 1988).

2-2. Mechanism of Lipid Oxidation

The mechanism of lipid oxidation has been well defined by a number of studies (Chan, 1987; Frankel, 1984) and can be described as an autocatalytic chain reaction that can be viewed as involving three major steps, namely:

(1) initiation, (2) propagation, and (3) termination. The oxidative mechanism is influenced by several factors such as oxygen, light, heat, heavy metals, and enzymes. Below, each step of the autoxidation mechanism is discussed briefly.

Initiation: $RH \longrightarrow R\bullet + \bullet H$

$RH + O_2 \longrightarrow R\bullet + \bullet OOH$

Propagation: $R\bullet + O_2 \longrightarrow ROO\bullet$

$ROO\bullet + RH \longrightarrow ROOH + R\bullet$

Termination: $R\bullet + R\bullet \longrightarrow RR$

$R\bullet + RO\bullet \longrightarrow ROR$

$R\bullet + ROO\bullet \longrightarrow ROOR$

The initiation step occurs when a labile hydrogen is abstracted from the unsaturated lipid (RH) to produce the alkyl radical (R •). In the propagation step, oxygen reacts rapidly with the alkyl radical to form the peroxyl radical (ROO •). The peroxyl radical reacts with a hydrogen atom abstracted from another unsaturated lipid molecule to form an

unstable hydroperoxide (ROOH), and another free alkyl radical (R •). The decomposition of hydroperoxides (ROOH) leads to the formation of aldehydes and esters, and other secondary products. In the initial stages of the propagation step, one begins to observe the deterioration of product flavor. In the termination step, the chain reaction can be stopped by the formation of non-free radical reaction products. This same trend is reflected in the length of the induction period for lipid oxidation, which was determined by Maskan (1993) from storage stability studies using an accelerated shelf-life testing procedure.

An alternative mechanism of lipid oxidation involves the reaction of singlet oxygen with the double bond of a fatty acid. The reaction between a lipid and oxygen typically proceeds with the lipid molecule in a singlet electronic state, and the oxygen molecule in a triple state (Bradly and Min, 1992), which is the common ground state energy level for oxygen. For initiating the autoxidation reaction involving the singlet lipid with the triple oxygen directly, a high activation energy is required for the reaction to proceed (Jadhav, *et al.*, 1996). Therefore, an initiator such as a sensitizer, high temperature, or a lipoxygenase enzyme plays an important catalytic role to provide the capability of altering triplet oxygen to singlet oxygen for lipid oxidation. Singlet oxygen can react at the end of the double bond of a lipid and yield a hydroperoxide (Raws and Vansanten, 1970). Singlet oxygen is generated by the transfer of energy from a sensitizer such as chlorophyll or myoglobin with ultraviolet light. Ultraviolet light, as the main factor, is required for this oxidation mechanism to occur. (Frankel, 1984).

Lipid oxidation is the result of a series of specific individual reactions, with each reaction having its own activation energy. A number of theories have been proposed, describing

the reaction mechanism for lipid oxidation (Labuza, 1971). Lipid oxidation begins with the initial reaction process, which has a high activation energy, being about 30 to 40 kcal/mole. At this point, singlet oxygen plays a very important role in the formation of peroxides in the initial reaction. Trace metals and ultraviolet light, with the proper sensitizers, also function as initiators of the autoxidation process. Higher temperatures in this reaction process affect the formation of increased singlet oxygen species. The activation energy, under UV light, is about 4 kcal/mole for the initial reaction. Normally, the initial process in lipid oxidation involves metal catalysis. The activation energy, in the absence of a metal cation, is about 20 kcal/mole (Labuza, 1971). Once the initial reaction occurs, the autoxidation mechanism involves the propagation reaction, which has an activation energy of about 3 to 5 kcal/mole. The activation energy of the termination reactions is about 5 to 8 kcal/mole.

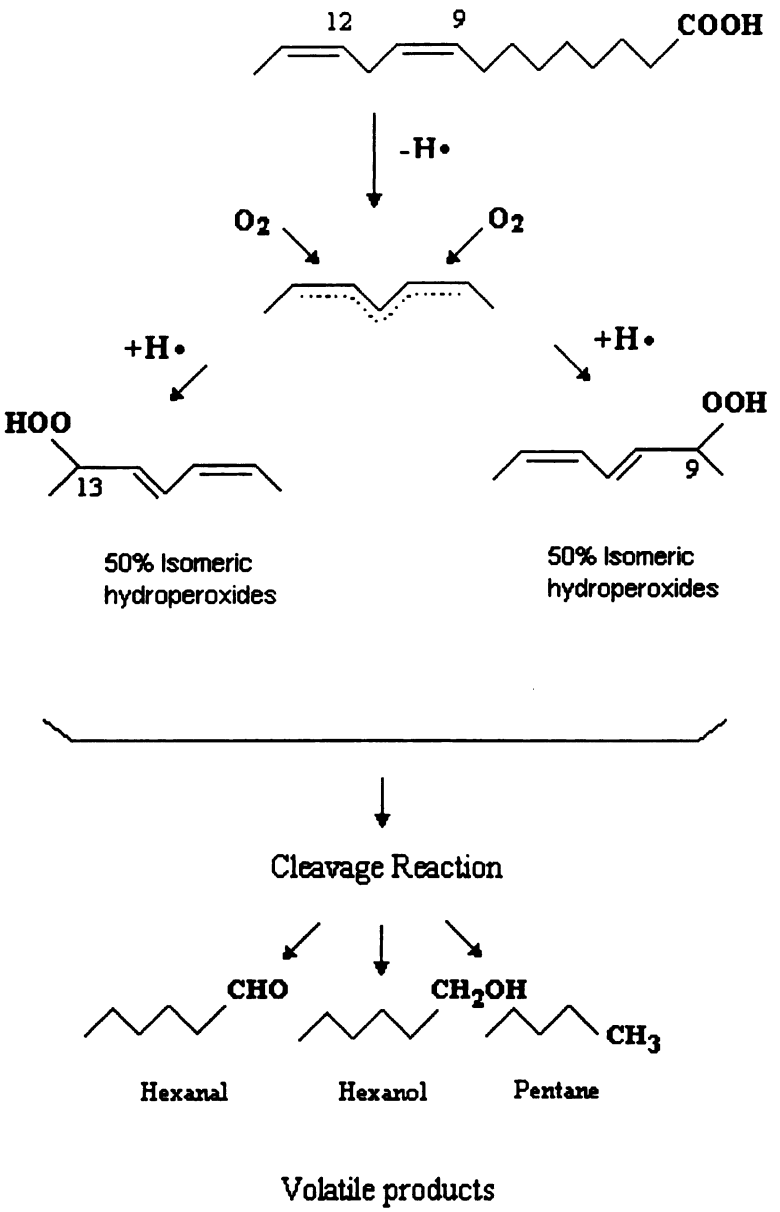

Figure 1. The typical autoxidation pathway of linoleic acid (Frankel, 1984 and Labuza, 1971).

As shown in Figure 1, the autoxidation mechanism of linoleic acid (18:2) involves the initial abstraction of a hydrogen atom, followed by the reaction of oxygen at the 9- and 13- end positions of the carbon chain to produce conjugated 9- and 13-hydroperoxide isomers. These isomers have the trans, cis-configuration which has the double allylic methylene group on carbon-11, to generate a pentadieny radical. Linoleic acid produces 4 isomers that have 2 conjugated 9- and 13-diene hydroperoxides and 2 unconjugated 10- and 12-diene hydroperoxides. The acyl hydroperoxides that are formed by these reactions, undergo subsequent reactions, leading to hydrocarbons, carbonyl and alcohols, and various volatile compounds (Table 1).

Table 1. Relative amounts of volatile compounds from autoxidation of linoleic acid at moderate temperature (20°C) (Chan, 1987).

Compounds	Percent (weight of a compound per total weight of all compounds identified)
Pentanal	0.7
Hexanal	66.4
Heptanal	0.7
Octanal	0.6
trans-2-Heptenal	5.9
cis-2-Octenal	13.0
trans-2-Octenal	5.5
trans-3-Nonenal	0.4
cis-3-Nonenal	0.4
trans-2-Nonenal	0.4
cis-2-Decenal	0.3
trans-2,trnas-4-Nonadienal	0.4
trans-2,cis-4-Decadienal	3.2
trans-2,trnas-4-Decadienal	2.0
1-Octen-3-one	<0.1

2-3. Secondary Products of Terminal Oxidation Reactions

Hydroperoxides formed in lipid oxidation decompose into secondary products. A general scheme for the fragmentation of monohydroperoxides involves carbon-carbon cleavage on either side of the alkoxy radical to produce two types of aldehydes, an olefin radical, and an alkoxy radical. These radicals can react with either OH • or H •. The vinyl alcohol derived from the reaction with OH • is unstable and tautomerizes into saturated aldehydes (Frankel, 1984).

The product from the reaction with H • is either an α-olefin, or a short chain ester. These products include carbonyls, alcohols, esters and hydroperoxides. The linoleic acid of one substrate yields four major hydroperoxides of 9- and 13-positions in the trans-cis and trans-trans configurations. These hydroperoxides decompose into a large number of volatile products, including hexanal as one of the major secondary products (Martin, *et al.,* 1990). The qualitative data presented in most studies (Frankel, *et al.,* 1989, Hallberg, *et al.*, 1991, Gardner, 1985) shows that hexanal is the major adehyde formed from autoxidation of polyunsaturated fatty acids. Quantitatively, hexanal has also been identified as one of the major oxidation products, resulting from autoxidation of linoleic acid (Schieberle and Grosch, 1981; Henderson, *et al.*, 1980). The total amounts of hexanal and pentanal present among the volatile aldehydes formed from linoleic acid (18:2) during autoxidation were 199.0 and 6.7 (nmole/mg fatty acid), respectively (Esterbauer, *et al.*, 1990). Jeon and Bassette (1984) determined the levels of n-hexanal and n-pentanal in headspace gas and found these to be good indicators for determining the degree of rancidity and flavor quality of potato chips. The analysis for n-hexanal in

low fat, dehydrated foods by gas chromatography was reported by Fritsh and Gale (1977). The quantification of hexanal in low fat food products, as a measure of oxidative rancidity, is a simple and effective analytical method, since hexanal is a stable compound and less reactive in the low fat model food product than other secondary products. When the hexanal level increases above a certain concentration in dehydrated and low-fat foods containing linoleic acid, quality deterioration by lipid oxidation is indicated.

Roozen, *et al.*, (1994) also investigated the levels of hexanal formed from methyl linoleate hydroperoxides prepared by autoxidation and produced by a lipoxygenase preparation, using a low fat food model. The lipoxygenase preparation was found to more readily yield hexanal.

2-4. Factors Affecting Lipid Oxidation

Water activity, temperature, oxygen concentration, antioxidants, trace metals, and light are among the various factors that can influence the rate of lipid oxidation in food products.

2-5. Water Activity

The physical and chemical deterioration of dehydrated food products is related closely to the vapor pressure of water surrounding the product, which is commonly expressed as water activity.

Water activity (*Aw*) is defined as the ratio of the vapor pressure (*P*) of water in the food to the vapor pressure of pure water (*Po*) at the same temperature.

$$Aw = \frac{P}{Po} = \frac{RH}{100}$$

where, P = water vapor pressure equilibrated over the food

Po = vapor pressure of pure water at same temperature

RH = relative humidity

The control of Aw in food products controls the change in food quality during storage. The amount of moisture in a food product is related to the following physical and chemical changes. The food system can undergo: (i) loss in nutritional quality of proteins, and vitamins; (ii) the oxidation of lipids; (iii) the growth of microorganisms; (iv) changes in enzymatic activity; and (v) changes in the texture of food products (Troller, 1989).

2-5-1. Moisture Sorption Isotherm

The moisture sorption isotherm can be used to describe the relationship between the moisture content of the food product as a function of water activity. This corresponds to a range of moisture content values and represents the change in moisture content, with a change in the water activity. The moisture sorption isotherm of most food products

shows a sigmoid type curve over a broad range of water activity values. The specific regions of the moisture sorption isotherm can be related to the physical characterization of water within the food product and provides an important prediction of the type of chemical reactions food products may experience.

Water contained in the food product consists of two types, referred to as 'free' and 'bound' water. Various food products have different levels of bound water, which is typically less than 10 %, on a wet weight basis. The B.E.T. (Brunauer, Emmett and Teller, 1938) monolayer value represents the most stable bound water (Karmas, 1980).

The generalized moisture sorption curve or isotherm is divided into three regions, with the level of water varying from dry to high moisture in the product. The first region has Aw values between 0 and 0.25, which is mostly water bound by the ionic groups of the product, such as NH_3^+ and COO^-, which are related to proteins, pectin, etc. The second type of bound water range has Aw values between 0.25 and 0.75, which includes water molecules H-bonded to hydroxyl and amide groups of the product. The third region of sorbed water has Aw values between 0.75 and 1.0, which represents the least strongly bound and multilayer moisture levels in the food product. The zone (Aw range from 0.2 to 0.3) between the first range and second range corresponds to the monolayer value and represented the maximum amount of water, with very strong binding to the dried product (Fennema, 1996). The monolayer value is very useful to express the most stable condition of a food product, based on the binding of water molecules. When the moisture level of a food product is determined by drying, the bound water can be removed from the food contents. The monolayer value from the B.E.T. equation and the moisture sorption isotherm of food product can also be obtained.

2-5-2. Water Activity related with Lipid Oxidation

The water activity level in dehydrated food products, containing unsaturated fatty acids, influences the development of oxidative rancidity and is a major factor in lipid oxidation, since a relatively narrow range of water activity can inhibit or activate lipid oxidation of food products (Rockland and Nishi, 1980). For example, at very low levels (below 0.3) of water activity in the food product there is a high rate of oxidation of fatty acids, until the monolayer level of moisture content is reached. As shown in Figure 2, the rate of oxidation of food products containing unsaturated fatty acids, at normal oxygen concentration, increases continuously over a water activity range between Aw = 0.3 to 0.7, and is then followed by a near constant rate of oxidation (Labuza, 1971).

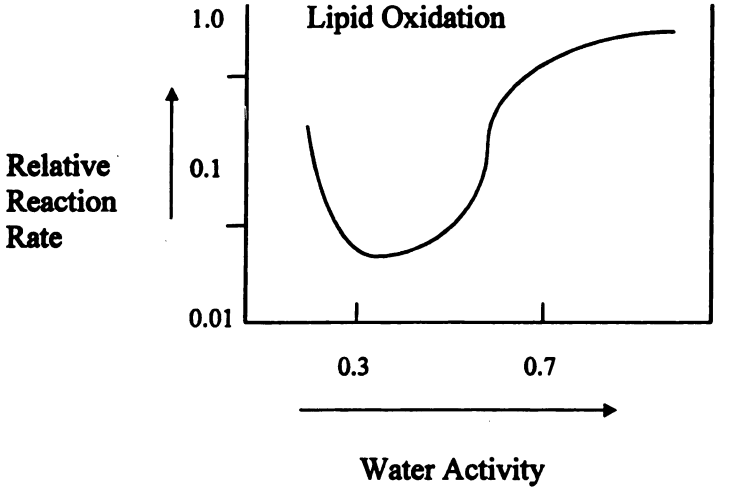

Figure 2. The rate of lipid oxidation according to the effect of Aw on the food system (Labuza, 1971).

The above figure illustrates the effect of Aw on the rate of lipid oxidation for a food model system. At Aw values below the monolayer value, the rate of lipid oxidation decreases with increasing Aw. The rate of lipid oxidation reaches a minimum around the B.E.T. monolayer value and increases again with a further increase in Aw, until it reaches a constant rate of oxidation (Leung, 1987). The moisture contained in the food product system affects the rate of lipid oxidation by hydrating metal ions and hydrogen bonding with peroxides formed, thus decreasing the rate of lipid oxidation by decreasing the catalytic activity of metal cations and promoting the recombination of free radicals at low moisture content. The hydration of hydroperoxides reduces the rate of free radical formation.

Berends (1993) showed the effect of water activity on the rate of lipid oxidation in a food product model system. The rate of lipid oxidation was calculated using the activation energy at different water activity ranges. The low water activities showed a high rate of oxidation. As the water activity increased to near the monolayer value, the rate of lipid oxidation decreased. The lipid oxidation rate was then found to increase, up to a constant level after the monolayer value point.

The shelf life of food products associated with flavor rancidity can be extended by controlling the products, water activity during storage. The B.E.T. monolayer level in food products has been shown to provide optimum conditions to minimize lipid oxidation, which causes food rancidity.

Gopala and Prabhakar (1995) observed a change in the rate of autoxidation in raw peanut oil by the addition of water throughout the storage period. The addition of moisture, at a

low level, into raw peanut oil was thought to inhibit the formation of peroxides from the fatty acids. Furthermore, Nelson and Labuza (1992) stated the importance of the relationship between the rate of lipid oxidation and water activity, based on the glass transition theory in polymeric systems. The physical conditions of the food system such as a crystalline or amorphous state can affect lipid oxidation, since the moisture content influences the state of the food system. For a packaged product, the free volume in a polymer matrix allows oxygen to diffuse through to the food system. Kumor (1986) mentioned that dry cereal product containing unsaturated lipids in the presence of air resulted in development of a rancid flavor at low water activities. Lipid oxidation in cereal products can result in color loss and flavor deterioration associated with the reaction of unsaturated lipids with oxygen, as well as quality loss.

2-5-3. Monolayer Moisture Content

The monolayer value can describe the amount of water required to form a monolayer over the highly polar groups of a dehydrated food product. The monolayer value is associated with the minimum reaction rate for lipid oxidation in a number of dehydrated food products, when the moisture content reaches the level of the B.E.T. monolayer value. The initial moisture content, sorption isotherm data, and the Brunauer, Emmett, and Teller (B.E.T.) equation (Brunauer, *et al.*, 1938) provides the monolayer moisture content of dehydrated food products. The monolayer water content corresponds to a specific water activity of the products' sorption isotherm plot. The rate of lipid oxidation at Aw below the monolayer value decreases with an increase in the products

water activity. The rate of lipid oxidation also increases with an increase in water activity, after a minimum point at the monolayer value is reached (Quast and Karel, 1972).

2-6. Temperature

Temperature is the most important acceleration factor in the lipid oxidation process. Elevated temperatures increase molecular movement and accelerate the rate of lipid oxidation. The higher temperatures result in increased free radical activity by providing the activation energy values required for the reactions associated with the autooxidation process. The activation energy, determined from higher temperature level studies, is important for the prediction of shelf life at room temperature for food products. Berends (1993) determined the rate constants for lipid oxidation of a food system model at three temperatures and compared the respective rate values. This comparison was based on an assumed first order rate equation and showed that at a constant oxygen concentration, greater amounts of hexanal are produced as the temperature increases from 23, to 40, and to 66°C. The change in temperature shows a significant effect on the rate of lipid oxidation. Gloria (1993) investigated the effect of chemical oxidation, photosensitized oxidation and autoxidation in a microcrystalline cellulose model system on the formation of volatile oxidation compounds and the loss of β-carotene. The loss of β-carotene was faster during autoxidation at 80°C than the chemical oxidation, photosensitized oxidation and autoxidation at 20°C. Autoxidation at 20°C and chemical oxidation yielded several volatile oxidation products from β-carotene. Autoxidation at

80°C and photosensitized oxidation led to more specific oxidation products, namely; dihydroactinidiolide and beta-ionone, respectively (Gloria, 1993).

2-7. Oxygen Concentration

Oxygen is an essential factor required to initiate formation of hydroperoxides in the lipid oxidation reaction. Thomas (1994) studied the effect of varying initial oxygen concentration levels, using oxygen absorbers, on the shelf life of packaged potato chips. An initial oxygen concentration of 0.2 % (v/v) in the package headspace showed significantly less hexanal formation than that found at an oxygen concentration of 2 %, after 22 weeks without an oxygen absorber. Koelsch (1989) found the rate of lipid oxidation at a headspace oxygen concentration of 15.4 % to be faster than that at 1.2 % oxygen, using a system for measuring the rate of lipid oxidation. Berends (1993) showed that hexanal levels, at an oxygen concentration of 8 %, followed a first order rate equation and were greater than that for 1.5 % oxygen at accelerated temperatures, in a model food product system containing linoleic acid. The oxygen concentration in a package headspace, or a continually permeating low oxygen concentration can affect the rate of lipid oxidation reactions. The oxygen concentration can be controlled by the use of vacuum, or an inert gas and by controlling the headspace composition within the package system. Kishida, *et al.,* (1993) investigated the oxidation of oleic, stearic, linoleic and linolenic acids in foods at 170°C in a closed vessel and the oxygen consumption for autoxidation.

The yields of malondialdehyde (MDA) and 2-thiobarbituric acid-reactive substances (TBA-RS) were compared with the data for oxygen consumption. TBA-RS and MDA increased with the oxygen consumption up to 2000 μmol/L and 700 μmol/L respectively in the autoxidation of linoleic acid. Therefore, TBA-RS reflected the reaction course better than MDA, over a wide range of concentrations of consumed oxygen, in the autoxidation of linoleic acid.

2-8. Light

Light is a catalyst for oxidative rancidity in food products during storage. However, a light barrier provided by the packaging material can retard the rate of lipid oxidation reactions. Mathluothi (1986) showed the influence of light transmittance, using various packaging materials, on a series of physical, chemical, and sensorial characteristics of solid whole natural yogurt during storage. High light energy afforded considerable differences between the peroxide values of the yogurts exposed in different packages during storage. Jeon and Bassette (1984) reported the changes in n-pentanal and n-hexanal concentrations in potato chips exposed to 100 ft-candles of fluorescent light, using headspace gas analysis. The n-hexanal concentration in the potato chips exposed to light showed moderately higher levels than in the controls, during the first 60 hrs of storage. Rapid formation of n-hexanal occurred after 60 hrs of exposure to the light.

2-9. Trace Metals

Trace metals, to include Co, Cu, Fe, and Mn, can reduce the length of the induction period and increase the maximum rate of lipid oxidation. Metals act as prooxidants by electron transfer, liberating radicals from hydroperoxides via oxidation reactions. However, chelation of metal ions by food components reduces the prooxidative effect of these ions. The addition of disodium ethylenediaminetetraacetate (as chelating agent) in deep-fried instant noodles was found to prolong the shelf life of the product (Rho, 1986). In biological systems, copper and iron ions have both prooxidant and antioxidant properties which can promote free radical induced oxidative stress under certain conditions (Johnson and Fischer, 1994). Copper and iron metal ions catalyze the oxidation of lipids and show a decrease in the induction period, as well as an increase in the rate of lipid oxidation (Pershern, *et al.*, 1995).

3. Antioxidants

Antioxidants are a major class of compounds (21 Code of Federal Regulations (CFR) 170.3) that prolong the onset of deterioration, rancidity, or discoloration of food products, which occur due to oxidation, as defined by the United States Food and Drug Administration (FDA) (Dziezak, 1986). Antioxidants function by retarding or inhibiting the initiation, and propagation reactions in the free radical autoxidation process associated with lipid oxidation.

Such a reaction scheme is shown below.

$$R\bullet + AH \longrightarrow RH + A\bullet$$

$$ROO\bullet + AH \longrightarrow ROOH + A\bullet$$

Here, the antioxidant (AH), which has a phenolic hydroxyl structure, can donate a hydrogen atom to a free radical (R •) or a peroxyl radical (ROO •) of the lipid, thus terminating the propagation step. Reaction of a hindered phenolic antioxidant with a free radical forms a free phenoxy radical (A •), which is stabilized by the electron delocalization in the aromatic ring.

Antioxidants of the hindered phenolic type are classified as either synthetic or a natural product. Currently, the application of α-tocopherol to a food product directly or indirectly is increasing, as the trend toward the use of natural antioxidants increases (Shahidi and Wanasundara, 1995). This affords a greater biological benefit and reduces health risk, even though synthetic antioxidants applied to food products are effective and inexpensive (Landvik *et al.*, 1996). Many food manufactures tend to substitute synthetic antioxidants with foods containing natural antioxidant substances (Marshell, 1974). In general, the use of antioxidants for a food product directly is limited to 200-300 ppm (w/w) of butylated hydroxyanisole (BHA), butylated hydroxytoluene (BHT), and tertiary butylhydroquinone (TBHQ), or 200-500 ppm of the gallates, for the stabilization of fats and oils (Madhavi and Salunkhe, 1996).

Porter (1977) evaluated both natural and synthetic phenolic antioxidants in a dry model system that had linoleic acid monolayers on activated silica gel. BHA was found to be highly effective, even though a monohydric compound. Shahidi and Wanasundara (1995) reported that canola extracts and some of the flavonoids (morin, myricetin,

quercetin, and rutin) were more effective than BHA and BHT in preventing the oxidation of canola oil. The antioxidant molecule may react with the free hydroperoxide radicals. The free antioxidant radicals are produced after the active free radicals are deactivated. The antioxidant free radicals are more stable and can undergo oxidation to quinones or combine with other free radicals.

α-Tocopherol shows a good ability to inhibit lipid oxidation or to extend the induction period of free radical oxidation, as well as to slow the propagation step of the autoxidation process (Widicus and Kirk, 1981; Pershen, *et al.*, 1995).

3-1. Synthetic Antioxidants

Synthetic phenolic antioxidants are the most widely used in food products and include butylated hydroxyanisole (BHA), butylated hydroxytoluene (BHT), propyl gallate (PG) and tertiarybutyl hydroquinone (TBHQ) (King, *et al.*, 1993).

Butylated Hydroxytoluene (BHT)

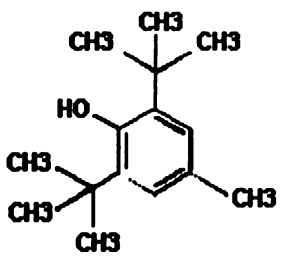

3,5-Di-Tert-Butyl-4-Hydroxy Toluene (BHT)

BHT is one of the most extensively used antioxidants in the food industry. BHT is used in low-fat food products, fish products, packaging materials, paraffin, and mineral oils. BHT is also widely used in combination with other antioxidants like BHA, propyl gallate, and citric acid for the stabilization of oils and high fat foods. BHT is a white crystalline solid readily soluble in fats and oils and insoluble in water. It is subject to loss during processing. BHT is Generally Recognized as Safe (GRAS) for use in food to a maximum antioxidant concentration of 200 ppm of fat weight (21 CFR 182.3173). BHT is permitted up to 50 ppm of maximum usage levels in dry breakfast cereals, as stated in the Code of Federal Regualtions (21 CFR 172.115) (Coulter, 1988). BHT in high doses has a toxic effect on the liver, lungs, and kidney, and on bloods coagulation mechanism (Madhavi, and Salunkhe, 1996). Cort (1974) reported that BHT and BHA were more effective than tocopherol in their role as an antioxidant in linoleic acid. All tocopherols were shown to be active in oleic acid, with dl-α-tocopherol equal to BHT, and dl-γ-tocopherol a more active antioxidant than BHT or BHA.

3-2. Natural Antioxidants

The list of natural antioxidants includes tocopherols, ascorbic acid, carotenoids, flavonoids, lecithin, rosemary extract, gum guaiac, and a few others. Tocopherols have the greatest popularity of the natural source products. They occur naturally in vegetable oils, with the prime commercial source being soybean (Giese, 1996).

Tocopherol

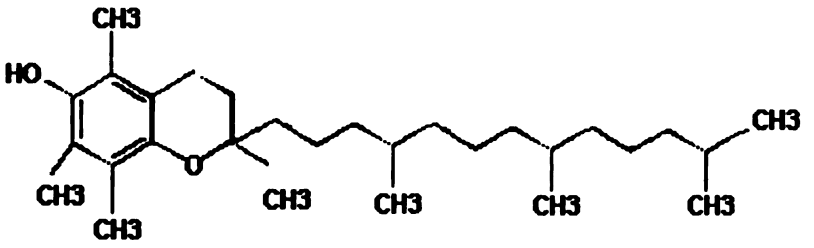

d,l-alpha-tocopherol (Vitamin E)

Tocopherol is designated as α-, β-, γ-, δ- types, which are based on the number and position of the methyl groups on the chromane ring. α-Tocopherol has methyl groups in the 5-, 7-, and 8- positions in the aromatic ring. β-Tocopherol has methyl groups in the 5-and 8-positions, and γ-Tocopherol has methyl groups in the 7- and 8-positions. δ-Tocopherol has a single methyl group in the 8-position of the aromatic ring (Machlin, 1984). α-Tocopherol has the greatest biological activities in varying potencies (Schuler, 1990). Tocopherol comes from the vegetable oil source more than from an animal fat source. Cereal grains, vegetables, and fruits are also good sources of tocopherol.

Tocopherol functions as a good chain-terminating antioxidant. Tocopherol has GRAS status for use as a food preservation (21 CFR 182.3890). Tocopherol is an effective antioxidant in various food products for use at relatively low concentrations, in the range of 100 to 300 ppm of fat weight (Dougherty, 1988). The most effective concentrations of

α - tocopherol are in the range of 100-200 ppm in the food system (Dziezak, 1986). The loss of tocopherol in food processing is affected directly by oxygen, light, heat, and trace metals (Eitenmiller, 1997). However, tocopherol has heat stability and is not volatile under normal conditions of cooking, compared to the instability of some antioxidants to heat (Dougherty, 1988).

McCord (1994) reported that vitamin E plays a role in inhibiting the progress of chain reactions involving propagation of lipid radicals produced as oxidant productions in the presence of iron ions. Burton, *et al.*, (1993) proposed that the α-tocopherol functions as an antioxidant by rapidly transferring its phenolic hydrogen atom to a lipid peroxyl radical, resulting in the formation of two molecules that are relatively unreactive towards polyunsaturated lipid, a lipid hydroperoxide and the α-tocopheroxyl radical. Cort (1974) showed that the antioxidant activity of the dl-γ-tocopherol was greater than α-tocopherol, and increased as the concentration increased in chicken, pork, and beef fats, and with oleic acid. Pershern, *et al.*, (1995) reported that a relationship existed between total fat, fatty acid and α-tocopherol contents and lipoxygenase (LOX) activity and the shelf-life of hazelnuts. The α-tocopherol content in hazelnuts played an important role in controlling off-flavor at a level of 20mg per 100g hazelnuts. A higher α-tocopherol level in hazelnuts improved shelf-life stability.

3-3. Antioxidants for the Polymer Plastic Film

Currently, polymeric packaging materials are widely used due to commercial advantages of their cost and good control of their physical and mechanical properties. Among the polymeric food contact materials, a commercial HDPE has shown high usage in food packaging such as for milk bottles, drinking water bottles, and as a package for edible oil containing fatty acid components (Till, *et al.*, 1982). Polyolefins have incorporated antioxidants to maintain the stability of the polymer to oxidation during processing and at environmental conditions, as well as to retard the oxidation of packaged food products. The oxidation of polyolefins is related to the degree of chain branching in the polymer. The oxidative degradation of polyolefins in the presence of oxygen, during melt processing at high temperatures, may be related to the packaging article's inability to withstand a stress associated with aging or deteriorating effects (Birley, 1991).

The use of α–tocopherol to prevent oxidative reactions in extrusion processing for HDPE bottles and LDPE film packaging at high temperatures has shown the effectiveness of α–tocopherols performance as an antioxidant, through sensory evaluations. Its application at low temperatures has also been determined (Zambetti, 1995). Laermer and Nabholz (1990) evaluated α–tocopherol as a highly effective melt stabilizer, alone at low concentrations and in synergistic mixtures with other secondary antioxidants, including phophites (such as TNPP, Hostanox PAR204, Weston 619) and thioesters (such as DSTDP) in polypropylene. The melt and color stabilization observed for a series of mixtures of tocopherol with phosphite and thioester antioxidants with polypropylene and polyethylene showed such mixtures to have excellent stability properties, as compared

with other antioxidants (Laermer and Zambetti, 1992). Tocopherols incorporated into polymeric packaging afford commercial advantages to the polymer system and to commercial applications of the polymer. Polymers stabilized with α-tocopherol were found to have fewer taste and odor problems, as well as better color stability, than those with typical commercial polymer antioxidants. Further, there is a reduction of contamination risk from the packaging components, and good thermal stability during processing (Laermer *et al.*, 1994). At accelerated stability tests, HDPE/EVA liner packaging films with various concentrations of tocopherol added, showed a noticeable reduction of flavor loss from a packaged cereal product at 37°C, over a three month storage period (Laermer *et al.*, 1994). Ho and Yam (1994) reported that HDPE drinking water bottles containing tocopherol had less odor and higher acceptability than these containing the antioxidants, Irgonox 1010 or BHT, through sensory evaluation of the off-flavor problem. This problem can be identified with the following possible factors associated with odor threshold, namely: molecular weight, and polarity of the compounds released from the polymer, such as ketones and aldehydes. Lin (1996) observed that cereal product packaged in pouches without antioxidant showed a significantly higher level of hexanal, as compared to the rate of oxidation of cereal product packaged in antioxidant (α-tocopherol, BHT) impregnated structures, following the 20th week of storage (23°C/50%RH). The hexanal levels detected in cereal product packaged in α-tocopherol impregnated pouches and BHT impregnated pouches showed no significant difference, over a 44 week storage period at ambient conditions (23°C/50%RH).

4. The Mechanism of the Migration of Antioxidants from the Packaged Film Structures to a Contained Product.

Antioxidant migration from a packaging film structure into a contained food product can be described by the following basic mechanism. First, diffusion of antioxidant molecules contained within the void volume between the polymer chains through the polymer bulk phase to the polymer surface. Second, evaporation of antioxidant molecules from the surface of the packaging material to the internal package environment. Third, sorption of antioxidant molecules onto the surface of the packaged product. High molecular weight antioxidants would be expected to migrate slowly into the food product, as compared with low molecular weight migrants. The mechanism for the three step migration process is illustrated in Figure 3.

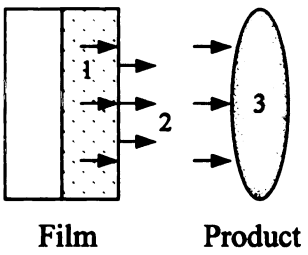

Figure 3. A three step migration process

Generally, migration from a polymeric packaging material can be described as either global or specific migration. These terms refer to whether the total mass of migrant is considered, or a number of restricted migrating components from the package into the contained food, under specified conditions, are being considered (Crosby, 1981). The migration system can be divided into the three types based on migrant diffusion, such as described by Robertson (1993): (1) migration takes place only from the packaging surface regardless of the presence of a food product. (2) the presence of food may affect migration from the packaging surface; However, migration is not controlled by the food product, but by the rate of diffusion of the migrant through the polymer bulk phase. In this case a diffusion coefficient can be measured under the test conditions and during a specified contact time. (3) migration is controlled by the food product at the packaging surface, and the food system plays an important role in the transfer of migrants from the film structure to the contained product. Here, penetration of the film structure by a component of the contacting food system can increase the rate of diffusion of the migrant from the packaging film. The relationship describing the loss of antioxidants from the packaging film structure into the food product can be expressed by the rate of migration of the antioxidants. The migration rate of the antioxidant is affected by the following factors (Calvert and Billingham, 1979): the additive solubility, the diffusion coefficient of the additive, and additive volatility, which are discussed briefly below. (1) The solubility of antioxidants in the film structures. This is described by the solubility coefficient, which is determined by the morphology of the polymer and the chemical properties of the antioxidants. The temperature and vapor pressure also affect the solubility of antioxidants. (2) The diffusion coefficient of antioxidants within the film structures,

describes how rapidly molecules are advancing through the polymer bulk phase and the time to reach steady state. The molecular size of the antioxidant affects the magnitude of the diffusion coefficient.

The diffusive flux of antioxidants in a film structure can be expressed as the amount passing through a plane of unit area normal to the direction of flow during unit time.

$$F = M/A \cdot t \qquad \text{---------- (1)}$$

Fick's first law applies where the rate is directly proportional to the concentration gradient.

$$F = -D\left(\partial C/\partial X\right) \qquad \text{---------- (2)}$$

Where,

F = the flux (the rate of transfer of the diffusing substance per unit area)

M = the amount of the substance which passed through the film

A = area of surface at which diffusion occurs

C = the concentration of diffusing substance

X = the distance of diffusion

t = time

D = the coefficient of diffusion

For an infinite plane or sheet, across which diffusion occurs in a linear direction (x) of a thin membrane, in most cases, migration from a film structure into a food system can be expressed by Fick's second law (Equation 3).

$$(\partial C/\partial t) = D(\partial^2 C/\partial X^2) \qquad \text{---------- (3)}$$

The amount of antioxidant transferred per unit time, through a film structure with constant dimensions, can be represented by the transmission rate. Factors affecting antioxidant diffusion within the film structure include the chemical nature of the film structure, the size of antioxidants, the thickness of the film structure (an inverse proportion), and environment conditions (temperatures, humidity).

(3) The loss rate of the antioxidants by volatilization from the film surface.

A mathematical model describing the loss of an antioxidant from the polymer to the environment in which the polymer is stored requires two parameter factors; namely: (1) a mass transfer constant, characterizing transfer across the boundary of polymer surface-air interface; and (2) a constant characterizing antioxidant mass transfer within the polymer bulk phase.

A mathematical equation has been described by Crank (1975) for the additive loss from a film by surface evaporation with finite boundary conditions. To calculate the loss of antioxidant concentration as a function of time, the total amount of additive M_t leaving the film at time (t) is expressed as a fraction of the corresponding amount M_∞ leaving the film at infinite time by the mathematical equation (4).

$$\frac{M_t}{M_\infty} = 1 - \sum_{n=1}^{\infty} \frac{2L^2 \exp(-\beta n^2 T)}{\beta n^2 (\beta n^2 + L^2 + L)} \qquad \text{---------- (4)}$$

Where, M_t = amount of additive leaving the film in time (t)

M_∞ = amount of additive leaving the film at infinite time

$T = Dt/l^2$

$L = l\alpha /D$

l = half of film thickness, cm

t = time, sec

D = diffusion coefficient of additive in film, cm^2/sec

α = mass transfer constant of additive from film, cm/sec

βn values are the positive roots of $\beta n \tan \beta n = L$

Calvert and Billingham (1979) reported the rate of loss of a low molecular weight compound, such as 3,5-di-tertiary-butyl-4-hydroxytoluene (BHT), from thick polymeric slabs was determined by bulk phase diffusion, while the loss from thin films was dominated by the rate of surface evaporation.

The rate of loss of 2-tertiary-butyl-4-methoxyphenol (BHA) from a high-density polyethylene film as a function of the storage time and temperature, based on the theoretical model, was reported by Han, *et al.*,(1987).

From the following equation (5), for a first-order rate expression, the loss of BHA from HDPE film as a function of storage time and temperature was analyzed.

$$Ln \frac{C}{Co} = -Kt \qquad \text{----------} (5)$$

where, Co : the initial concentrations of BHA in the film sample (w/w)

C : the concentrations of BHA in the film sample (w/w) at time (t)

K : the rate constant

t : the time interval

If the term for n = 1 is assumed in Equation 4, the following form is derived after rearrangement,

$$1 - \frac{M_t}{M_\infty} = \frac{2L^2 \exp(-\beta n^2 T)}{\beta n^2 (\beta n^2 + L^2 + L)} \qquad \text{---------- (6)}$$

or

$$Ln[(1 - \frac{M_t}{M_\infty})(\frac{\beta^2(\beta^2 + L^2 + L)}{2L^2}] = -\beta^2 \frac{Dt}{l^2} \qquad \text{---------- (7)}$$

Equation (7) is the same form as Equation (5). Since (1-Mt/M∞) = C/Co and the equations describe the same phenomenon, the two following equations can expressed by

$$\frac{\beta^2 D}{l^2} = K \qquad \text{---------- (8)}$$

and

$$\frac{\beta^2(\beta^2 + L^2 + L)}{2L^2} = 1 \qquad \text{---------- (9)}$$

The β value is used to calculate the value of D from Equation 8, and the values of L and D are used to calculate the values of α from Equation of $L = l\alpha$ /D.

The above methods, as described by Calvert and Billingham (1979), give a calculation of the diffusion coefficient, the volatilization coefficient, and the expected shelf-life of the polymer. Han, *et al.* (1987) found that the loss of BHA from HDPE followed a first-order rate expression and described a method for the calculation of the diffusion coefficients (D) and the mass transfer coefficient (α) from sorption or desorption data for BHA and BHT in HDPE. The controlling parameter factor for mass transfer of the antioxidants was found to be volatilization rather than diffusion.

5. Product Model System

A number of researchers have used a model system to provide a specific, as well as a well characterized system, to study the complex autoxidation reaction. The product model gives a constant composition and can minimize the number of variables, which can result in unexpected reactions. Widicus and Kirk (1981) reported the storage stability properties of α-tocopherol using a dehydrated model food system containing methyl linoleate for lipid oxidation. The rate of lipid oxidation was found to be dependent on the accessibility of the surface area of the food system to oxygen. Thus, oxygen diffusion is difficult to control in a model system. To minimize the problems associated with the product surface area, the model system required a large surface area and a minimal thickness. In this case, oxygen is readily accessible and the reaction rate is not dependent on oxygen diffusion (Leung, 1987). Berends (1993) used a model product to represent an oxidation-susceptible freeze-dried product containing linoleic acid. The uniformity of the model product and a consistency of the oxidation rate to exposed oxygen were proved

from product components adapted by Koelsch (1989) and Berends (1993). The product model used for this research has been developed to predict the rate of lipid oxidation, based on the oxidation of linoleic acid during storage. This model system can also provide additional information on the effectiveness of antioxidants on retarding lipid oxidation of the model product system, according to various affected factors.

6. Analytical Technique for Measurement of Lipid Oxidation in Food System

The analytical measurements to monitor lipid oxidation have been based on a number of techniques (Allen and Hamilton, 1994). As previously discussed, lipid oxidation is a complex sequence of reactions, which involves the formation of intermediate products such as hydroperoxides and peroxides, as well as a number of different breakdown products, depending on the types of lipids in the product. The peroxide value (PV), which is based on an iodometric titration procedure, is a common measurement that has been used to quantify peroxide or hydroperoxide type intermediate-products. Mate, *et al.* (1996) determined the peroxide value of peanut oil by reaction with ferric thiocyanate as a colorimetric method. The anisidine value (AV) estimates the level of aldehydes (2-alkenals) in fat containing products, which are treated with p-anisidine reagent in iso-octane solution, and is useful for fat containing products with a low PV. The thiobarbituric acid (TBA) method is used to determine the level of aldehyde products formed. Here, thiobarbituric acid reacts with malondialdehyde to produce a red chromogen and is useful for monitoring the initial steps of lipid oxidation. Warner, *et al.* (1996) used a modified TBA method to determine the total extent of lipid oxidation of

stored ground peanuts. The 10% peanut homogenate with deionized water was added to TCA (trichloroacetic acid) solution. The absorbance of a filtered aliquot was then measured at 443nm using an UV-VIS spectrometer, after reaction with TCA at 60°C for 30min. The Kreis test measures a red color obtained when phloroglucinol reacts with oxidation products in hydrochloric acid solution (Gray, 1978). The red color is related to the reaction of epoxy aldehydes and acetals extracted from oil products. High performance liquid chromatography (HPLC) methods have also been used to measure aldehydic products (2,4-dinitrophenylhydrozones) of lipid peroxidation, and are most often used with biological systems. Gas chromatography (GC) is useful for determining volatile compounds of lipid oxidation (Frankel, *et al.*, 1989). GC is applied to volatile compounds in fat containing products through headspace or extraction procedures. GC offers high resolution, in addition to providing a strong possibility of identification of oxidation products by mass spectroscopy.

6-1. Gas chromatography / Mass spectrometry

Gas chromatography/Mass spectrometry (GC/MS) is an important analytical method to provide characteristic information of molecular structure and as a quantitative tool with a high sensitivity and specificity. Gas chromatography/Mass spectrometry (GC/MS) combines two techniques for the separation and identification of the sample product. Gas chromatography (GC) provides a separation technique and mass spectrometry (MS) an identification technique (Watson, 1985). A mass spectrometer provides a useful analysis function that converts sample molecules into ions and then

separates the ions according to their mass-to-charge ratio. Such a process provides definitive qualitative and quantitative information on sample molecules, based on their molecular composition. Generally, the mass spectrometer has three basic functions; namely: (1) to ionize the substance; (2) to separate the constituent ions according to mass-to-charge ratio; and (3) to detect the relative abundance of the individual mass-to-charge fragments (i.e., ions) and record the mass spectrum of the substance.

There are a number of different ways to separate the ions of different mass-to-charge values, when the various mass-to-charge ions from the ionized samples are formed. The different types of mass spectrometers are: (i) magnetic-sector; (ii) double-focusing; (iii) transmission-quadrupole; (iv) quadrupole ion traps; (v) time-of-flight; and (vi) ion cyclotron resonance (Watson and Sparkman, 1996).

In the magnetic-sector mass spectrometer, ions with a positive unit charge are created from the sample that exists in the gas phase, at a pressure of about 10^{-3} or 10^{-5} Torr. The ions then are accelerated into a magnetic field. The magnetic field deflects the ions according to their mass and ions with a certain mass strike the detector.

The quadrupole mass spectrometer is the most generally used instrument for the separation of ions produced in the analysis systems such as gas chromatography/mass spectrometry (GC/MS) and liquid chromatography/mass spectrometry (LC/MS). Radio frequency (Rf) and direct current (dc) fields applied to opposing sets of four parallel surfaces are used to separate the ions of differing mass-to-charge ratios (m/z values) in the quadrupole mass spectrometry.

Mass spectrometers are used in both organic and inorganic chemistry. In organic mass spectrometry, the most widely used ionization technique for volatile compounds is

electron ionization (EI). This technique uses a beam of electrons at 70 eV to ionize the compound being analyzed and at the same time impart energy to the molecular ions that are formed. Some of the molecular ions then will fragment. Detection of the molecular and fragment ions produces the mass spectrum. Some molecular ions do not last long enough to be detected, because of unstable fragment ions. This introduces some difficulty with interpretation of the data.

In these cases, it sometimes is possible to employ chemical ionization (CI) to produce ions representative of the impact molecule. CI is often used in conjunction with EI to identity compounds. Nonvolatile ionization compounds such as sugars and peptides are analyzed using desorption ionization techniques.

A library search is an important procedure to identify a compound by comparison of its mass spectrum with a database of mass spectra of known compounds. Two of the most general data bases of mass search programs that provide electron ionization (EI) generated mass spectra for use on PCs are the NIST/EPA/NIH and the Wiley database (Watson and Sparkman, 1996). Interpretation of mass spectrum data is also used for identification of unknown spectrum, using information of the fragmentation of molecules related to structural elements.

Quantification based on GC-MS analyses, is usually determined using selective ion monitoring (SIM), because it is more sensitive than full scanning. However, it produces less information as only a limited number of ions are monitored. An SIM analysis is obtained for specific compounds and can increase the sensitivity by 50 to 500 times, as compared to total ion monitoring data (Watson and Sparkman, 1996). The mass spectrometer incorporating the SIM (selected ion monitoring) mode is equipped with a

peak selector to record selected ions characteristic of a compound of known identity. SIM analysis that has selected several mass ions of specific m/z values provides several advantages which include: (1) greater sensitivity due to more time at the few selected ions rather than total scanning; (2) shorter scan cycle times since only a few ions in the total m/z range need to be examined; (3) more accurate quantitation since a shorter cycle time allows the m/z range selected to be scanned more frequently; and (4) higher resolution of overlapping peaks in a complex sample by monitoring characteristic ions of each peak.

Dawson, *et al.* (1991) monitored headspace volatiles to evaluate the effect of adding glycerophosphorylcholine (GPC) and Glycerophosphorylethanolamine (GPE) on the oxidation of linoleic acid using GC/MS analysis that was set at 30-300 m/z scan range. Rosiers, *et al.* (1993) used the GC/MS method for the measurement of specific aldehydes, such as malondialdehyde, hexanal, and 4-hydroxynonenal, to evaluate the extent of lipid peroxidation. Selected ion monitoring was applied to GC/MS analysis in the positive chemical ionzation mode for malondialdehyde and 4-hydroxynonenal, and in the electron impact mode for other aldehydes (Rosiers, *et al.*, 1993). Hall, *et al.* (1985) studied the optimum model for describing the kinetics of the formation of hexanal in a dry milk sample, which was stored under air and which had a low concentration of Maillard reaction product during storage, and derived an expression to fit the experimental data obtained by GC/MS analysis. Buttery and Ling (1995) identified hexanal, which represented major MS ions, as the principle volatile flavor component present in tortillas by capillary GC/MS.

7. Isolation Techniques of Volatile Compounds Present in Food Systems

The off-flavor compounds related to various food products have a large number of different functional groups and chemical structures, which are derived from biochemical-metabolism or from external factors (Charalambous, 1992). Specifically, lipid oxidation leading to the unacceptability of a food product can be estimated by the development of unpleasant flavors. The major secondary oxidation products from linoleic acid, among a variety of fatty acids, are representative aldehyde type compounds, which include hexanal, pentanal, octenal, and decadienal etc. The aldehydes and vinyl ketones formed in the lipid phase of food products are mainly responsible for the off-flavors, due to their low threshold levels for human sensory response (Kochhar, 1993). Such volatile compounds are in low concentration and therefore must be concentrated from the food prior to instrumental analysis. The volatile compounds resulting from the oxidation of food products can be isolated by static headspace, dynamic headspace, or distillation-solvent extraction techniques (Reineccius, 1984). The headspace sampling techniques were found to give accurate data for the level of volatile compounds derived from a food product. Gas chromatography/Mass spectrometry is an excellent method for analysis of volatile compounds, due to the high resolution and sensitivity afforded by this method. The respective procedures are reviewed briefly below.

7-1. Static Headspace Analysis

For static headspace analysis, the headspace gases above a food sample, in a sealed container, are injected directly into a gas chromatograph for analysis of volatile compounds. The direct headspace sampling procedure has been widely used, due to the advantages of simplicity and rapidity. The direct headspace sampling procedure can reduce the loss of volatile compounds during opening of the container. Direct headspace sampling, however, also has the disadvantages of limited sample size, and less sensitivity than other procedures which involve sample concentration. This system is useful for measurement of oxidation at a particular time, as well as the extent of oxidation of foods. Mate, *et al.* (1996) used the static headspace method for nut samples, using gas chromatography, for analysis of hexanal resulting in oxidative rancidity at accelerated tests. Moreau and Rosenberg (1996) reported the analysis of hexanal to monitor for the oxidative stability of an anhydrous milkfat microencapsulated in whey proteins, using headspace methods. Leino (1992) identified the volatiles of fresh, frozen, freeze-dried, and air-dried chive samples, using a static headspace gas analysis procedure.

7-2. Purge and Trap System (Dynamic Headspace Analysis)

The purge and trap technique is a dynamic system designed to improve the low sensitivity faced by the direct headspace sampling system. The volatile compounds are purged from the sample by a stream of inert gas, such as nitrogen or helium, and are trapped with a cartridge tube filled with a sorbant, such as Tenax, Chromosorb or

activated charcoal. The volatile compounds are then desorbed from the sorption tube by rapid heating in a desorption system and are analyzed by GC or GC/MS. Sakakibara, *et al.* (1988) used activated charcoal to trap the volatile flavor compounds from the headspace of powdered dried bonito (katsuobushi) during storage. Luning, *et al.* (1994) studied the differences in flavor of fresh green and red bell peppers, using Tenax sorption to first sorb and then desorb the volatile flavor compounds by a dynamic headspace technique. Hall, *et al.* (1985) analyzed quantitatively for compounds with higher boiling points, such as the headspace concentration of hexanal, by the dynamic purge and trap method. Hall, *et al.* (1985) reported the use of Chromosorb 105 for adsorbing volatile compounds from a dry milk sample, with fat content of 23.8-24.5 % and containing various antioxidants, by the dynamic headspace sampling system. The purge and trap system has a higher sensitivity for analyses involving trace levels of volatile compounds. However, there are some disadvantages with this procedure, such as: (i) breakdown of the very volatile compounds due to high temperature during thermal desorption; (ii) low recovery of high boiling point compounds; and (iii) transfer of water from a product sample with a high moisture content to the chromatography column. The conditions of the purge, trap, and desorption steps must be controlled to optimize the sensitivity according to the volatile compounds and analytical system. A Tenax trap is very widely used for trapping of volatile compounds. Tenax has a low affinity for polar compounds and a high affinity for nonpolar compounds (Reineccius, 1993).

7-3. Distillation System

The distillation system includes a high vacuum molecular distillation, stream distillation, or simple heating of the food and taking the distilled aroma constituents into the analytical apparatus (Reineccius, 1993). Stream distillation has two general types. One type of distillate system involves isolation of product volatiles with a rotary evaporator. The other is a more complex simultaneous distillation/extraction procedure (SDE), based on the apparatus of Likens and Nickerson (1964). This system is most commonly used for extraction of flavors today. Both approaches require distillation and solvent extraction.

Most of the volatile compounds in food products are isolated by simultaneous distillation/extraction. The distillation/extraction method, when compared to headspace techniques, has the advantages of greater extraction efficiencies of high boiling point substances and higher concentrations to allow identification by GC/MS. The Likens and Nickerson method also has the disadvantages of the potential destruction of volatiles during distillation, and loss of volatiles during concentration. Beal and Mottram (1994) examined the off-odor compounds of malted barley, sampled as a function of storage time, by GC analysis of the volatile isolates using a simultaneous distillation/extraction procedure (a modified Likens and Nickerson apparatus). Chung and Cadwallader (1994) reported the use of simultaneous steam distillation and vacuum simultaneous steam distillation-solvent extraction techniques for volatiles extracts from cooked blue crab (*Callinectes sapidus*) claw meat. These extracts were analyzed by gas chromatography/olfactometry for odor activity.

MATERIALS AND METHODS

3-1. Product Model

A product model was designed to simulate a low moisture content, fatty acid-containing food product, such as a cereal product or snack food. As formulated, the product model had a uniform thickness, density, moisture content, and surface area. Product model ingredients included linoleic acid, to provide the substrate for lipid oxidation, distilled and deionized water (Mallinckrodt Baker Inc., Paris, Kentucky), Tween 20 (Fisher Scientific, Pittsburgh, PA), and sodium carboxymethycellulose (CMC) (Aqualon Co., a division of Hercules Inc. Hopewell, VA). Linoleic acid is an unsaturated fatty acid that has two-double bonds at the 9 and 12 carbon positions in the eighteen-carbon chain (18:2). Generally the main source of linoleic acid is vegetable oils such as soybean, sunflower, cottonseed, and corn oils. The linoleic acid for the product model was obtained from Acros Organics (99%, $C_{18}H_{32}O_2$, FW 280.45, Fisher Scientific, Pittsburgh, PA). CMC, as cellulose gum, is an anionic water-soluble polymer derived from cellulose. The main function of CMC is the binding of water, or to increase the viscosity of an aqueous system. The main applications of sodium carboxymethylcellulose are as a stabilizing agent in ice cream, and as a high water binding agent of dietetic foods (Dreher, 1987). Tween 20 (polyoxyethylene-20-sorbitan monolaurate) is an emulsifier which promotes mixing between water and oil. The ingredients and uniformity of the mixture were based on a similar product model

described by Berends (1993). The composition of the product model formulation is summarized in Table 2 of the Results and Discussion Section.

Linoleic acid, Tween 20, and distilled and deionized water were mixed with a homogenizer (Model K5-A, Hobart, Kitchenaid), operated at a level 4 on the speed control. Sodium carboxymethylcellulose was slowly added to the aqueous mixture. The mixed ingredients were homogenized for approximately 10 minutes, or until the formation of a uniform product that contained a constant moisture content. Samples of the uniformly mixed product were added to a depth of approximately 15mm thick into plastic petri dishes (100 x 15mm size). The petri dishes were weighed and tared before adding the product samples and applying the petri dish covers. The sample products in the petri dishes, covered by a paperboard box, were placed into a freezer (-30°C) for freezing over a 24 hour period. The frozen products were placed in a laboratory freeze drier (Vitris Model II, Repp Industry, Gardiner, NY), after the petri dish covers were removed. The operating conditions of the freeze-drier were 100 micro torr at -50°C, with a plate temperature of -38°C. The frozen product samples were dried for 5 days. The completely dried products were immediately covered with petri dish covers, weighted, and placed in a paperboard carton. The freeze-dried product was then stored in a conventional freezer (- 30°C), until samples were required for characterization and stability studies. For storage stability studies, samples were prepared by placing the homogenized product to a depth of 15mm thick into 60 x 15mm size aluminum weight dishes and then freeze drying the product samples as described above.

3-2. Packaging Materials

Three coextruded laminate films were used to fabricate the flexible pouches to be evaluated in this study. All of the films contained a heat seal layer (Suryln-EVA) coextruded to a high density polyethylene (HDPE) layer. The primary difference between the three test films was in the nature and level of antioxidant incorporated within the heat seal layer. Film I contained α-tocopherol in the heat seal layer, film II contained 3,5-di-tert-butyl-4-hydroxytoluene (BHT) in the heat seal layer, and film III had no antioxidant in the heat heal layer. Film samples were obtained from the James River Corporation (Flexible Packaging Group, Cincinnati, OH). The average thickness of the test laminate films was measured using the Model 549 micrometer of Testing Machines, Inc (Amityville, L.I., NY). The average thickness and the thickness measurements of each film are summarized in Table 24. Each side of the film samples was identified by Fourier Transform Infrared Spectroscopy (Perkin Elmer Model 1000). The results obtained for each film are presented in Appendix E. The concentration levels of the antioxidants in the film structures were determined by high pressure liquid chromatography (HPLC) analysis. The antioxidant concentration levels determined for the film structures are presented in Table 11.

3-3. Initial Moisture Content

The initial moisture content of the model product system was determined using a modified vacuum-oven method performed on the freeze-dried samples. This method was based on a similar product model described by Berends (1993) and is described in Section 28 of the Official Method of Analysis of the Association of Official Analytical Chemists (1975). The freeze-dried samples were added to tared aluminum weighing dishes (50 x 15mm) and weighed. The samples in the aluminum weighing dishes were then placed in the vacuum oven and the samples maintained at 30mmHg and 90°C for eight hours. The samples were placed in a desiccator for 1 hour to allow equilibration to room temperature after removing them from the vacuum oven. The samples were then reweighed. The initial moisture content of the samples was calculated using the average data.

The initial moisture content was obtained using the following equation:

$$\left(\frac{Wi - Wf}{Wf}\right) \times 100 = \%IMC \ (on \ dry \ weight \ basis) \quad \text{-------} (10)$$

where; Wi = initial weight of product sample (grams)

Wf = final weight of product after drying (grams)

The results for the determination of the initial moisture content of the sample are summarized in Table 4 of the Results and Discussion Section.

3-4. Sorption Isotherm

A sorption isotherm was developed to determine the Equilibrium Moisture Content (EMC) of the model product at different water activities (Aw). A series of salt solutions were prepared using the procedure described in Hygrodynamics Technical Bulletin No. 5 (Creating and Maintaining Humidities by Salt Solutions) and placed in eight tightly sealed recloseable 5 gallon high density polyethylene buckets, thus creating a series of constant relative humidity environments. The buckets were allowed to equilibrate for two weeks before the test began. The relative humidity inside the buckets was monitored with a hygrometer sensor (American Instrument Company, Silver Springs, MA) mounted in the plastic lid. Freeze-dried product was taken immediately from the petri dish and weighed on an analytical balance into tared aluminum weighing dishes. Three replicate samples, in aluminum weighing dishes, were then placed into each relative humidity storage bucket. Isotherm data were obtained gravimetrically by measuring product weight change over five day intervals, at a constant relative humidity and temperature. Isotherm data were obtained when the freeze-dried model product system reached an equilibrium weight, at each test condition. All humidity conditions inside the storage buckets were shown to be constant over the course of the experiment, as indicated by the readings from the hygrometer sensors installed in the respective relative humidity buckets. The storage temperatures were 18, 28, and 38°C, respectively. Isotherm results were obtained from the average of triplicate data values. The conditions

of relative humidity and the salts used to obtain the specific relative humidity are presented in Table 26.

The equilibrium moisture content (EMC) was calculated according to the following equation:

$$\left(\frac{Pf\,(1+IMC)}{Pi}\right)-1\times100 \;=\; \%EMC \;\; (on \;\; dry \;\; weight \;\; basis) \qquad \text{-------(11)}$$

where; P_f = final weight of product sample after equilibration

P_i = initial weight of product sample

IMC = gH_2O/g dry weight product

3-5. Moisture Equilibration System of Product Model

The freeze-dried product model system was equilibrated to a constant water activity (A_w = 0.30) under a nitrogen atmosphere, to retard lipid oxidation prior to initiating the storage stability studies. A dynamic flow procedure was developed, which is described below.

A multi-chamber test system was designed to equilibrate the freeze-dried product model to a fixed and constant relative humidity at constant temperature. The test chambers consisted of stainless steel desiccant chambers of dimensions, 30.5cm x 28cm x 31cm (length x width x height). Each chamber was equipped with seven open metal-link shelves with a 30mm interval between, to allow the exposure of multiple product samples under constant conditions. Each test chamber was also equipped with a gas inlet and

outlet port to provide continuous flow of the humidified nitrogen gas stream. A schematic diagram of the equilibrium system is given in Figure 4. The flow rate of the humidified nitrogen gas into the inlet port of the chamber was set at 30ml/min. Equilibration conditions in the test chambers were carried out at 23 $\pm$1°C. A constant concentration of water vapor to be flowed continually through the respective exposure test chambers was produced by bubbling nitrogen through a gas washing bottle, which contained distilled-deionized water, with a fritted dispersion tube. To obtain the required relative humidity, the humidified gas stream was mixed with another stream of dried carrier gas (nitrogen). Flow meter settings were determined to provide the desired relative humidity value of approximately 30% RH. A hygrometer sensor (model No.1243, American Instrument Company, Silver Spring, MA) was incorporated into the system design to allow continuous monitoring of the relative humidity of the gas stream, over the course of the equilibration process. The moisture equilibration system for the product model is shown in Figure 5.

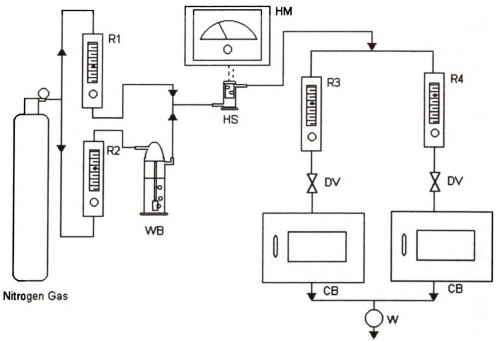

R1: rotometer of dried gas
R2: rotometer of humidified gas
R3, R4: rotometer of controlled gas
WB: water bubbler
W: exit of gas flux

CB: controlled chamber
HM: hygrometer indicator
HS: hygrometer sensor
DV: needle valve

Figure 4. A schematic diagram of the equilibrium system

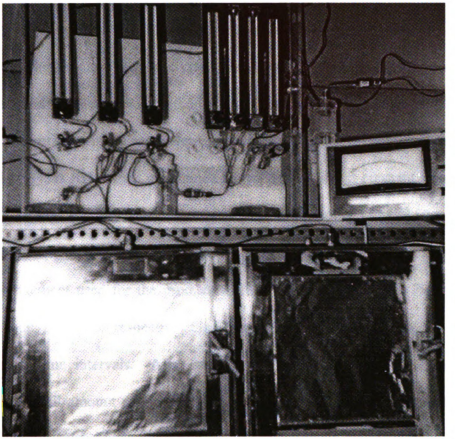

Figure 5. The moisture equilibration system for product model.

3-6. Product Stability Studies

A known amount of the model food system (approximately 6 gm) was packaged in 4.5" x 5" test pouches, fabricated from the three test films. The pouches were sealed by an impulse heat sealer (Sencorp Systems Inc.) at 35psi with a 0.9second heating time and a 0.4second cooling time, and then stored in an environmentally controlled room. The conditions of the storage room were selected to maintain the packaged product at 23 $\pm$ 2°C and 50 $\pm$ 5% RH, which maintained the product model at constant water activity. Accelerated storage stability studies were also performed at 45 $\pm$ 1°C and 50 $\pm$ 5% RH in a controlled chamber (Hotpack corp. Philadelphia, PA). A schematic diagram of the storage arrangement used for the product stability studies is shown in Figure 6. Test pouches made from the respective film structures were removed from storage at predetermined time intervals. After sampling the pouches, the product model was removed. A small amount of the product model was used for the hexanal analysis to determine the extent of lipid oxidation. The pouch structure was assayed to determine the relative concentration of antioxidant retained as a function of the storage time, at given environmental conditions. Samples were stored and assayed for hexanal levels, as a function of storage time and temperature and product oxidation rates compared to the other test samples. A flow diagram of the test scheme is shown in Figure 7.

(23°C, 50 % RH)

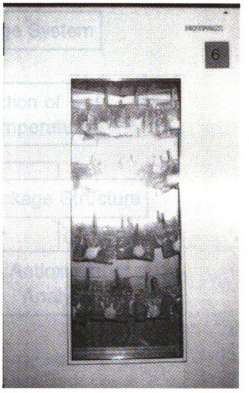

(45°C, 50 % RH)

Figure 6. The storage arrangement of the pouched model product at 23°C, 45°C.

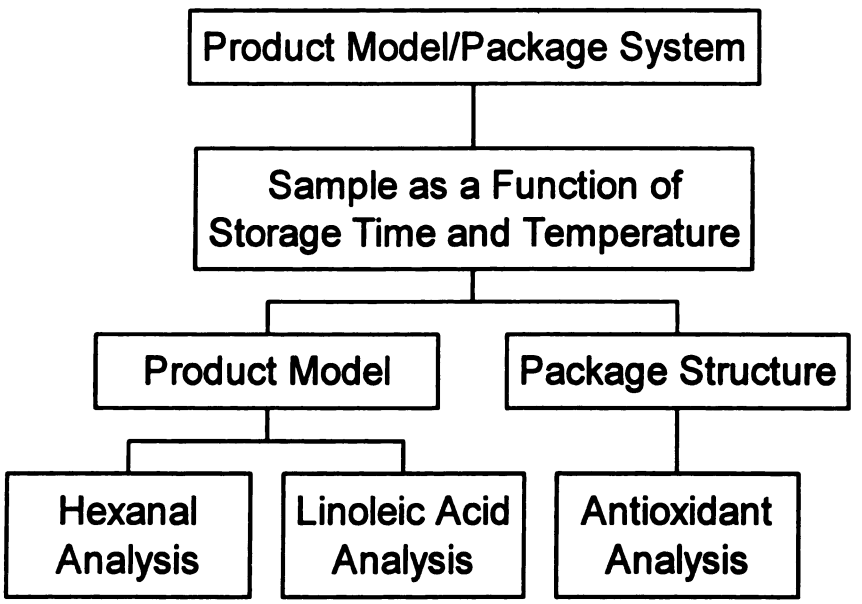

Figure 7. Flow diagram of the test scheme.

3-7. Analytical Procedure for Antioxidants in the Packaged Films

3-7-1. Soxhlet Extraction System

A soxhlet extraction apparatus was used to extract the antioxidants from film samples obtained either directly from roll stock or from the fabricated pouches, as a function of storage time and temperature. About one gram of the film was weighed and cut into pieces approximately 1cm x 1cm. The film samples were transferred to the extraction thimble and were extracted with 100ml of acetonitrile solvent for 24 hours. After cooling, the extracted solutions were transferred to 100ml volumetric flasks and brought to volume with acetonitrile (99.9%, HPLC grade solvent, EM science). A 10ml aliquot of the respective extraction solution was filtered using microfilter (0.45μ, HV, Millipore Corp.) and transferred to 4ml glass vials (Supelco Inc, Bellefonte, PA) with screw caps (Supelco Inc, PA) and PFTE covered septum (Waters, Millipore Corp., MA), which were designed for the auto-sampling system of the high pressure liquid chromatograph.

3-7-2. Percent Recovery of Antioxidants for Extraction System

The determination of antioxidant recovery was defined as the percentage loss of antioxidants from the extraction system. Sample solutions of each antioxidant were prepared by weighing about 0.02 gram of BHT or α-tocopherol and the weighed sample transferred to a 200ml volumetric flask with acetonitrile solvent.

The concentration of the respective antioxidants was determined by HPLC analysis. The area response of the antioxidant solution (i.e. control) obtained from HPLC analysis was used as a basis for determining the percent recovery.

The antioxidant solutions were carried through the soxhlet extraction procedure, with no film added to the extraction thimble. Here, 100ml of the antioxidant solution, of known concentration, were transferred to the soxhlet extraction system. The conditions of the extraction procedure were similar to those described for the extraction procedure for the test films. Following the extraction period, the extraction solution was transferred to a 100ml volumetric flask, made up to volume and assayed for antioxidant concentration by HPLC. The area response obtained from the extraction solution was compared with the area response of the initially prepared antioxidant solutions. The percent recovery test of each antioxidant was performed in triplicate.

3-7-3. High Pressure Liquid Chromatography (HPLC) Analysis

Quantification of antioxidant levels in the test films following Soxhlet extraction was determined by a HPLC procedure. Analyses were carried out on a Waters Model 150-C ALC/GPC equipped with a Waters 486, Tunable Absorbance Detector and interfaced to a Waters Model 730 Data Module. The chromatographic conditions were as follows:

The mobile phase for BHT analysis was Methanol (85%) and Water (15%) by volume, while pure Methanol (99.9%, HPLC grade solvent, J.T.Baker Inc.) was the mobile phase for the analysis of α-tocopherol. Absorbance was recorded at 280nm. A HPI C18 (Delta- Pak™, Waters Corporation, Milford, MA) column, 3.9mm x 150 mm length, was used for analysis. The volume of injected sample from the 4ml single vials was 20 μl. The flow rate of the mobile phase was 1 ml/min; the total run time of one sample was 6 minutes at room temperature. The retention time for BHT was 3.58 minutes. The retention time for α-tocopherol was 4.5 minutes. Typical peak profiles of the BHT and α-tocopherol solution, obtained from the integrator are shown in Figures 39 and 40, respectively. The sample compounds were detected with the UV detector set at 280nm wavelength. The detector sensitivity was set at 0.03 AU; the filter of the detector was set at 0.1 seconds. The integrator (Water, Data Module Model 730) interfaced to the detector had a chart speed of 0.8 cm/min. The integrator conditions were set at 5 for peak width; 15 for noise rejection; and 100 for area rejection.

α-Tocopherol ($C_{29}H_{50}O_2$, MW 430.72) from Eastman Kodak Company (Rochester, New York) was used for preparation of standard solutions for calibration. BHT ($C_{15}H_{24}O$, MW

220.35) was obtained from the Eastman Chemical Company (Kingsport, TN). The antioxidants (BHT, d-α-tocopherol) were quantified by peak area, by comparison to a external standard calibration curve which was constructed, using a serial dilution procedure with concentrations of 2, 4, 6, 8, 10ppm (w/v). The calibration data of each standard antioxidant solution are presented in Figure 37 for BHT and in Figure 38 for α-tocopherol.

The level of antioxidants extracted from the films was determined by substitution into the following equation:

$$\%\ Antioxidant\ (w/w) = \left(\frac{(Rs \times C.F. \times Vtotal)}{(Vinj \times Wtfilm)}\right) \times 100 \qquad \text{-------} (13)$$

where: Rs = detector response values for the sample (A.U.)

V_{total} = total volume of solution (ml)

V_{inj} = volume of unknown solution injection (ml)

C.F. = calibration factor from the standard calibration curve (g/A.U.)

Wt_{film} = the tested film weight (grams)

4. Analytical Test for Lipid Oxidation in the Model Product

4-1. Linoleic Acid Analysis

4-1-1. Extraction

Linoleic acid in the model product system was extracted with chloroform/methanol (2:1, (v/v)) at a ratio of 20:1, solvent to sample, as described by Nelson (1991). A 3g sample of the model product system was cut into small pieces. The test sample was placed into a 500ml separatory funnel. Chloroform (100ml, Mallinckrodt Chemicals Co., Paris, Kentucky) was added to the sample and the mixture shaken slowly for 1 minute; 50ml of methanol (99.9%, HPLC solvent grade, J.T.Baker, Phillipsburg, NJ) were then added and the mixture shaken again for 1 minute. After mixing, the solution was stored in the separatory funnel for 4 hours at room temperature. The chloroform-methanol solution from the separatory funnel was collected into a 250ml volumetric flask. After collecting the chloroform-methanol solution from the test sample, 50ml of fresh chloroform were added to the separatory funnel and then 25ml of methanol were added. The second mixture was shaken for 1 minutes and stored in the separatory funnel for 4 hours at room temperature. The second extraction solution was collected, added to the initial extraction solution in the volumetric flask and evaporated to dryness using a dried nitrogen gas stream for 28 hours.

4-1-2. Preparation of Methyl Esters

The preparation of methyl esters of fatty acids for capillary gas chromatography analysis has been reported by several researchers (Slover, 1979; Luddy, 1968; Morrison, 1964), to obtain a rapid and quantitative analysis.

To the residue remaining, following concentration to dryness, was added 1ml of boron fluoride-methanol reagent (10% methanol, Supelco Inc, Bellefonte, PA) as an acidic catalyst for the methylation of linoleic acid. The volumetric flask was then closed tightly with the cap using a Teflon and paraffin sealing tape. The flask was heated in a boiling water bath for 2 minutes and then cooled to room temperature. Methanol (249ml, 99.9%, HPLC grade solvent, J.T.Baker Inc.) was added to the volumetric flask (250ml), and a 1μl sample of this solution was injected with a 5μl (series 800) syringe (Hamilton Co., Reno, Nevada) directly into the gas chromatograph, for analysis of the methyl ester of linoleic acid. A Hewlett-Packard Model 5890A gas chromatograph equipped with dual flame ionization detectors and a fused silica capillary SPB-5 nonpolar column (30m x 0.32mm ID) was employed (Supelco Inc., Bellefonte, PA). The GC conditions were as follows. The column temperature was programmed from the initial stage of 150°C for 4 minutes to the final stage of 220°C for 8 minutes at the rate of 5°C/min. Helium was used as a carrier gas, at a flow rate of 2.2ml/min. Injector temperature, 220°C; and detector temperature, 250°C.

Standard calibration solutions were prepared using a serial dilution procedure with 14, 20, 27, and 34 n mole concentrations of trans-9, 12 –octadecadienoic methyl ester (methyl linoleate) with chloroform (99.9%, Mallinckrodt Chemical Co., Paris,

Kentucky). Trans-9, 12–octadecadienoic methyl ester was obtained from the Supelco Company (Bellefonte, PA). The data obtained for standard calibration of trans-9, 12–octadecadienoic methyl ester is shown in Figure 42. The retention time of trans-9, 12 – octadecadienoic methyl ester was 18.7 minutes.

The level of linoleic acid in the model product was calculated by substitution into the following equation:

(Rs x C.F.(mole/Rs) x Vt (ml)) / Vi (ml) = mole ester ------- (i)

1 mole acid with mol. wt acid equals 1 mole ester with mol. wt ester ------- (ii)

From the Equation (i) and (ii):

Concentration of linoleic acid (mole/gram product)

$$= \frac{(Rs \times C.F. \times Vt)}{(Wtsample \times Vi)} \qquad \text{------- (14)}$$

where: Rs = detector area response values for the sample (A.U.)

C.F. = calibration factor from the standard calibration curve (mole/A.U.)

Wt_{sample} = the tested sample weight (grams)

Vt = the tested total volume (ml)

Vi = injection volume (ml)

mol. wt acid = Linoleic acid ($C_{18}H_{32}O_2$) = 280.46 (FW)

mol. wt ester = Linoleic acid methyl ester ($C_{19}H_{34}O_2$) = 294.5 (FW)

4-1-3. Percent Recovery of Linoleic Acid through Extraction and Methylation

The percent recovery of linoleic acid was determined by performing the extraction and methylation procedures with a known amount of linoleic acid. A weighed amount of pure linoleic acid (99%, Acros Organics, Fisher Scientific) was used for quantitative analysis. A 1μl volume from the methyl ester solution was injected directly into the gas chromatograph for analysis. The area response obtained by GC was applied for calculation of the amount of linoleic acid.

The amount of linoleic acid obtained by GC analysis was used to determine the percent recovery, where the determined value is compared with the amount of the original weighed linoleic acid. Injections of GC analysis were done in triplicate.

4-2. Hexanal Analysis

4-2-1. Apparatus for Trapping of Hexanal Compound (A Dynamic Purge and Trap System)

A dynamic purge and trap system was designed for headspace sampling of volatiles from the model product system. Erlenmeyer flasks of a 250ml size were modified with 29/42 standard taped male joints, to fit the dispersion tube assembly of a gas washing bottle (Stopper assemblies for Corning 31770 gas washing bottles, Fisher Scientific, Pittsburgh, PA). Modification of the dispersion tube assembly of the gas

washing bottles and the Erlenmeyer flasks were performed by the Glass Blowing Shop of the Chemistry Department at Michigan State University. A schematic diagram of the dynamic purge and trap system is shown in Figure 8. A modified Erlenmeyer flask was interfaced to a flow meter and needle valve assembly, connections were through 1/8" O.D. copper tubing and swagelok fitting. A constant rate of flow of nitrogen gas was controlled by the flow meters.

An amount of the model product system (approximately 6 gm), was removed from the packaged pouch, weighed and placed into a modified Erlenmeyer flask (250ml) equipped with an inlet and outlet port. The inlet port of the dispersion head was connected to a flow meter and needle valve (Nu Pro type B-25G) to regulate the flow of nitrogen gas. The sorption trap was connected to the exit port of the dispersion head via swagelok adapters. The dispersion head exit port of 8 mm O.D. glass tubing was connected by a 5/16" swagelok nut and a series of reducing adapters to a 1/4" male swagelok fitting. The sorption trap was mounted to the dispersion head with a 1/4" thumb wheel swagelok fitting (Supelco Inc., Bellefonte, PA) for easy removal and could be affixed to both glass and metal desorption traps. Figures 8 and 9 show the trapping cell and the complete purge and trap system. The glass thermal desorption tubes (Carbotrap 300, 6mm I.D. x 4mm I.D. x 11.5cm) used in the present study were prepacked by Supelco Inc. (Bellefonte, PA). The trapping tubes were packed with 300μg of Carbotrap C absorbent, 200μg of Carbotrap B absorbent and 125μg of Carbosieve S-III absorbent. Nitrogen was flowed through the assembled purge and trap system at room temperature to remove oxygen from the system prior to heating. After one hour, the water bath (Blue M Constant Temperature Bath, Blue Island, IL) was turned on and

allowed to heat for one hour to reach 50°C. The modified Erlenmeyer flasks were then placed in the water bath and the system purged for 24 hours. Repetitive analyses of the model product showed no additional hexanal detected. Each sample was analyzed in triplicate.

The thermal desorption unit (Model 890, Dynatherm Analytical Instruments, Inc supplied by Supelco, Bellefonte, PA) conditions were as follows:

Helium was used as the carrier gas with a flow rate of 7.5ml/min. at 40psi.

The desorption temperature was set at 250°C for 6 minutes; The temperatures of the valve and transfer line were set at 230°C: The conditioning temperature for cleaning the sorption tubes, prior to reuse, was 280°C for 30 minutes.

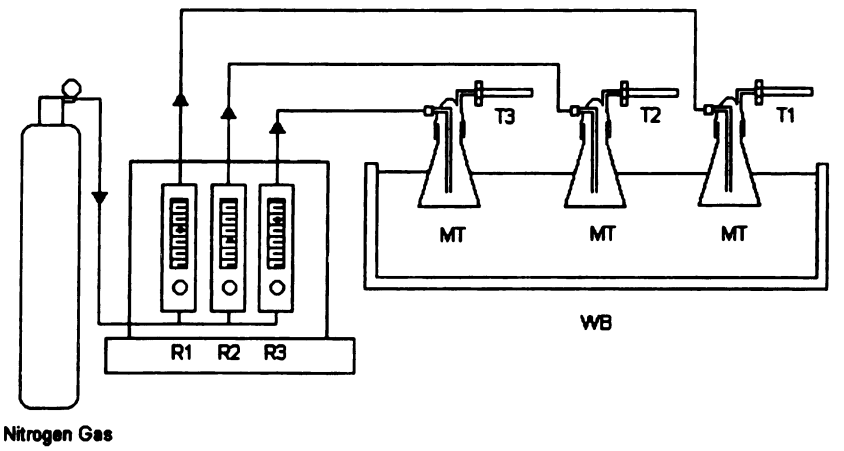

R1, R2, R3 : rotometers MT : modified Erlenmeyer flasks
T1, T2, T3 : trapping tubes WB : water bath

Figure 8. A schematic diagram of the dynamic purge and trap system

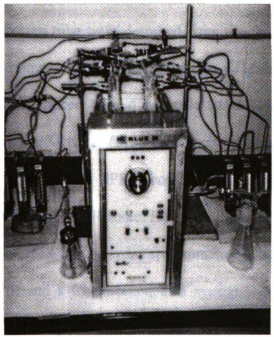

(Dynamic and trap system)

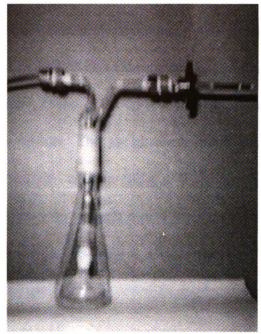

(Trapping cell apparatus)

Figure 9. A Dynamic and trap system for the model product

4-2-2. The Analysis Procedure of Hexanal Compound

The levels of sorbed hexanal were quantified by a gas chromatography-mass spectrometry (GC/MS) procedure. Volatile compounds including hexanal, sorbed on the carbotrap tube were desorbed from the thermal desorption unit (Dynatherm Analytical Instruments, Inc.) and transferred to a Hewlett-Packard 5890 Gas Chromatograph, which was interfaced to a quadrupole mass spectrometer (Model HP 5970) with a Mass Selective Detector (MSD) and a chemstation data system. The gas chromatograph was equipped with a SPB-5 non-polar fused silica capillary column (60m x 0.32mm ID, Supelco Inc., Bellefonte, PA). The level of hexanal in the product model was analyzed by GC/MS using a mass spectrometer (Model HP 5970) interfaced to a GC (Model HP 5890) and a Chemstation data system. The conditions of Gas chromatography/Mass spectrometry analysis for hexanal were as follows:

The initial temperature was set at 40°C for 6 min; the temperature was then raised at 5 degree/min; and the final temperature and time were held at 200°C for 10 minutes. Helium was used as a carrier gas, with a flow rate at 10 ml/min. The solvent delay was 5 minutes, and the cycles per second were 1.70. The temperature of the injection port was set at 220°C. The temperature of the transfer line between the gas chromatograph and the mass spectrometer was set at 250°C.

The total ion chromatogram peaks, or the individual ion profiles were integrated, based on the integrator events that were set up with 0.2 as the peakwidth and 14 as the threshold. The electron multiplier voltage was 2600eV.

Calibration of the GC/MS system, for quantitative analysis of hexanal, was performed by direct injection of 1μl of known hexanal standard solutions onto the carbotrap tube. Hexanal standard solutions of known concentration were prepared by a serial dilution procedure with methanol. Hexanal for the standard calibration was obtained from the Aldrich Chemical Company, (98% grade, Milwaukee, WI). The hexanal external standard calibration data by GC/MS are shown in Figure 43.

4-2-3. Mass Spectrometer

The gas chromatograph (Model HP 5890, Hewlett Packard, Avondale, PA) was interfaced to a quadrupole mass spectrometer (Model HP 5970) with a Mass Selective Detector (MSD). The analysis of hexanal by the GC/MS system was carried out with the Chemstation (Model HP 5970), at an ionization energy of 70eV. The analysis of hexanal was performed using a gas chromatograph/mass spectrometer at the Mass Spectrometer Laboratory in the Department of Biochemistry at Michigan State University. The desorbed compounds from the thermal desorption system were separated by gas chromatography with helium carrier gas. A library search for the identification of hexanal by the mass spectrometer was performed with the NIST Mass Spectral Search program. Autotuning was employed when operating in the election impact mode, using perfluorotributylamine (PFTBA) as the tuning compound. An ion group, containing five selected ions, identified from the hexanal library search, namely 29, 44, 56, 72, and 100 m/z, was used for quantification.

The total ion chromatogram of the five selected ions in SIM was used for the quantification of hexanal. The ratios of the selected ions from the mass spectrum were identified for qualitative identification of hexanal, by comparison with the standard hexanal mass spectrum from the library search. The retention time of the chromatographic ion peak in SIM also supports the identification of hexanal, when compared with the retention time of the external hexanal standard. The calibration data for the standard hexanal relations is presented in Table 58. The retention time for hexanal from SIM analysis was 8.5 minutes.

The concentration of hexanal in the product model was determined in duplicate for each time interval. The hexanal level of the product model was calculated by substitution into the following equation:

$$Hexanal\ \ level\ \ (mole/g)\ =\ \left(\frac{(Rs \times C.F.)}{(Wtsample)}\right) \qquad \text{------- (15)}$$

where: Rs = detector response values for the sample (A.U.) obtained by GC/MS

C.F. = calibration factor from the standard calibration curve (mole/A.U.)

Wt_{sample}= the tested sample weight (grams)

4-2-4. Percent Recovery of Hexanal through a Dynamic Purge and Trap System

The percent recovery study was carried out to determine the percentage loss of hexanal from the dynamic purge and trap system. A sample solution of hexanal, of a known concentration level in methanol, was added directly to the carbotrap glass tube. A 1μl aliquot of the sample solution was injected into the top section of the carbotrap glass tube. The carbotrap glass tube was then transferred to the thermal desorption unit interfaced with the GC/MS system for hexanal analysis. The area response obtained from a sample of known concentration using the GC/MS analysis was used as a basis for determining the percent recovery. An aliquot containing hexanal of the same concentration level as used above was carried through the dynamic purge and trap system. A 1μl sample of hexanal solution of known concentration was transferred to the erlenmeyer flask of the dynamic purge and trap system. The carbotrap glass tube was installed and the hexanal adsorbed by a constant flow of nitrogen gas for 24 hours at 50°C in the waterbath, after flushing at room temperature for 1 hour. The carbotrap glass tube was then transferred to the thermal desorption unit interfaced with the GC/MS system for hexanal analysis. The area response obtained by a dynamic purge and trap system was used to determine the percent recovery by comparison with the area response obtained from the carbotrap tube by direct injection. This percent recovery test was performed in triplicate.

RESULTS AND DISCUSSION

4-1. Product Model

Two model product systems were prepared, which were formulated with high and low levels of lipid content. The product formulations are summarized in Table 2. The model product systems were characterized by the relationship between water activity and moisture content in the product. The effectiveness of antioxidant-impregnated laminate film was determined by studying the oxidation of linoleic acid in the model product with time. For these studies, model product system (B)(low loading level of lipid) was used.

Table 2. Components of the model product (A, B) on a wet weight basis

	Model Product (A)		Model Product (B)	
Components	Weight (g)	% (w/w)	Weight (g)	% (w/w)
Linoleic Acid	40.59	4.06	3.6	0.36
Tween 20	0.11	0.01	0.11	0.01
CMC	130	13	130	13
Deionized water	829.3	82.9	866.29	86.63
Total	1000	100	1000	100

The composition of the model product, on a wet weight basis, is shown in Table 2. The weight of the model product, on a dry weight basis, was based on the sample weight after freeze-drying. The weight percent of the linoleic acid in the test product, on a dry weight basis, was determined after freeze-drying. Summarized in Table 3 are the weight percentages and actual weight values for linoleic acid for the product B formulation samples on a wet basis, following freeze drying, sample weight following equilibrium to

30% RH and the sample weight typically used for the purge and trap analysis for hexanal concentration.

Table 3. The percent of linoleic acid in model product (B) calculated.

Product sample	Sample weight (g)	% of linoleic acid (w/w)
Wet basis	33.7501	0.36
Dry basis	5.6143	2.2
Equilibrated To 30% RH	5.8422	2.1
Test weight	0.1737	2.0797

The initial concentration of linoleic acid in the model product (B) following equilibrium at 30 percent relative humidity was estimated at 0.021(g/g), based on the initial product composition (i.e., wet basis). The initial moisture content (IMC) of the product formulations was determined on the freeze-dried samples. Freeze dried samples were also used to construct sorption isotherms for the respective product formulations.

4-2. Initial Moisture Content

The initial moisture content was determined and an equilibrium sorption isotherm was developed to describe the relationship between Aw and moisture content of the model product. The results of the initial moisture content for model products A and B are tabulated in Table 4. The analysis was carried out in triplicate. The initial moisture content (IMC) of the freeze-dried products was determined by a gravimetric method and was obtained by substitution into Equation 14 of the Material and Method section.

Table 4. The initial moisture content of freeze-dried model products A and B.

	(gH_2O/100g dry basis product)	
	Model Product (A)	Model Product (B)
IMC (%)	3.46 ± 0.25	3.63 ± 0.22

All values are the average ± standard deviation of three replicated samples.

The initial moisture content values for each model product were 3.46 (A), and 3.63 (B) gH_2O/100g dry product, respectively. The calculations of experimental data are given in Appendix A.

4-3. Equilibrium Sorption Isotherm

The relative humidity levels for the respective test chambers were monitored with a hygrometer (Troller and Christian, 1978) and were found to be in good agreement with those reported by Rockland, *et al.* (1980) and Labuza (1976). A constant weight of the model products was obtained at each relative humidity condition, at three different temperatures.

Values for the equilibrium moisture content and the associated relative humidity values for the freeze-dried product, determined at 18, 28, and 38°C are summarized in Tables 5 - 7 (model products A) and Tables 8 - 10 (model products B), respectively. The equilibrium sorption isotherms for the obtained sorption data are plotted in Figures 10 - 13 (model products A), and Figures 14 – 17 (model products B), respectively. The calculations for the equilibrium sorption isotherms are included in Appendix A (see Tables 26 to 31, respectively).

The equilibrium sorption isotherms of the model products (A, B) showed the typical sigmoid shape at each test temperature. The equilibrium sorption isotherms, at increased temperature, also showed a slightly higher water activity at the same moisture content for the model product.

The equilibrium sorption isotherms of the model products (A, B), as represented by the relationship between moisture content and water activity, provided data which allowed for characterization of the model product, as well as for the selection of storage conditions for the product stability studies.

With respect to the equilibrium sorption isotherms obtained for the model product system, a series of equations developed to describe the characteristic geometric configuration of sorption isotherm shapes were evaluated to select the best-fit model. A detailed description of the isotherm expressions evaluated and the mathematical treatment followed is presented in Appendix B. The linearized plots of the best-fit model are also presented graphically in Appendix B (see Figures 25 to 30, respectively).

For all cases, the mathematical equation that best described the sorption isotherm of the model products was the Halsey equation, except for model product B at 38°C, which was best described by the Henderson equation. The monolayer moisture content at each temperature was 8.57 (18°C), 9.12 (28°C), and 8.38 (38°C) for model product containing high linoleic acid levels and 9.88 (18°C), 9.84 (28°C), and 9.23 (38°C) (g H_2O/100g dry product) for model product containing low linoleic acid levels.

Table 5. The Equilibrium moisture content for the freeze-dried product (A) as a function of water activity, at 18°C.

Water Activity	Average EMC (%)
0.096	8.1504
0.214	10.8778
0.355	13.2473
0.46	15.5210
0.56	19.0749
0.745	30.1573
0.805	35.9295

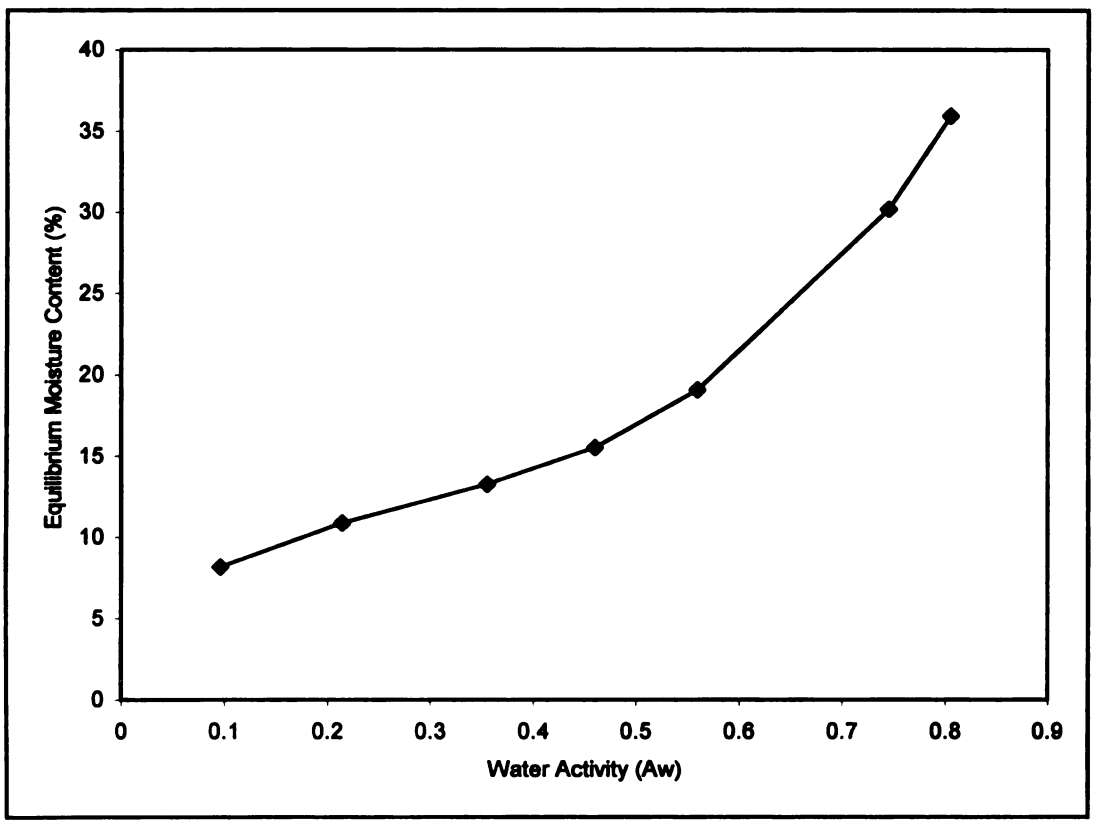

Figure 10. The Sorption isotherm at 18°C of model product (A).

Table 6. The Equilibrium moisture content for the freeze-dried product (A) as a function of water activity at 28°C.

Water Activity	Average EMC (%)
0.14	8.5393
0.25	10.5386
0.38	13.5261
0.455	15.9322
0.55	18.1299
0.63	21.9630
0.735	29.3419
0.815	34.2381

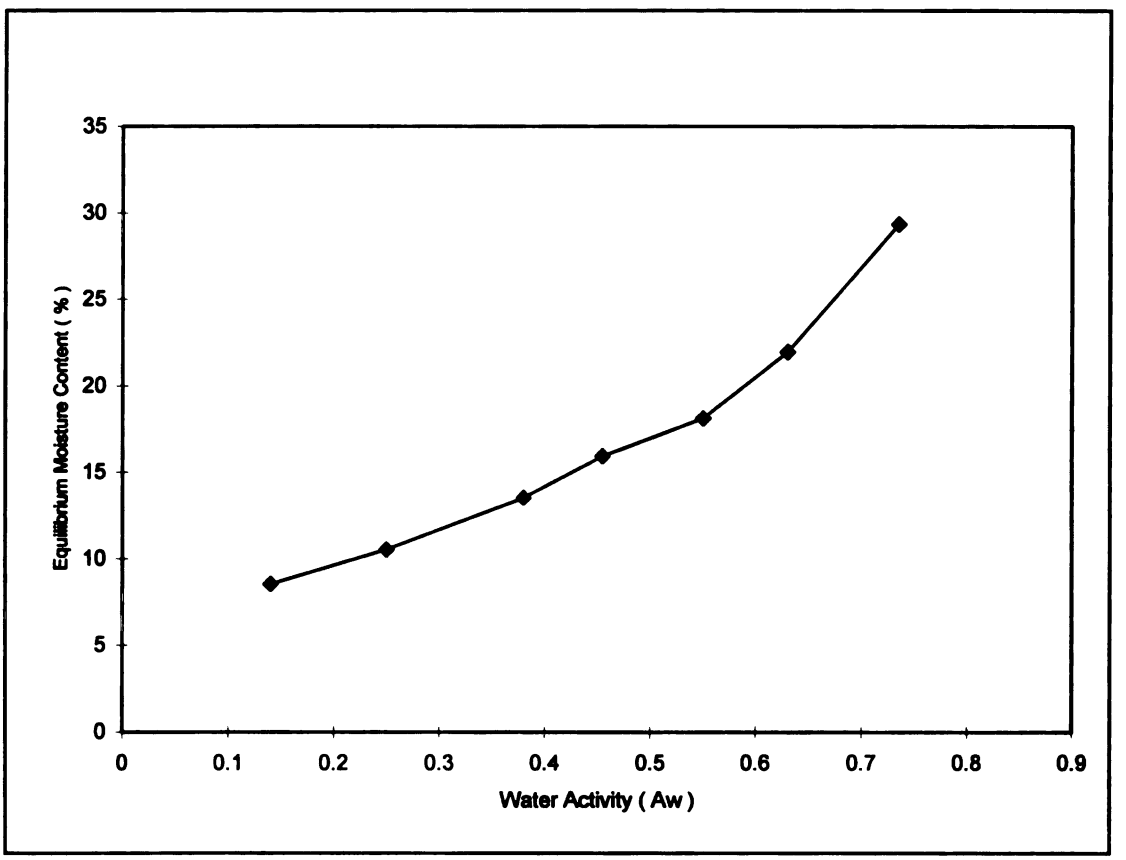

Figure 11. The Sorption isotherm at 28°C of model product (A).

Table 7. The Equilibrium moisture content for the freeze-dried product (A) as a function of water activity at 38°C.

Water Activity	Average EMC (%)
0.116	8.7792
0.2	10.2812
0.345	12.6412
0.445	14.9042
0.535	16.2677
0.755	27.7705
0.815	32.2779
0.905	55.0928

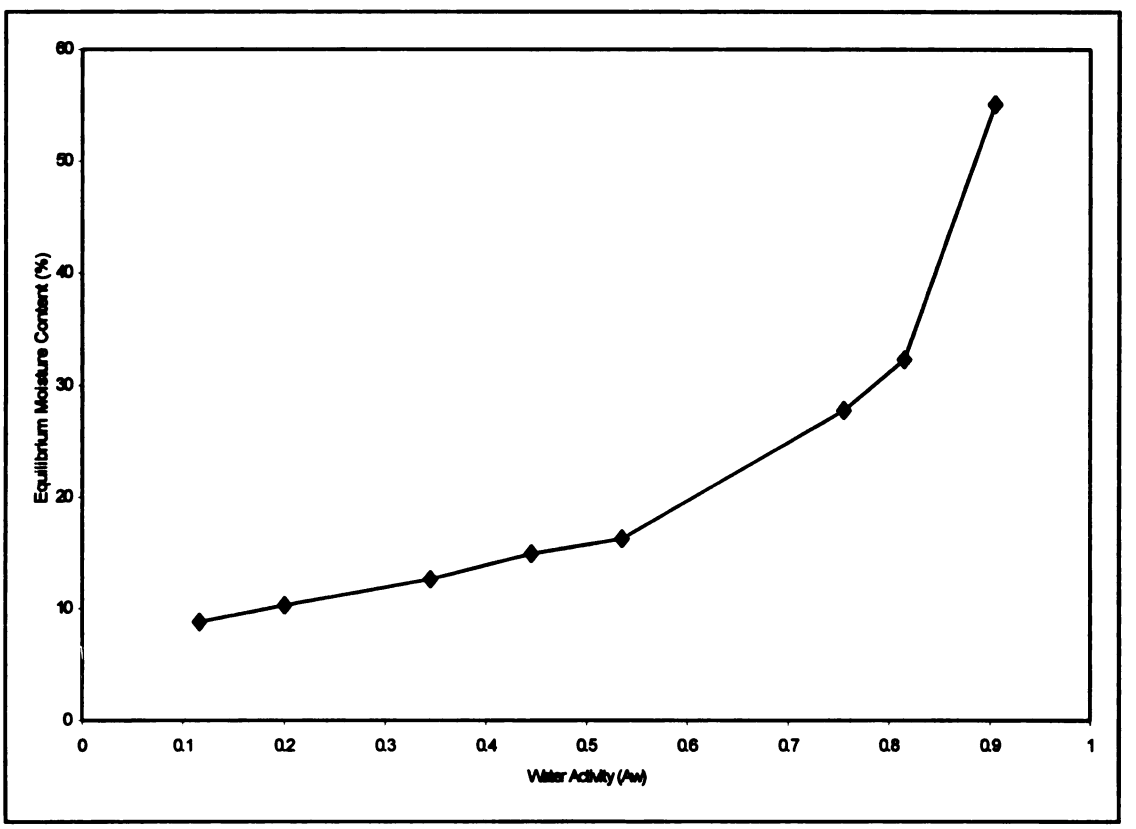

Figure 12. The Sorption isotherm at 38°C of model product (A).

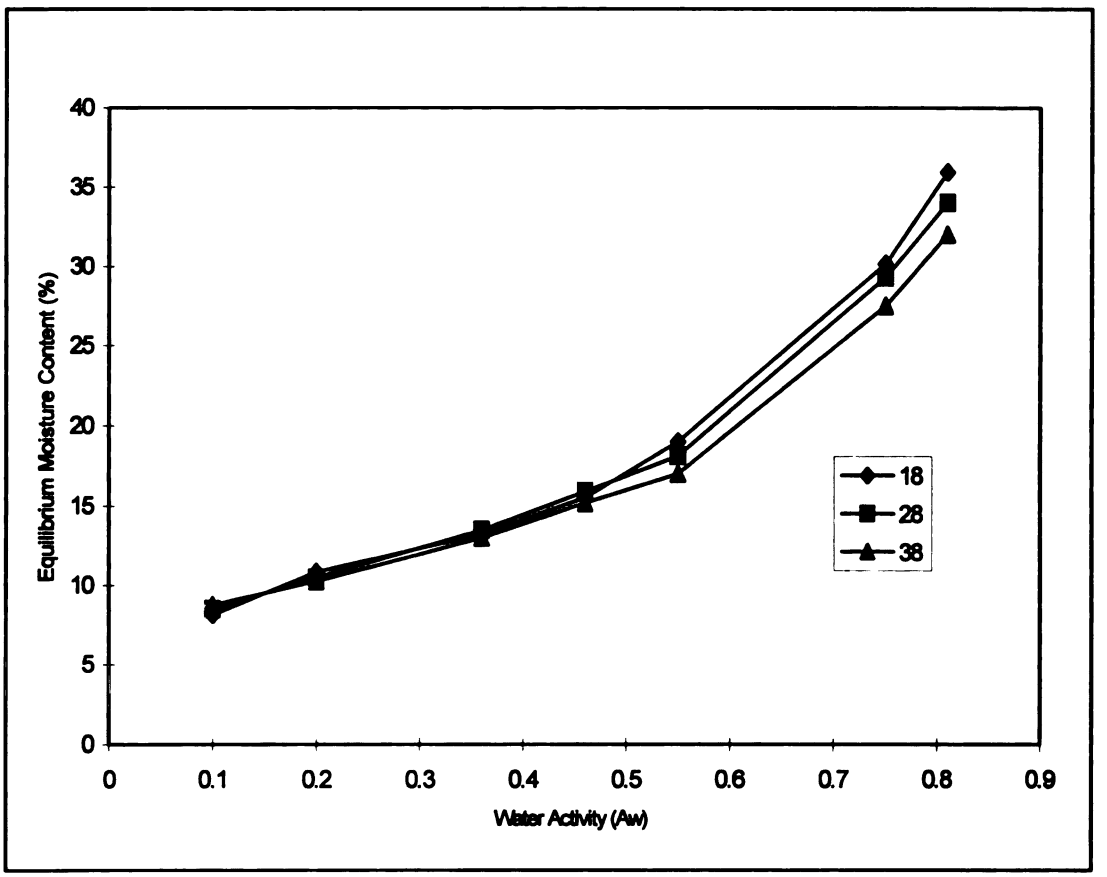

Figure 13. The Sorption isotherms at 18, 28, and 38°C for model product (A).

Table 8. The Equilibrium moisture content for the freeze-dried product (B) as a function of water activity at 18°C.

Water Activity	Average EMC (%)
0.094	8.04579
0.215	10.6671
0.35	14.3611
0.46	17.4871
0.58	21.4555
0.756	36.3225
0.815	43.5431

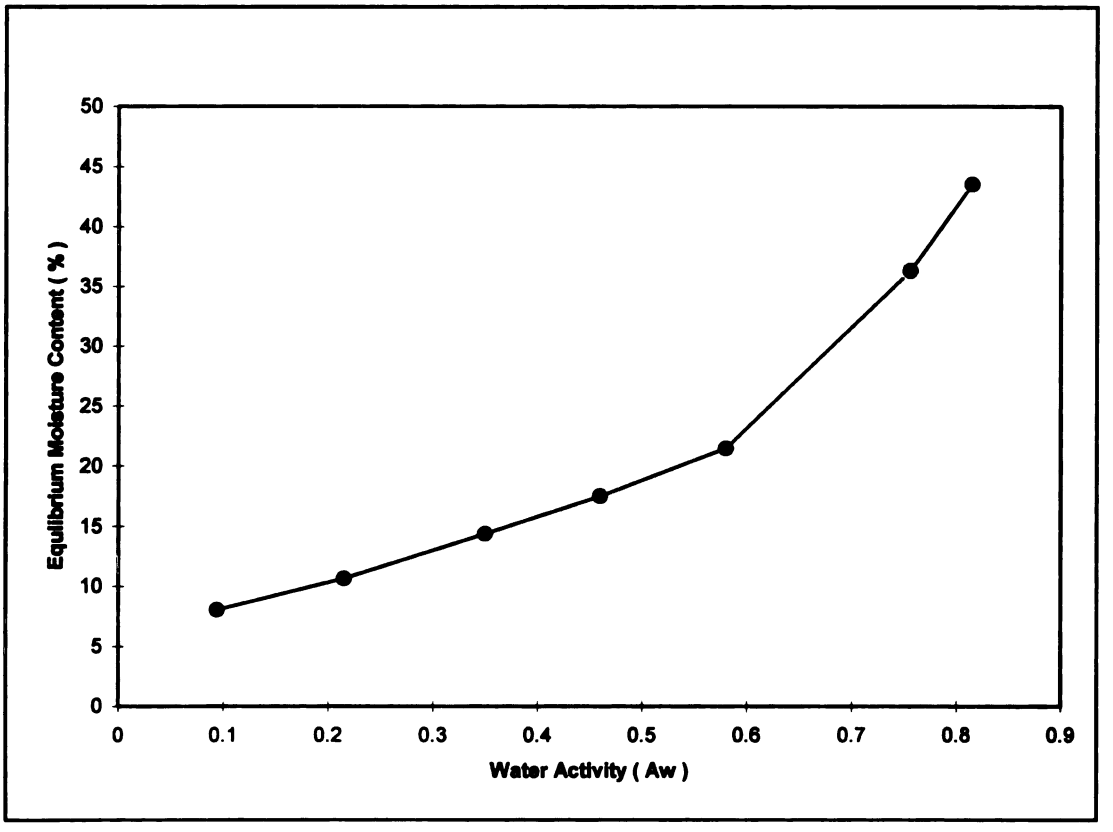

Figure 14. The Sorption isotherm at 18°C of model product (B).

Table 9. The Equilibrium moisture content for the freeze-dried product (B) as a function of water activity at 28°C.

Water Activity	Average EMC (%)
0.11	6.6965
0.235	9.3052
0.345	12.6711
0.455	16.4800
0.545	18.8241
0.75	30.1192
0.805	39.4153

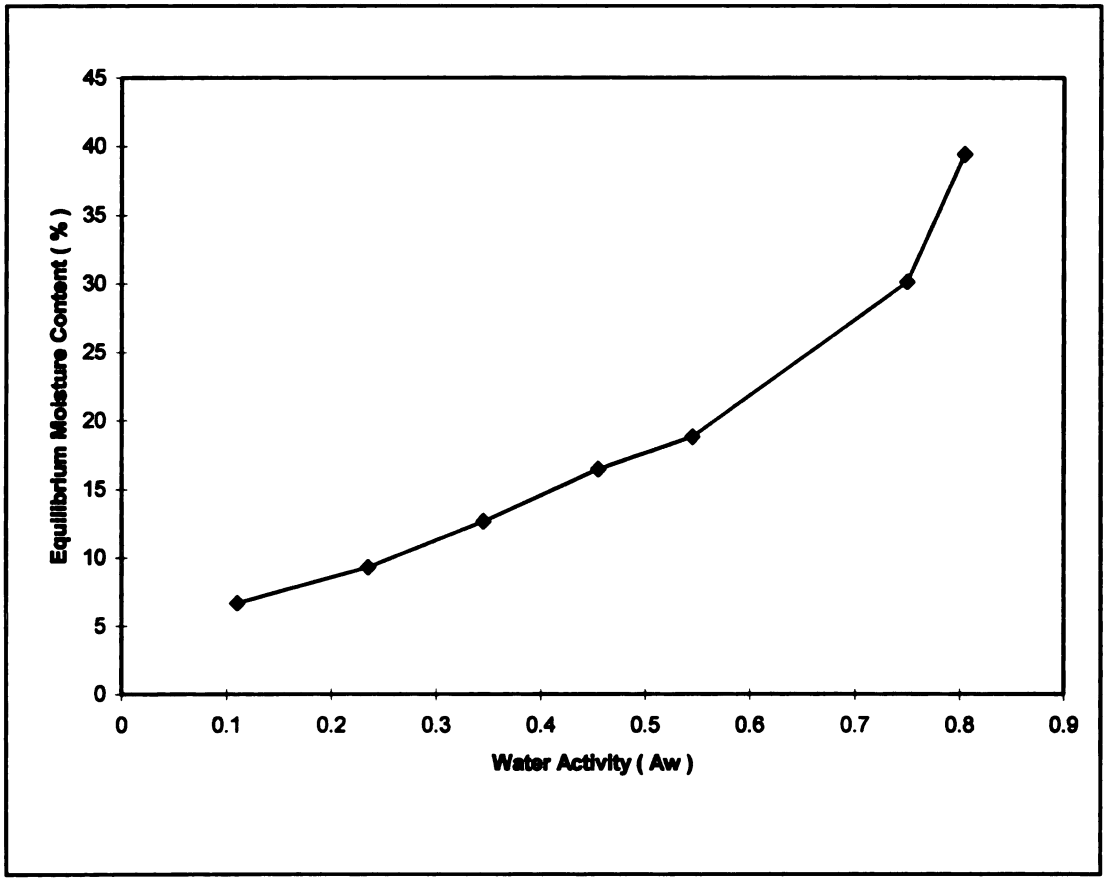

Figure 15. The Sorption isotherm at 28°C of model product (B).

Table 10. The Equilibrium moisture content for the freeze-dried product (B) as a function of water activity at 38°C.

Water Activity	Average EMC (%)
0.114	5.4358
0.198	9.4891
0.345	11.6215
0.47	15.7390
0.51	17.3351
0.755	31.3016
0.815	36.0693

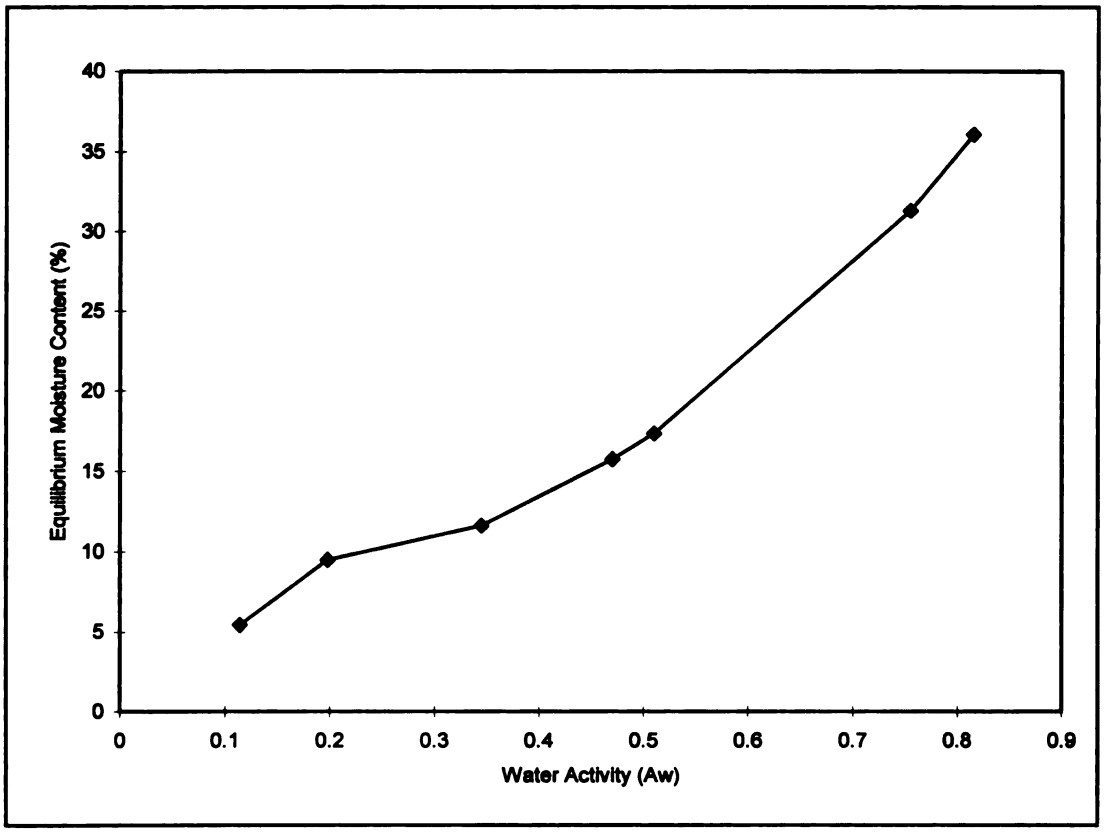

Figure 16. The Sorption isotherm at 38°C of model product (B).

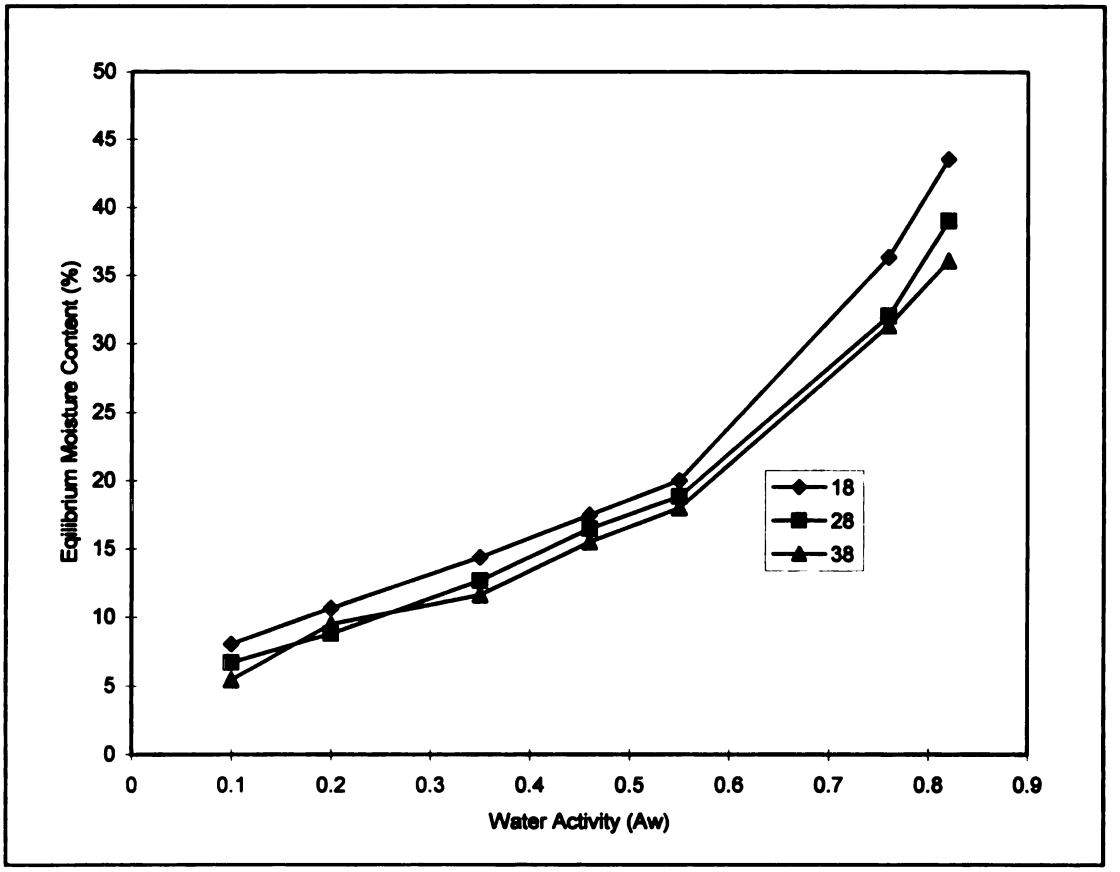

Figure 17. The Sorption isotherms at 18, 28, and 38°C for model product (B).

4-4. The Moisture Content Equilibrium of the Model Product at a Specific Water Activity, and Temperature

Prior to packaging the product and initiating the storage studies, the freeze-dried model product system was equilibrated to the desired water activity level (A_w = 0.30) to minimize the effect of water activity (A_w) on the rate of lipid oxidation. Here the dried model product was placed in an equilibration chamber at ambient temperature (23°C), and humidified nitrogen gas was continually flowed through the chamber to allow equilibration of the product model to the required water activity. The results of the hexanal analysis of the product model following equilibration showed that lipid oxidation did not take place to a significant extent during the equilibration period.

4-5. Model Product Shelf Life and Stability of Antioxidants

A flow diagram of the test scheme followed is presented in Figure 7 in the Materials and Methods section. The storage stability of the model product system was determined to evaluate the ability of antioxidant impregnated films to inhibit lipid oxidation, via the evaporation/sorption mechanism previously described. The storage studies were performed at conditions of 23°C and 45°C, respectively. Oxidation of the model product, stored at each condition, was monitored over a period of 28 weeks at 23°C and over a 6 day period at 45°C.

The pouch film was assayed over a 20 week period for the studies carried out at 23°C and for 6 days at 45°C, to allow monitoring of the relative concentration of antioxidant retained by the package structure with time.

4-6. Loss of Antioxidants (BHT, α-tocopherol) from Coextruded Laminate Films

The level of antioxidants present in the packaging films was determined as a function of time and temperature. The results of the initial antioxidant concentration levels are summarized in Table 11.

Table 11. The package film structures evaluated.

Film (HDPE/Sealant Lamination)	The initial concentration of antioxidants (wt/wt %)
I. Control	No antioxidants
II. BHT (3,5-di-tert-buthyl-4- hydroxytoluene)	0.1137 %
III. α-tocopherol	0.0073 %

The initial concentration of BHT incorporated into the laminate film structure for storage stability studies was 0.1137 %(w/w). The initial concentration of α-tocopherol incorporated into the test laminate film structure was 0.0073 %(w/w).

The levels of antioxidant remaining in the packaging pouch structures, as a function of storage time at 23°C, are summarized in Table 12. The relative percent loss at BHT and α-tocopherol from the coextruded pouch materials, as a function of storage time at 23°C, is represented graphically in Figure 18, where the relative percent antioxidant retained is plotted as function of storage time. Statistical analysis was performed using Sigma stat

1.0 (Jandel Corp., San Rafael, CA). Appropriate comparisons were made using the Student-Newman-Keuls test for multiple comparisons by a one-way analysis of variance (ANOVA).

Table 12. The level of antioxidants from coextruded packaging pouches as a function of storage time (23°C, 50 %RH).

Storage Time	Conc. Of antioxidants ppm (w/w)		Relative percent retained antioxidants(Ct/Co)x100	
Weeks	BHT	Tocopherol	% BHT	% Tocopherol
0	1137±5.9 [a]	73±1.0 [a]	100	100
2	608±5.7 [b]	63.5±3.6 [b]	53.5	87
4	446.5±49.0 [c]	62±6.7 [b]	39.3	85
6	279±26.1 [d]	61.5±2.6 [b]	24.5	84
8	211±8.9 [e]	60±2.4 [b]	18.6	82.2
10	149±4.9 [f]	45±9.5 [c]	13.1	61.6
12	112±20.5 [g]	40.5±15.3 [c]	9.9	55.5
14	79.5±13.2 [h]	29±11.9 [c]	7.0	39.7
16	36.5±2.3 [I]	27±3.7 [c]	3.2	37
18	32±13.2 [I]	26±7.1 [c]	2.8	35.6
20	N/A	N/A	N/A	N/A

Average ± standard deviation of each pouch as a function of time.
[a-i] Means with different superscripts in same column are significantly different ($p<0.05$).
N/A means it is not available due to a limit of the detector sensitivity.

The relative percent of antioxidant retained in the packaging pouches was 2.8% of BHT and 35.6% of α–tocopherol, after 18 weeks of storage at 23°C. As shown, within a two week storage period at 23°C, approximately 50 % of the included BHT was lost from the packaging pouch material. The loss of α-tocopherol from the packaging pouches over the same period of time was approximately 10%, with nearly 50% α-tocopherol

remaining after 12 weeks of storage at 23°C. The concentration of BHT retained in the packaging pouches showed statistically significant differences ($p<0.05$) between samples, as a function of storage time. After a 10 week storage period at 23°C, the level of α–tocopherol exhibited highly significant differences ($p<0.05$) when compared with the initial concentration in the packaging pouch material, with a statistically significant difference after the first two weeks, while the BHT concentration retained in the pouch structures, showed a highly significant difference within the first two weeks.

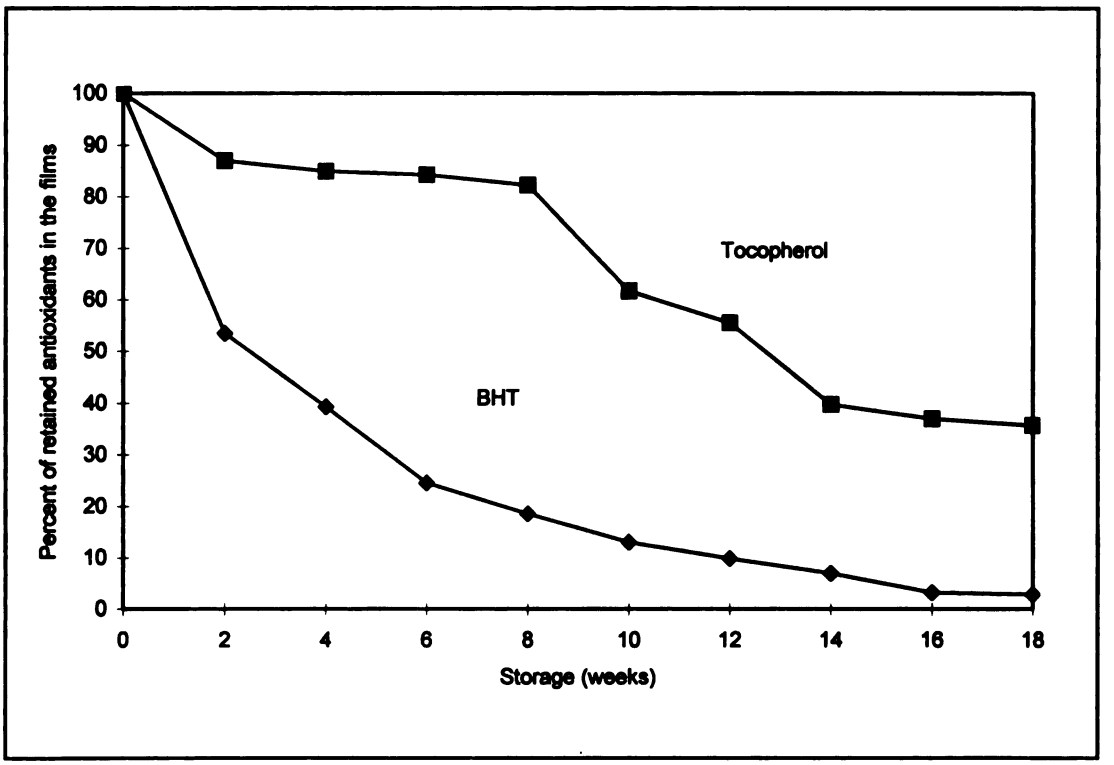

Figure 18. The relative percent loss at BHT and α-tocopherol from coextruded pouch films as a function of storage time (23°C).

Comparing these results, with the data obtained by Lin (1996) for three layer laminate films, showed similar loss rates of α–tocopherol as a funtion of storage time (23°C).

After removing the model product, the BHT and α-tocopherol content of the pouch material was also determined as a function of storage time, for the product stability studies carried out at 45°C and 50% RH. The results of these acclerated stability studies, involving determination of antioxidant levels from the package structures with time, are summarized in Table 13 and presented graphically in Figure 19.

Table 13. The level of antioxidants from coextruded packaging pouches as a function of storage time (45°C, 50% RH).

Storage Time	Conc. of antioxidants ppm (w/w)		Relative percent of retained antioxidants(Ct/Co)x100	
Days	BHT	Tocopherol	% BHT	% Tocopherol
0	1168±25.3 [a]	73±6.3 [a]	100	100
2	185±28.4 [b]	72.5±2.4 [a]	15.8	98.9
4	40±3.3 [c]	72±2.5 [a]	3.5	98.0
6	N/A	55.5±1.0 [b]	N/A	74.8

Average ± standard deviation of each pouch as a function of time.
[a, c] Means with different superscripts in same column are significantly different ($p<0.05$).
N/A means it is not available due to a limit of the detector sensitivity.

As shown, no BHT was found in the BHT-impregnated laminate pouch structure after 6 days of storage at 45°C. For the α–tocopherol level, approximately 25% of the initial quantity was lost, after 6 days at 45°C. The concentration of α–tocopherol retained in the packaging pouch film structure showed no significant difference ($p>0.05$) until a 6 day storage period at 45°C. The levels of BHT retained in the antioxidant impregnated packaging pouch film indicated a significant difference ($p<0.05$), as a function of storage time, until the complete loss of BHT at 45°C.

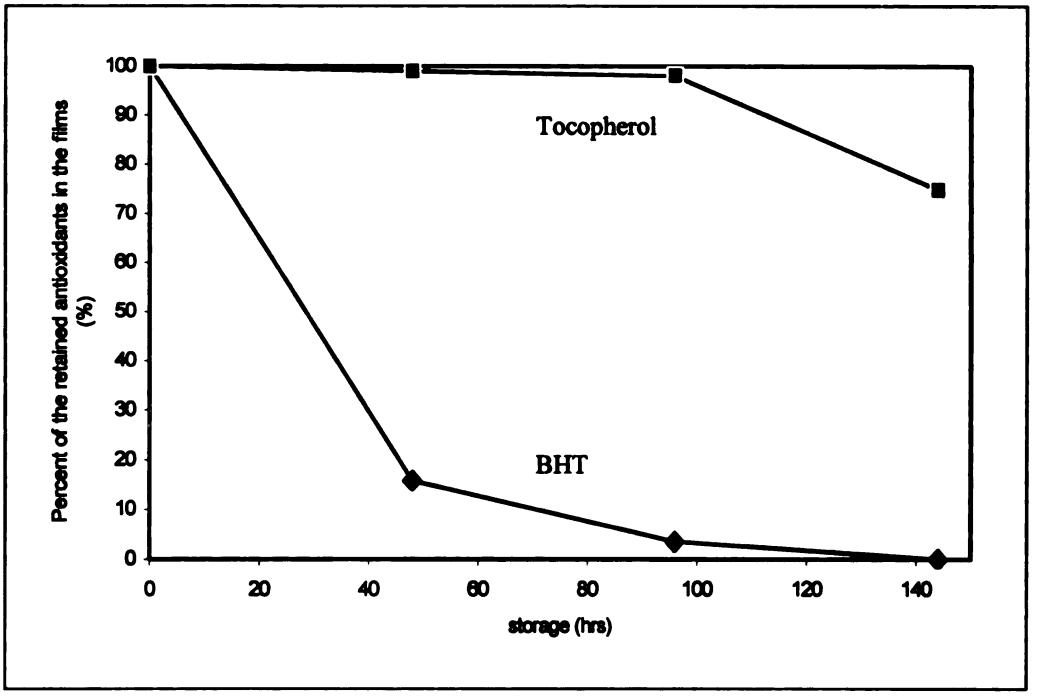

Figure 19. The relative percent loss at BHT and α-tocopherol from coextruded pouch films as a function of storage time (45°C).

The rate of loss of BHT from the package film structures was found to be much higher than the rate of loss of α-tocopherol, at both storage conditions.

The observed differences between the rates of loss of BHT and α–tocopherol from the laminate packaging pouch may be attributed to a higher rate of diffusion of BHT through the laminate surface layers, or a difference in the rate of evaporation of the BHT from the HDPE and heat sealant layers, as well as to the equilibrium partition distribution of the antioxidants between the respective layers of the lamination. Antioxidant migration is related to the solubility of the additive within the respective layers of the lamination and

the diffusion of the additive through it. Differences in either the solubility or diffusivity can affect the transmission characteristics of the respective antioxidants. The solubility difference depends primarily on the difference in the physical and chemical nature of the migrating molecules and the respective laminate layers and will be reflected in the partition distribution of the antioxidant between the laminate layers. On the other hand, the difference in antioxidant diffusivity is determined mainly by the size and shape of the molecules, and by the degree of aggregation among the diffusing molecules within the polymer layers. The fact that the initial concentration of the BHT was significantly higher than the initial level of α–tocopherol impregnated into the laminate film structure may also be a contributing factor to the observed lower rate loss for α–tocopherol.

4-6-1. The Rate of Loss of Antioxidants from Laminate Film Structure

The rate of loss of antioxidants from coextruded pouch film was reported by Bailey (1995) and Lin (1996) to follow a first-order or pseudo first-order rate expression:

$$\ln (Ct/Co) = - kt \qquad \text{-------- (17)}$$

Where Co : the initial concentration of antioxidants in the film

Ct : the concentration (w/w, %) at time = t

k : the rate constant of the antioxidant loss

t : the time interval

A plot of log(Ct/Co) as a function of storage time for antioxidant losses at storage temperatures at 23 and 45°C, indicated that a first order expression provided a good

description of the rates of loss of the respective antioxidants from the laminations evaluated in the present study (see Figures 20 and 21).

The first-order rate equation constants (k) for the loss of antioxidants from pouch films were determined at each temperature and are summarized in Tables 14 and 15, respectively.

The following expressions were derived from a least square fit of the rate loss data.

<u>23°C (t = weeks unit)</u>

$(Ct/Co) \times 100 = 87.452 * \exp(-0.1925t)$ ..... BHT R^2 :0.9887

$(Ct/Co) \times 100 = 109.74 * \exp(-0.0625t)$ ..... Tocopherol R^2 :0.9204

Table 14. Rate constants for the loss of antioxidants from the packaging pouch structure (23°C).

Antioxidants	Loss Rate Constant k (hr^{-1})
BHT	0.00115
Tocopherol	0.00037

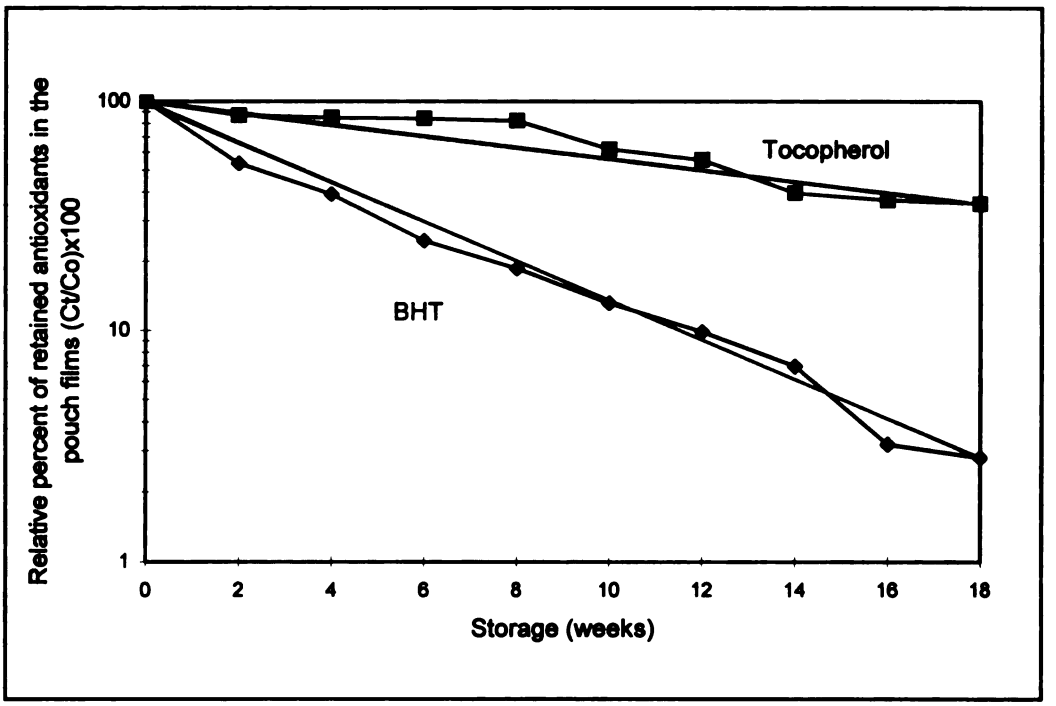

Figure 20. Relative percent loss of BHT and α-tocopherol from the pouch films as a function at storage time (23°C).

45°C (t = hours unit)

$(Ct/Co) \times 100 = 96.416 * \exp(-0.0350t)$ ..... BHT R^2 :0.9968

Table 15. Rate constant for the loss of BHT from the packaging pouch film structure (45°C).

Antioxidant	Loss Rate Constant k (hr^{-1})
BHT	0.0350

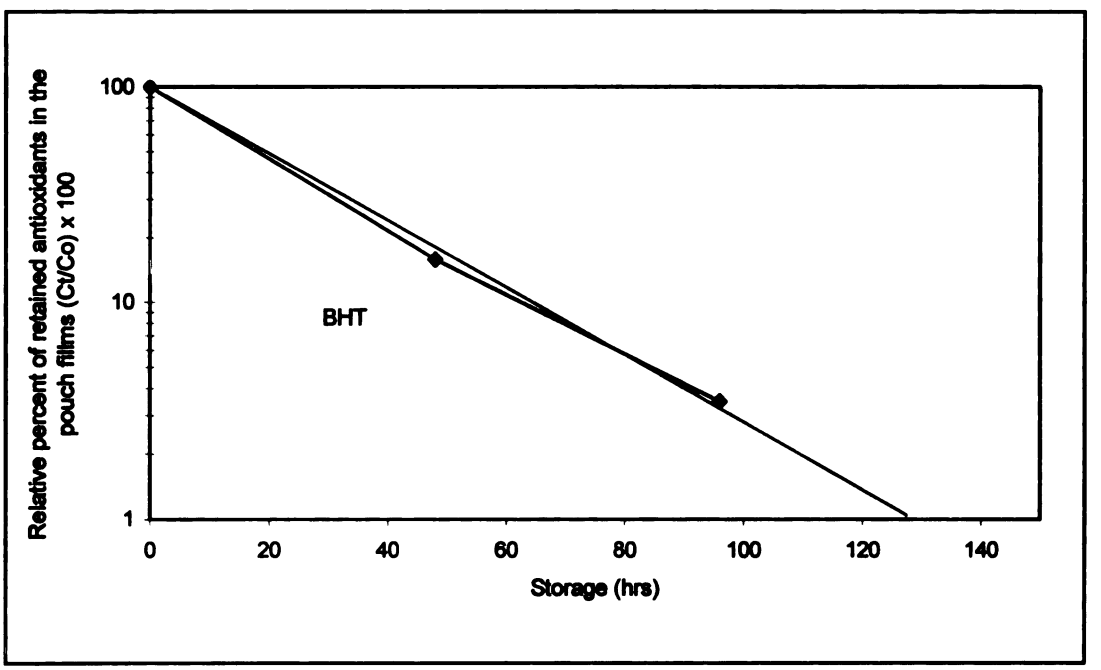

Figure 21. Relative percent loss of BHT from the pouch film as a function at storage time (45°C).

As shown in Tables 14 and 15, the rate loss constant values for BHT from the packaging pouch film structure, at the respective temperatures, were much greater than the rate constant for the loss of α–tocopherol from the packaging pouch film structure. The loss of α-tocopherol from the packaging pouch film structure at 23°C showed a similar loss

rate value (k= 0.00037 hr^{-1}), as compared to the loss rate constant (k= 0.0004 hr^{-1}) of α-tocopherol obtained by Lin (1996) from the coextruded laminate film structures.

4-6-2. Percent Recovery of Antioxidants from the Pouch Film

The percent recovery of antioxidants carried through the soxhlet extraction / HPLC analysis procedure is summarized in Tables 16 and 17, respectively.

Table 16. The percent recovery of BHT for extraction system.

Injection	Conc.	Area Response	
(20 μl)	10 ppm	Initial Conc.	After extraction
1		547024	534472
2		551967	534732
3		545764	538658
Average		548251.7	535954
Percent recovery		97.76 %	

Table 17. The percent recovery of α-tocopherol for extraction system.

Injection	Conc.	Area Response	
(20 μl)	10 ppm	Initial Conc.	After extraction
1		290202	282072
2		288542	287768
3		286662	289199
Average		288468.7	286346.33
Percent recovery		99.26 %	

A recovery of 98% and 99% for BHT and α-tocopherol, respectively showed good stability of antioxidants through the extraction procedure and HPLC analysis.

4-7. Level of Linoleic Acid in the Model Product following Storage at 45°C

The level of linoleic acid remaining in the model product packaged in the respective test pouches and stored at 45°C, as a function of time, is summarized in Table 17 and presented graphically in Figure 22, where the linoleic acid concentration is plotted as a function of storage time for the two antioxidant containing package pouches and the antioxidant-free control.

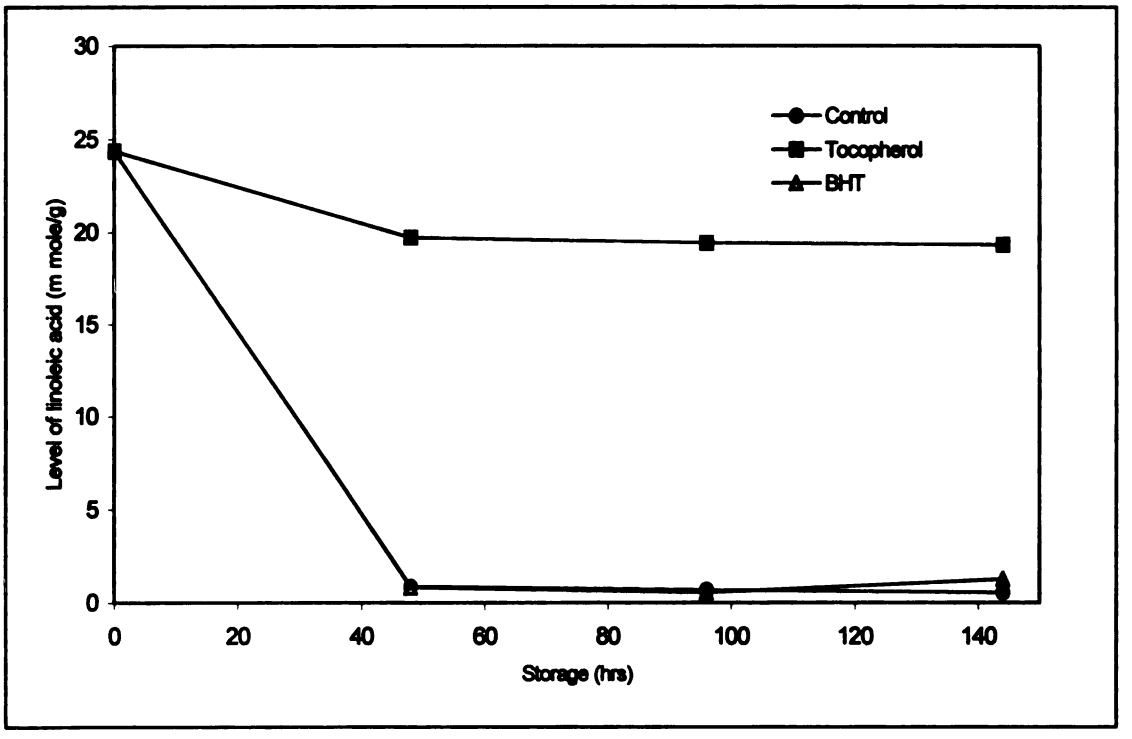

Figure 22. The concentration of linoleic acid in the model product as a function of storage time (45°C).

As shown, the concentration of linoleic acid in the model product packaged in the control and in the α-tocopherol impregnated laminate pouch structures decreased rapidly during storage over a 2 day period at 45°C. Over a 4 day storage period, there also appeared to be no statistically significant difference ($p>0.05$) between the level of linoleic acid in the model product packaged in the control and in the α-tocopherol impregnated laminate pouch structures. This result indicates that the α-tocopherol impregnated laminate pouch had no effect on retarding lipid oxidation in the model product, as compared to the control non-impregnated laminated pouch, when stored at 45°C. This was attributed to extensive fatty acid oxidation under the conditions of storage. However, the model product packaged in the BHT impregnated laminate pouch did not show a notable change in linoleic acid concentration, during storage for 6 days at 45°C, suggesting minimal lipid oxidation. These data showed a correlation between the concentration of linoleic acid present in the model product packaged in the respective laminate film pouches and the level of antioxidants retained by the respective packaging pouches, as a function of storage time at 45°C, 50% RH. (see Table 18)

Table 18. The concentration of linoleic acid from the model product as a function of the storage time at 45°C, 50% RH.

(m mole/g)

Storage (hrs)	Control	BHT	Tocopherol
0	24.38 ± 0.28^{aA}	24.38 ± 0.28^{aA}	24.38 ± 0.28^{aA}
48	0.87 ± 0.04^{bA}	19.71 ± 1.32^{aB}	0.83 ± 0.04^{bA}
96	0.70 ± 0.03^{bA}	19.42 ± 0.28^{aB}	0.56 ± 0.11^{cA}
144	0.55 ± 0.01^{bA}	19.31 ± 0.27^{aB}	1.27 ± 0.04^{dC}

Average ± standard deviation of each model product as a function of time.

$^{a-c}$ Means with different superscripts in same column are significantly different ($p<0.05$).

$^{A-C}$ Means with different superscripts in same row are significantly different ($p<0.05$).

The lack of observed loss of linoleic acid from the model product in the BHT impregnated laminate pouch, as a result of oxidation, can be attributed to a higher rate of loss of antioxidant from the pouch structure and subsequent sorption by the model product under these condition, than the rate of lipid oxidation of the model product. By comparison, under similar storage conditions, little or no α-tocopherol is migrated to the model product system to inhibit lipid oxidation. Also, significantly higher initial concentrations of the BHT than the initial level of α-tocopherol may be an important factor contributing to the observed inhibition of linoleic acid oxidation in the model product.

4-7-1. The Percent Recovery of Extraction for Linoleic Acid

The percent recovery for the methylation of linoleic acid was found to be approximately 72 %, based on the initial quantity of linoleic acid carried through the extraction step. However, when methyl linoleate was carried through the extraction step (see page 57 in Materials and Methods), a near quantitative recovery was observed (i.e. 97 %). Assuming a 72% recovery for the methylation step and a 97% recovery for the extraction step, the % recovery for the methylation/extraction procedure was nearly 70%, and while not quantitative, the percent recovery for this procedure was repeatable (see Table 19).

Table 19. The percent recovery of linoleic acid through the extraction and methylation procedures.

System	Sample1 (%)	Sample2 (%)	Sample3 (%)	Recovery Average(%)
1. Methylation	71	72.9	71.4	71.77
2. Extraction	96.5	96.8	96.2	96.5
3. Extraction and methylation	68.5	70.6	68.7	69.3

4-8. Difference in the Level of Linoleic Acid Between Model Product Preparation and Freeze-Dried Model Product

The model product for the storage studies was prepared by freeze-drying to simulate a low moisture food product, as well as to provide an initial moisture content which would minimize the rate of lipid oxidation of the resultant freeze-dried product system. To measure the effect of freeze drying on linoleic acid concentration in the freeze dried product, the methyl ester value of linoleic acid in the model product after freeze-drying was compared to the value in the original preparation (before freezing and freeze-drying). The percent recovery of linoleic acid in the model product following the freeze-drying procedure was 30.3%, as summarized in Table 20. The concentration of linoleic acid in the model product after freeze-drying showed a significant loss, as reflected by the methyl linoleate levels determined for the model product system following freeze-drying. The observed loss of linoleic acid may be due to volatilization of linoleic acid from the model product during the freeze-drying process, which involves

removal of water from the product. The composition of a model product with low lipid levels may be affected significantly by even small environment changes: such as the freeze-drier condition and run time.

Table 20. The percent recovery of the linoleic acid in the model product between before freezing-dry and after freezing-dry condition.

	Sample conditions (wet basis product)		% Recovery
Level of linoleic acid in model product	Before freezing-dry	After freezing-dry	30.3%
	0.33% (g/g)	0.1% (g/g)	

Noormarji (1990) determined the extent of lipid oxidation on both the functional and nutritional properties of chicken breast myofibrillar proteins during different stages of freeze drying by TBA tests. A series of experiments showed that freeze drying for 48 hr increased lipid oxidation in the control and methyl linoleate treated sample, as compared to freeze drying for 24 hr. Freeze drying for 48 hr showed much higher lipid oxidation levels than that for 24 hr, in the presence of oxidized methyl linoleate. The longer periods of freeze drying increased lipid oxidation as measured by TBA numbers (Noormarji, 1990). Such results suggest that the time of freeze drying of the model product system can play an important role in product lipid oxidation.

4-9. Product Storage Studies

The results of hexanal analysis carried out on model product samples packaged in pouch I (control pouch structure), pouch II (BHT impregnated pouch structure), and pouch III (α-tocopherol impregnated pouch structure) and stored at 23°C/50%RH are summarized in Table 21. The relationship between the extent of lipid oxidation and the

respective laminate package structures evaluated is presented graphically in Figure 23, where hexanal concentration in the product model system is plotted as a function storage time. Data were analyzed with the use of a Sigma stat 1.0 statistical analysis program (Jandel Corp., San Rafael, CA). The statistical analyses were compared using the Student-Newman-Keuls test for all pairwise multiple comparisons by a one-way repeated measure analysis of variance (ANOVA), with a significance difference of $p<0.05$.

Table 21. The hexanal concentration of model product system packaged in pouches fabricated from coextruded laminate structures (23°C, 50 %RH).

(n mol/g product system)

Storage Time (weeks)	Pouch I (Control)	Pouch II (BHT)	Pouch III (α-tocopherol)
0	3.39±0.68	3.39±0.68	3.39±0.68
2	5.59±2.01	4.83±0.79	5.89±0.72
4	6.25±0.36	5.54±2.08	6.81±0.86
6	6.45±1.94	6.25±1.37	4.62±1.51
8	4.42±0.79	4.01±1.94	4.32±1.37
10	4.27±1.01	7.11±5.46	6.50±1.29
12	5.23±1.94	7.21±0.86	4.37±1.87
14	3.86±2.87	7.32±1.58	4.22±0.50
16	5.94±1.51	5.28±1.44	4.93±2.80
18	5.18±1.72	5.64±1.51	4.42±0.22
24	8.18±2.87	7.98±4.10	5.99±0.29
26	7.87±1.65	8.79±0.50	7.52±0.72
28	5.84±0.50	9.50±2.37	8.18±2.37

Average ± standard deviation of each pouch as a function of time.
All values in same column are not significantly different ($p>0.05$).

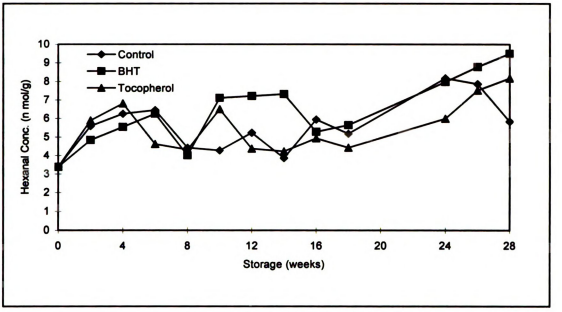

Figure 23. The concentration of the hexanal in the model product system packaged in pouches fabricated from coextruded laminate film structures (23°C, 50 %RH).

The initial concentration of hexanal in the model product at 0 day storage was 3.39 n mole/g product. As shown up through 28 weeks of storage, the levels of hexanal detected in the product model system packaged in these test structures were very similar. The concentration of hexanal in the model product packaged in the respective antioxidant impregnated laminate film pouches was not significantly different ($p>0.05$), as a function of the storage time at 23°C. Lin (1996) studied the effectiveness of α-tocopherol and BHT impregnated laminate films to retard the oxidation of a packaged oat cereal product and found a significant difference ($p<0.05$) in the level of hexanal in the cereal product packaged in pouches without antioxidant, as compared to the cereal product packaged in

the antioxidant impregnated laminate film pouches after 20 weeks of storage. Storage conditions for Lin's study were 23°C and 50%RH.

Based on the literature, lipid oxidation of the model product packaged in non-antioxidant impregnated laminate film pouches was expected to show, at the storage conditions of test (23°C/50%RH), a slow but constant rate of oxidation, followed by a rapidly accelerating rate of oxidation, at a certain point during the storage. This would result in hexanal concentrations many times greater than that observed at the initial stage of the storage stability study. However, as shown over the 28 week storage period (See Table 21), the level of hexanal in the model product packaged in non-antioxidant impregnated laminate film pouches showed no statically significant increase, as compared to the initial concentration of hexanal in the model product. Further, the model product packaged in the respective antioxidant impregnated laminate film pouches showed hexanal concentration level of less than 10 n mole/g, as compared to an initial hexanal level of approximately 3.39 n mole/g. By comparison, the hexanal concentration in the model product packaged in the non-antioxidant impregnated laminate film pouch and stored at 45°C and 50%RH, was over 70.7 n mole/g after 48hrs, indicating significant levels of the lipid oxidation (see Table 22). This result suggests that the observed lack of effectiveness of the antioxidants for the model product packaged in the respective antioxidant impregnated laminate film pouches was due to the lack of the lipid oxidation in the model products stored at 23°C and 50%RH, as a function of time.

A possible explanation for the lack of observed linoleic acid oxidation for the model product system stored at 23°C and 50%RH is that in the absence of trace metals, which can act to promote lipid oxidation and are typically found in a product system such as a

cereal product (Tjhio and Karel, 1969), the model product studied has a longer induction period than the 28 week period over which oxidation was monitored prior to experiencing oxidation of the fatty acid. Furthermore, the water activity of the product was adjusted to be at or near the B.E.T. monolayer level, which would provide conditions to minimize lipid oxidation.

The extent of oxidation of the model product packaged in the respective antioxidant impregnated test structures and stored at 45°C was also monitored by the formation of hexanal and the results presented in Table 22.

Table 22. The hexanal concentration of model product system packaged in pouches fabricated from coextruded laminate structures (45°C, 50 %RH).

(n mole/g product system)

Storage (hrs)	Control	BHT	Tocopherol
0	2.1+0.34[a]	2.1+0.34[a]	2.1+0.34[a]
48	70.76±1.10[b]	2.3±0.48[a]	125.88±15.72[b]
96	4.78±0.37[c]	2.7±0.79[a]	5.65±1.09[a]
144	16.4±4.91[c]	1.9±0.27[a]	19.1±0.36[a]

Average ± standard deviation of each pouch as a function of time.
[a - c] Means with different superscripts in same column are significantly different ($p<0.05$).

As shown, the effect of the BHT impregnated laminate film structure was much greater than the effect of the α-tocopherol impregnated laminate film structure in inhibiting lipid oxidation. The concentration of hexanal in the model product packaged in the BHT impregnated laminate film pouches showed no significant difference ($p>0.05$) over 6 days storage at 45°C. This can be attributed to the fact that the rate of loss of BHT from

the film into the model product is much faster than the rate of loss of α-tocopherol from the laminate film structure to the product model system, at 45°C.

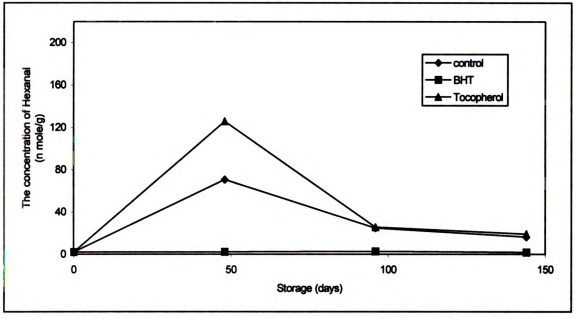

Figure 24. The concentration of the hexanal in the model product system packaged in pouches fabricated from coextruded laminate structures (45°C, 50 %RH).

The relationship between the extent of lipid oxidation and the respective laminate package structures that were evaluated in the present study are presented graphically in Figure 24, where the hexanal concentration in the model product system is plotted a function of time. The results of hexanal levels, determined in the model product showed the BHT impregnated laminate package structure to be effective in retaining lipid oxidation in the model product as a function of time, when stored at 45°C and 50%RH.

As shown in Figure 24, the highest values of hexanal were observed in the model product packaged in the control (free-antioxidant) and α-tocopherol impregnated pouches, after a 2 day storage period at 45°C/50%RH, which was followed by decreasing hexanal levels over the remaining stage period. This can be attributed to the partitioning of hexanal into the package headspace, its sorption and subsequent permeation through the package structures, or further oxidation at the elevated test temperature.

Henderson, *et al.* (1980) observed the effects of heating temperature and time on the mechanism of linoleate decomposition. Hexanal were found in significantly greater amounts from the propyl linoleate heated at 70°C than those heated at 180°C, 250°C. The authors proposed that hexanal was the major volatile compound formed during autoxidation at the low temperature, whereas decadienal levels increased at the high temperatures due to thermal decomposition.

4-10. Qualitative Identification of Hexanal Compound in Model Product Using the Selected Ion Monitoring GC/MS Procedures.

The characteristic ions of hexanal, at selected m/z values were monitored throughout the GC/MS analysis by operating the mass spectrometer in the SIM (selected ion monitoring) mode. The selected ion detector monitored only the ion current selected by the mass analyzer, for the ion current at m/z 29, 44, 56, 72 and 100, respectively. At a retention time of 8.6 min for the selected ions, the ion currents at m/z 44, 56, 72 were found to be from the same source. Furthermore, the ratio of the three peaks for the ion current profiles at 44:m/z, 56:m/z and 72:m/z for the model sample was approximately 1: 0.65: 0.16. Here, m/z = 44. These ratios agreed well with that of the hexanal standard

compound (1: 0.63: 0.16) (see Table 23). Therefore, observation of simultaneous peaks at the three selected ion current profiles, in the expected abundance ratio and at the expected retention time for the model sample and hexanal standard compound, provided unequivocal evidence that hexanal was present in the model sample.

Table 23. The ratio of the selected ion profiles at m/z 44, 56, and 72 for hexanal.

	Hexanal standard (4 n mole)	Model product (B)
Ratio of m/z (44/44)	1	1
Ratio of m/z (56/44)	0.63	0.65
Ratio of m/z (72/44)	0.16	0.16

The external standard calibration curve was obtained from the total peak areas of the ion fragments (i.e. m/z), selected as being characteristic of hexanal and determined for a series of standard solutions of known concentration (2, 4, 6, 8 n mole). This is referred to as the total ion chromatogram. When operating the GC/MS in the selected ion monitoring mode, the level of hexanal in the model product was calculated using the calibration factor obtained from the external standard calibration curve. The peak obtained at retention time (8.6 min), represented the total ion chromatogram of the model sample and was identified as being due to hexanal, based on the following. First, the retention time for the selected ions, at m/z 29, 44, 56, 72, and 100, was identical to that of the standard hexanal. The abundance of the peak areas from the selected ion current at m/z 29, 44, 56, 72, and 100 in the model product sample was used to determine the hexanal level in the sample by comparison to the response factor from standard hexanal

solutions. A comparison of the ion ratios provided further supportive evidence for hexanal.

SUMMARY AND CONCLUSIONS

A lipid containing freeze dried model product was designed to determine the effectiveness of antioxidant impregnated laminate film pouches to retard lipid oxidation. All of the films contained a heat seal layer (Suryln-EVA) coextruded to a high density polyethylene (HDPE) layer. The type of antioxidant in the heat seal layer was based on three test films, which were film I containing α-tocopherol, film II containing BHT, and film III which had no antioxidant. The initial concentrations of α-tocopherol and BHT incorporated into the test laminate film structure were 0.0073 %(w/w) and 0.1137 %(w/w), respectively.

The equilibrium sorption isotherm of the model product was determined at three different temperature conditions (18°C, 28°C, and 38°C), to allow selection of storage conditions (i.e. Temperature and RH) which could exhibit minimal rates of oxidation. The model product was described by the Halsey and Henderson (38°C, for the model product with the low linoleic acid level) isotherm models. The monolayer moisture content at each temperature was 8.57 (18°C), 9.12 (28°C), and 8.38 (38°C), respectively, for the model product containing high linoleic acid levels and 9.88 (18°C), 9.84 (28°C), and 9.23 (38°C) (g H_2O/100g dry product), respectively, for the model product containing low linoleic acid levels.

The loss rate of antioxidant from the laminate pouch film structure was determined as a function of storage time at 25°C/50%RH, and at 45°C/50%RH. The rate of loss of BHT from the package film structures was found to be much higher than the rate of loss of α-tocopherol, at both storage conditions. The storage stability of the packaged model product, at the respective storage conditions, was used to determine the effectiveness of the antioxidant impregnated film structures in inhibiting lipid oxidation. Hexanal levels were determined as a measure of lipid oxidation. Analyses were based on a GC/MS procedure, operating the mass spectrometer in the selected ion monitoring mode.

The BHT impregnated laminate film was found to be more effective than the α-tocopherol impregnated laminate film in inhibiting lipid oxidation at accelerated storage conditions (i.e. 45°C/50%RH). This was attributed to the fact that the rate of loss of BHT from the package film structure to the model product is much faster than the rate of loss of α- tocopherol from the laminate film structure to the product model system at 45°C. However, the level of hexanal in the model product packaged in the respective antioxidant impregnated laminate film pouches showed no statically significant differences ($p>0.05$) following storage at 23°C/50%RH. A possible explanation for the lack of observed linoleic acid oxidation for the model product system stored at 23°C and 50%RH is that in the absence of trace metals, which can act to promote lipid oxidation and are typically found in a product system such as a cereal product, the model product studied has a longer induction period than the 28 week period over which oxidation was monitored, prior to experiencing oxidation of the fatty acid. Furthermore, the water activity of the product was adjusted to be at or near the B.E.T. monolayer level, which provides conditions which minimize lipid oxidation.

The results of this study demonstrate the ability of impregnating packaging materials with an antioxidants to extent the shelf-life for lipid-containing food products and to give the greatest advantages for polymeric packaging systems.

FUTURE STUDIES

An antioxidant used in plastic materials for food product contact is expected to be an important factor, with respect to indirect food additives for restricted migration regulations. Based on the results of this study, the following future studies are proposed.

1. Various storage stability studies can be carried out to evaluate the effect of relative humidity and temperature on the rate of transfer of antioxidant from film structures and the oxidation of a model product stored in antioxidant impregnated laminate film structures.
2. The study of the partition coefficient and solubility of antioxidants through the respective laminate film layers will provide thermodynamic parameters that measure antioxidant migration from the heat seal layer to HDPE layer and its partition distribution to the food product phase. In addition, knowledge of the diffusion coefficient will include information on the rate of loss of antioxidant from the heat seal layer to the HDPE layer. This study will provide a better understanding of antioxidant transfer between the respective laminate film layers and a food product, to provide information on the levels of antioxidant transfer to a packaged food product.
3. The potential effect of synergetic antioxidant combinations, or other stabilizer/ antioxidant in laminate film structures can be evaluated to provide a better understanding relation between levels of two such components and oxidation

of the film structures during processing as well as product stability during storage.

4. The applications of developed HPLC/MS or Radioactive labelling techniques for antioxidant analysis will be helpful to continue monitoring migrated antioxidants to the fatty food model product packaged in the respective package structures. This method will be useful for actual commercial food products, where it is difficult to isolate antioxidants from fatty food product.
5. To provide the consumer better quality for food products, a limited number of antioxidants in the film structures falling within regulatory requirements may be evaluated by a sensory study of the food products through the storage stability studies. Future studies are required to develop a mass transfer relationship between packaging films and food products for storage conditions where other natural or commercial antioxidants such as the Ascorbic acid, BHA, and Irganox series are considered.

APPENDICES

APPENDIX A

Table 24. The thickness of laminate structures used to fabricate the pouch structures for storage studies.

unit = mil*

Test	Control	BHT	α-tocopherol
1	2.3	2.25	2.3
2	2.35	2.21	2.2
3	2.38	2.01	2.25
Average	2.34	2.16	2.25

*(mil = 1/1000 inch)

Table 25. The initial moisture content of the model product (A, B).

Model(A)	Dw.	Tw	Td	Nw	Mw	IMC	Average
1	1.3081	4.3424	4.2359	2.9278	0.1065	3.6375	3.4606
2	1.3121	4.297	4.2021	2.89	0.0949	3.2837	±0.2502

Model(B)	Dw.	Tw	Td	Nw	Mw	IMC	Average
1	1.3221	3.0732	3.0169	1.6948	0.0563	3.3219	
2	1.3251	3.0678	3.0033	1.6782	0.0645	3.8434	3.6291
3	1.3261	3.0091	2.9494	1.6233	0.0597	3.6777	±0.2196
4	1.3391	3.0381	2.9779	1.6388	0.0602	3.6734	

Dw : Dish Weight (g)
Tw : Total Weight with Dish (g)
Td : Total Weight with Dish after drying (g)
Nw : Net Weight after drying (g)
Mw : Moisture Weight (g)
IMC : % Initial moisture content on a dry basis (gH_2O/g dry weight product)

Table 26. The conditions of relative humidity for the salt solutions according to each temperature.

The model product (A)

Salt solution	Relative humidity (%)		
	At 18 °C Temperature	At 28 °C Temperature	At 38 °C Temperature
Lithium Chloride	9.6	14	11.6
Potassium Acetate	21.4	25	20
Magnesium Chloride	35.5	38	34.5
Potassium Carbonate	46	45.5	44.5
Magnesium nitrate	56	55	53.5
Sodium Nitrate		63	
Sodium Chloride	74.5	73.5	75.5
Ammonium Sulfate	80.5	81.5	81.5
Potassium Nitrate			90.5

The model product (B)

Salt solution	Relative humidity (%)		
	At 18 °C Temperature	At 28 °C Temperature	At 38 °C Temperature
Lithium Chloride	9.4	11	11.4
Potassium Acetate	21.5	23.5	19.8
Magnesium Chloride	35.0	34.5	34.5
Potassium Carbonate	46.0	45.5	47.0
Magnesium nitrate	58.0	54.5	51.0
Sodium Chloride	75.6	75.0	75.5
Ammonium Sulfate	81.5	80.5	81.5

Table 27. Experimental data for equilibrium sorption isotherm of the model product (A) at 18 °C (64 °F). Unit = g (weight)

	Average obtained moisture content as a function of storage time					
Aw	0 days	5 days	10 days	15 days	20 days	25 days
0.096	0.0000	0.0850	0.0876	0.0904	0.0916	0.0910
0.214	0.0000	0.1316	0.1332	0.1346	0.1348	0.1346
0.355	0.0000	0.2310	0.2309	0.2310	0.2309	0.2318
0.46	0.0000	0.2410	0.2410	0.2411	0.2384	0.2410
0.56	0.0000	0.3100	0.3157	0.3158	0.3148	0.3125
0.745	0.0000	0.4883	0.4997	0.5006	0.5032	0.5044
0.805	0.0000	0.5896	0.6090	0.6177	0.6318	0.6449

*Average of three replicate sample data

Table 28. Experimental data for equilibrium sorption isotherm of the model product (A) at 28 °C (84 °F). Unit = g (weight)

	Average obtained moisture content as a function of storage time					
Aw	0 days	5 days	10 days	15 days	20 days	25 days
0.14	0.0000	0.0762	0.0805	0.0790	0.0966	0.0982
0.25	0.0000	0.0885	0.0941	0.0999	0.1432	0.1345
0.38	0.0000	0.1452	0.1495	0.1507	0.1867	0.2036
0.455	0.0000	0.1993	0.2033	0.2060	0.2453	0.2600
0.55	0.0000	0.2560	0.2598	0.2672	0.3074	0.3208
0.63	0.0000	0.3996	0.3885	0.3800	0.3778	0.3728
0.735	0.0000	0.4641	0.5007	0.5774	0.5657	0.5543
0.815	0.0000	0.5581	0.5941	0.6424	0.6250	0.6149

*Average of three replicate sample data

Table 29. Experimental data for equilibrium sorption isotherm of the model product (A) at 38 °C (100 °F). Unit = g (weight)

	Average obtained moisture content as a function of storage time					
Aw	0 days	5 days	10 days	15 days	20 days	25 days
0.116	0.0000	0.0786	0.1203	0.1263	0.1188	0.1149
0.2	0.0000	0.1127	0.1216	0.1505	0.1479	0.1425
0.345	0.0000	0.1445	0.1460	0.1758	0.1816	0.1779
0.445	0.0000	0.2046	0.2421	0.2454	0.2341	0.2403
0.535	0.0000	0.2591	0.2909	0.2994	0.2917	0.2866
0.755	0.0000	0.5498	0.5450	0.5413	0.5277	0.5225
0.815	0.0000	0.6611	0.6642	0.6562	0.6431	0.6425
0.905	0.0000	1.0498	1.0769	1.0830	1.0743	1.0691

*Average of three replicate sample data

Table 30. Experimental data for equilibrium sorption isotherm of the model product (B) at 18 °C (64 °F). Unit = g (weight)

	Average obtained moisture content as a function of storage time					
Aw	0 days	5 days	10 days	15 days	20 days	25 days
0.094	0.0000	0.0779	0.0862	0.0891	0.0858	0.0888
0.215	0.0000	0.1510	0.1536	0.1563	0.1485	0.1510
0.35	0.0000	0.1945	0.2090	0.2134	0.2094	0.2108
0.46	0.0000	0.2762	0.2816	0.2850	0.2820	0.2832
0.58	0.0000	0.3408	0.3479	0.3523	0.3486	0.3486
0.756	0.0000	0.7031	0.7073	0.7144	0.7080	0.7092
0.815	0.0000	0.7932	0.8146	0.8349	0.8252	0.8304

*Average of three replicate sample data

Table 31. Experimental data for equilibrium sorption isotherm of the model product (B) at 28 °C (84 °F). Unit = g (weight)

	Average obtained moisture content as a function of storage time					
Aw	0 days	5 days	10 days	15 days	20 days	25 days
0.11	0.0000	0.0559	0.0652	0.0632	0.0638	0.0597
0.235	0.0000	0.1014	0.1086	0.1095	0.1097	0.1101
0.345	0.0000	0.1819	0.1853	0.1872	0.1868	0.1873
0.455	0.0000	0.2454	0.2465	0.2484	0.2480	0.2496
0.545	0.0000	0.2927	0.2921	0.2945	0.2912	0.2935
0.75	0.0000	0.5029	0.5170	0.5236	0.5195	0.5208
0.805	0.0000	0.7128	0.7095	0.7084	0.7070	0.7153

*Average of three replicate sample data

Table 32. Experimental data for equilibrium sorption isotherm of the model product (B) at 38 °C (100 °F). Unit = g (weight)

	Average obtained moisture content as a function of storage time					
Aw	0 days	5 days	10 days	15 days	20 days	25 days
0.114	0.0000	0.0421	0.0306	0.0314	0.0308	0.0353
0.198	0.0000	0.1000	0.1045	0.1075	0.1063	0.1152
0.345	0.0000	0.1500	0.1506	0.1514	0.1496	0.1505
0.47	0.0000	0.2282	0.2286	0.2345	0.2320	0.2352
0.51	0.0000	0.2665	0.2664	0.2684	0.2666	0.2669
0.755	0.0000	0.5189	0.5127	0.5177	0.4863	0.5030
0.815	0.0000	0.6321	0.6325	0.6514	0.6363	0.6228

*Average of three replicate sample data

APPENDIX B

Isotherm Model using the Mathematical Expression

The equilibrium sorption isotherm of the model product describes the relationship between the product's moisture content at a given water activity. From an initial examination of a series of equations developed to describe equilibrium sorption isotherms, the following models or expressions were selected.

- Henderson Equation
- Chen Equation
- Halsey Equation
- Guggenhem-Anderson-de Boer (G.A.B.) Equation
- Brunauer, Emmett and Teller (B.E.T.) Equation

These equations represented a synopsis of the characteristic geometric configurations of sorption isotherm shapes that have been transformed to convenient linearized forms. The linearized equations are as follows:

Table 33. Isotherm Mathematical model (Berends, 1993).

Model	Equation
1. Henderson	Ln [-ln(1-aw)] = nln Meq + ln K
2. Chen	Ln (-ln aw) = K – aMeq
3. Halsey	Aw = exp (-a/Meq)
4. G.A.B.	Meq = C(K) (aw) (Wm) / (1-Kaw) (1-Kaw + Ckaw)
5. B.E.T.	Aw/Meq (1-aw) = 1/MmC + aw (C-1/MmC)

where; aw = water activity,
Meq = equilibrium moisture content,
Mm = monolayer moisture content,
n, K, C = constants

For the freeze-dried product model, the best fit of the experimental equilibrium sorption data to a linearized form of the isotherm expressions was determined by linear regression analysis. The correlation coefficient was determined and was applied to the degree of fit among the five equations. The estimation for the parameters in the respective expressions was calculated graphically using slope and intercept values.

By substituting these parameters back into the isotherm equations, calculated sorption data was obtained (see Tables 34-39). A comparison of the experimental and calculated isotherm data was given by a value of sums of squares, which provided the basis for selection of the best fit model.

For all cases, the mathematical equation that best described the sorption isotherm of the model products was the Halsey equation, except for model product B at 38°C, which was best described by the Henderson equation. The linearized plots of the best-fit model are presented graphically in Figures 25-30, respectively.

Table 34. The data of model product (A) for Halsey equation at 18°C (64°F).

Halsey Equation model

	X axis	y axis	Ln(-ln(aw))=-1.6011ln(Meq)+4.1983		
Aw	Ln(Meq)	ln(-ln(aw))	Actual	Mathematical	% difference
0.096	2.0981	0.8516	8.1504	8.0869	-0.7851
0.214	2.3867	0.4329	10.8778	10.5038	-3.5608
0.355	2.5838	0.0350	13.2473	13.4673	1.6335
0.46	2.7422	-0.2529	15.5210	16.1207	3.7199
0.56	2.9484	-0.5450	19.0749	19.3473	1.4077
0.745	3.4064	-1.2229	30.1573	29.5455	-2.0707
0.805	3.5816	-1.5283	35.9295	35.7532	-0.4930

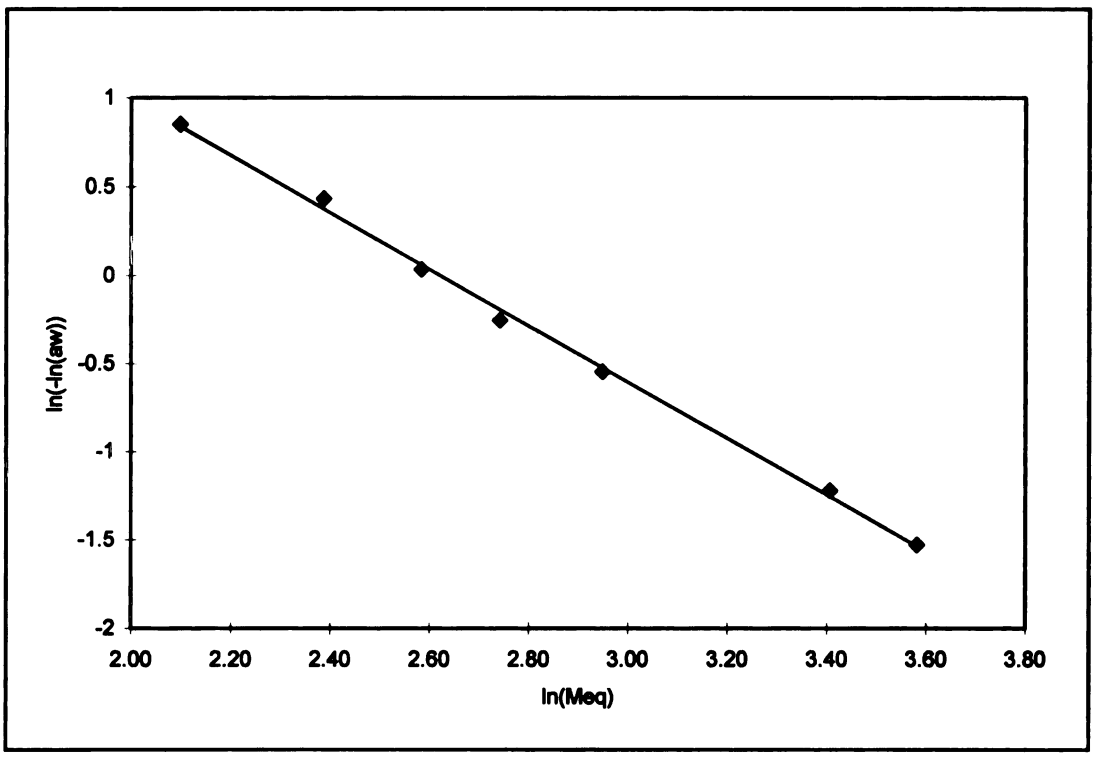

Figure 25. The plot of linear regression of Halsey equation for model product (A) at 18°C.

Table 35. The data of model product (A) for Halsey equation at 28°C (84°F).

Halsey Equation model

	X axis	y axis	Ln(-ln(aw))=-1.6719ln(Meq)+4.392		
Aw	Ln(Meq)	ln(-ln(aw))	Actual	Mathematical	% difference
0.14	2.1447	0.6761	8.5393	9.2312	7.4950
0.25	2.3550	0.3266	10.5386	11.3769	7.3684
0.38	2.6047	-0.0330	13.5267	14.1069	4.1126
0.455	2.7683	-0.2390	15.9322	15.9566	0.1526
0.55	2.8976	-0.5144	18.1299	18.8149	3.6406
0.63	3.0894	-0.7721	21.9630	21.9501	-0.0590
0.735	3.3790	-1.1780	29.3419	27.9819	-4.8604
0.815	3.5333	-1.5869	34.2381	35.7334	4.1847

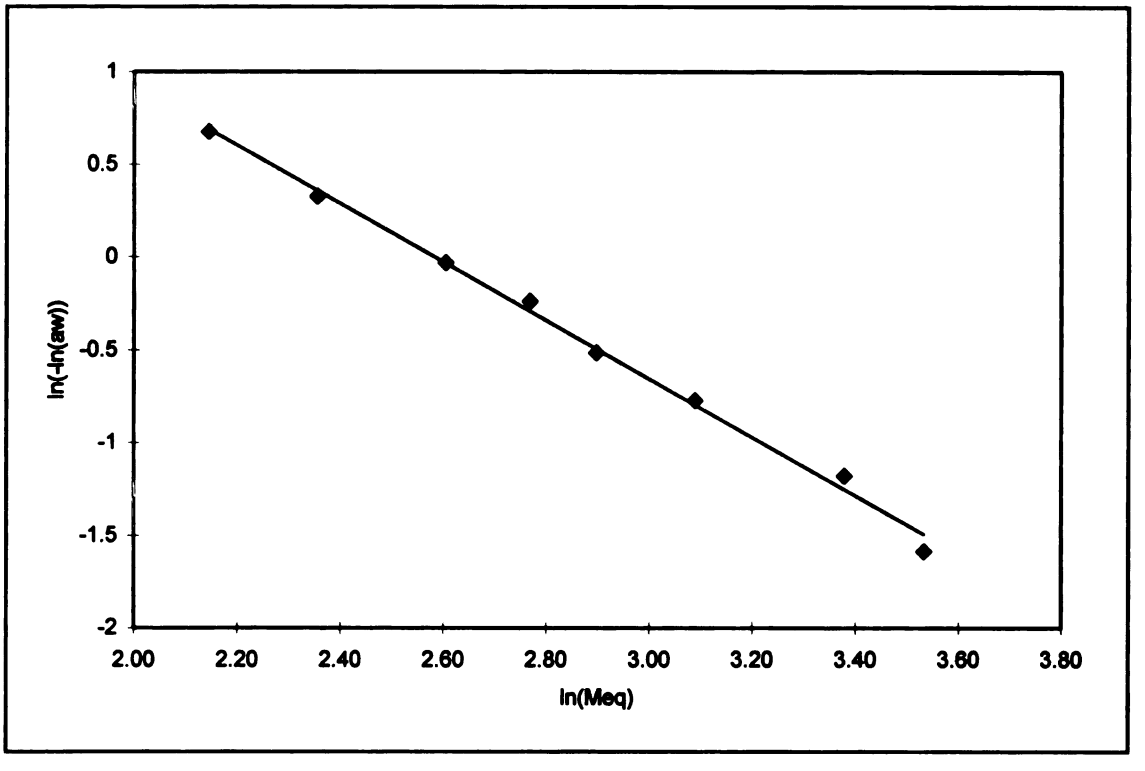

Figure 26. The plot of linear regression of Halsey equation for model product (A) at 28°C.

Table 36. The data of model product (A) for Halsey equation at 38°C (100°F).

Halsey Equation model

	X axis	y axis	Ln(-ln(aw))=-1.6886ln(Meq)+4.3592		
Aw	Ln(Meq)	ln(-ln(aw))	Actual	Mathematical	% difference
0.116	2.1724	0.7674	9.2381	8.3904	-10.1031
0.2	2.3303	0.4759	10.7463	9.9714	-7.7710
0.345	2.5370	0.0622	13.1163	12.7393	-2.9593
0.445	2.7016	-0.2111	15.3889	14.9778	-2.7443
0.535	2.7892	-0.4692	16.7582	17.4515	3.9728
0.755	3.3240	-1.2693	28.3094	28.0283	-1.0029
0.815	3.4744	-1.5869	32.8359	33.8282	2.9335
0.905	4.0090	-2.3044	55.5797	51.7393	-7.4226

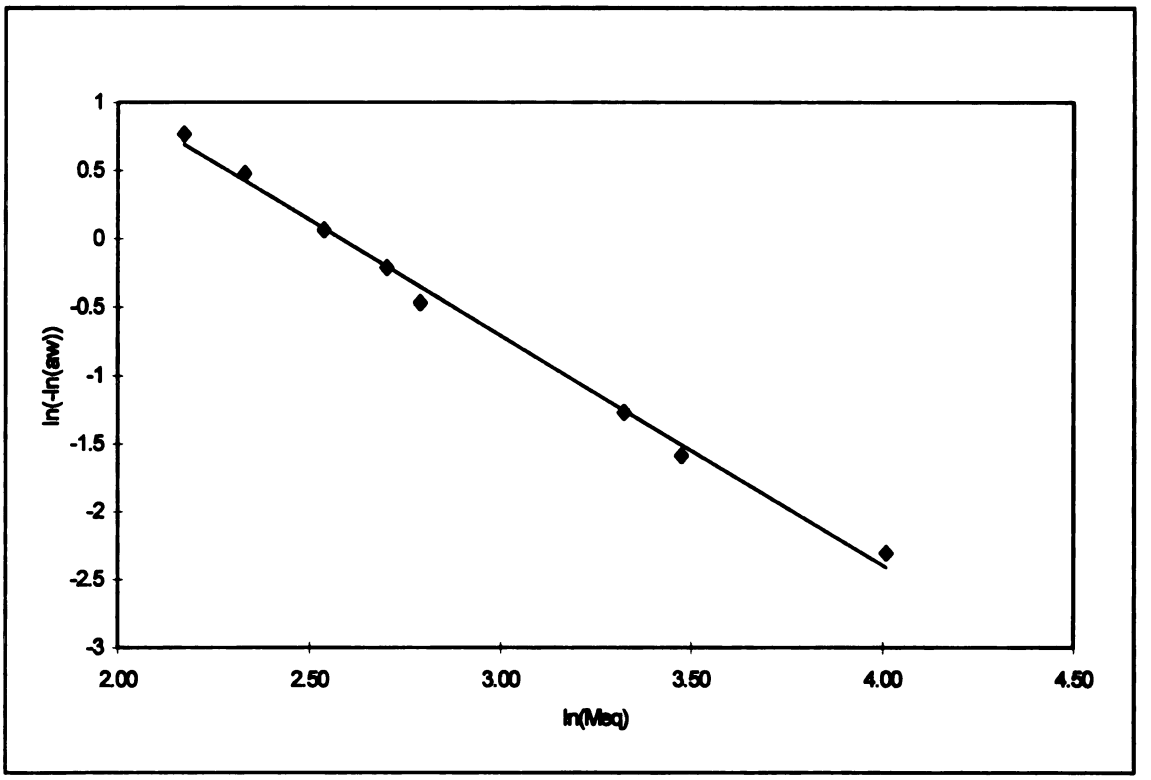

Figure 27. The plot of linear regression of Halsey equation for model product (A) at 38°C.

Table 37. The data of model product (B) for Halsey equation at 18°C (64°F)

Halsey Equation model

	X axis	y axis	Ln(-ln(aw))=-1.4356ln(Meq)+3.8456		
Aw	Ln(Meq)	ln(-ln(aw))	Actual	Mathematical	% difference
0.094	2.0852	0.8606	8.0458	7.9989	-0.5862
0.215	2.3672	0.4299	10.6671	10.7971	1.2043
0.35	2.6645	0.0486	14.3611	14.0817	-1.9846
0.46	2.8615	-0.2529	17.4871	17.3730	-0.6565
0.58	3.0660	-0.6075	21.4555	22.2399	3.5272
0.756	3.5924	-1.2740	36.3225	35.3807	-2.6620
0.815	3.7738	-1.5869	43.5431	43.9962	1.0298

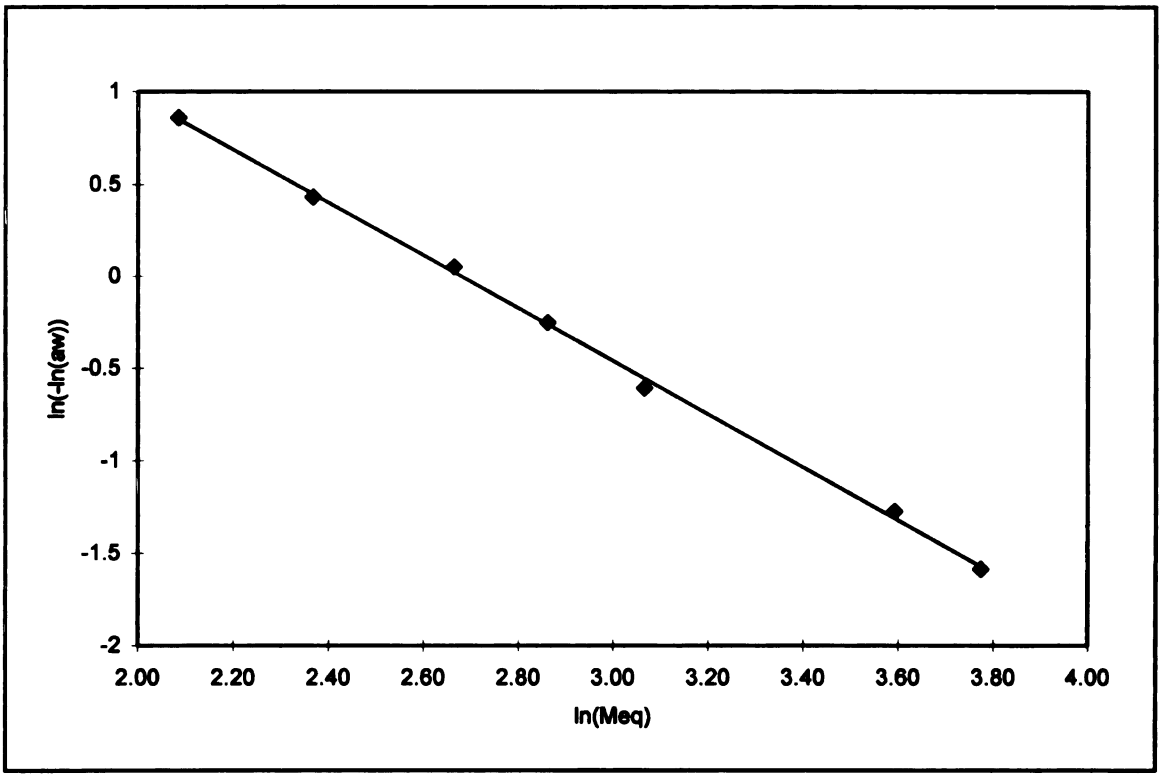

Figure 28. The plot of linear regression of Halsey equation for model product (B) at 18°C.

Table 38. The data of model product (B) for Halsey equation at 28°C (84°F).

Halsey Equation model

	X axis	y axis	Ln(-ln(aw))=-1.3353ln(Meq)+3.3906		
Aw	Ln(Meq)	ln(-ln(aw))	Actual	Mathematical	% difference
0.11	1.9016	0.7918	6.6965	7.0025	4.3698
0.235	2.2306	0.3703	9.3052	9.6012	3.0833
0.345	2.5393	0.0622	12.6711	12.0927	-4.7837
0.455	2.8022	-0.2390	16.4800	15.1523	-8.7624
0.545	2.9351	-0.4993	18.8241	18.4140	-2.2274
0.75	3.4052	-1.2459	30.1192	32.2092	6.4889
0.805	3.6742	-1.5283	39.4153	39.7938	0.9510

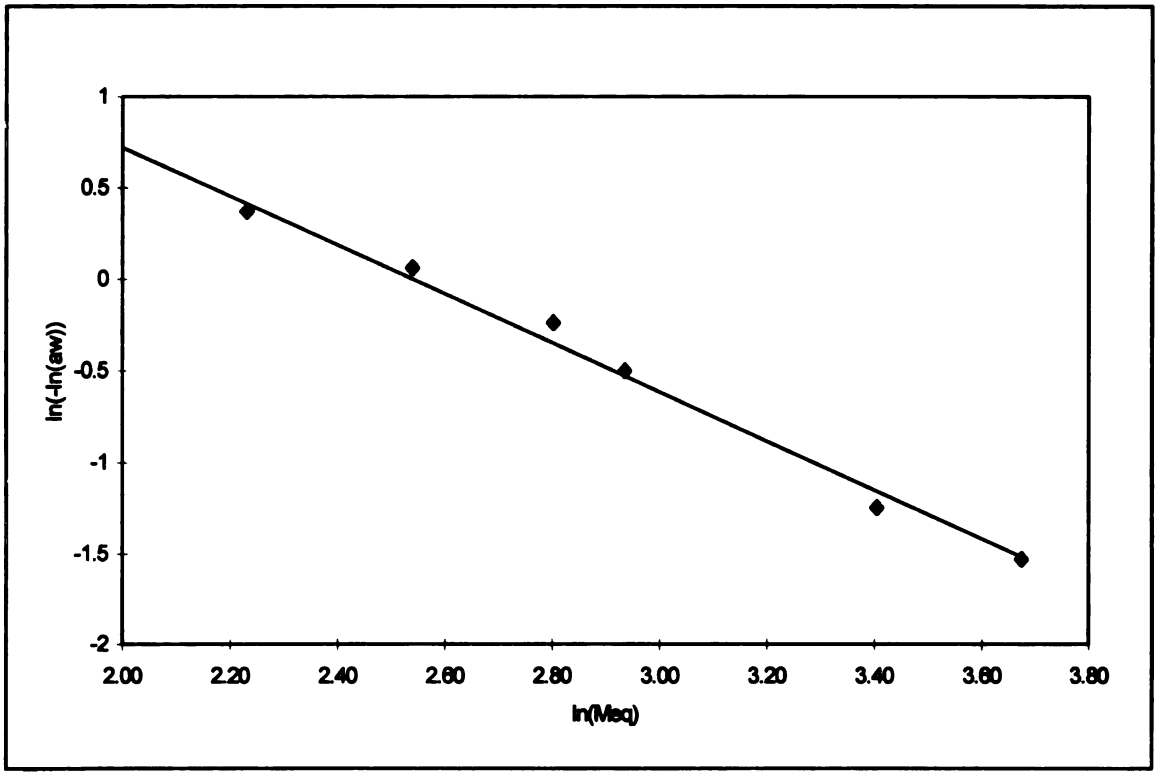

Figure 29. The plot of linear regression of Halsey equation for model product (B) at 28°C.

Table 39. The data of model product (B) for Henderson equation at 38°C (100°F).

Henderson Equation model

	X axis	y axis	Ln(-ln(1-aw))=1.4187ln(Meq)-4.4876		
Aw	Ln(Meq)	ln(-ln(1-aw))	Actual	Mathematical	% difference
0.114	1.6930	-2.1117	5.4358	5.3374	-1.8441
0.198	2.2502	-1.5112	9.4891	8.1497	-16.4353
0.345	2.4529	-0.8601	11.6215	12.8960	9.8831
0.47	2.7561	-0.4543	15.7390	17.1661	8.3138
0.51	2.8527	-0.3378	17.3351	18.6358	6.9793
0.755	3.4437	0.3411	31.3016	30.0725	-4.0873
0.815	3.5854	0.5232	36.0693	34.1908	-5.4940

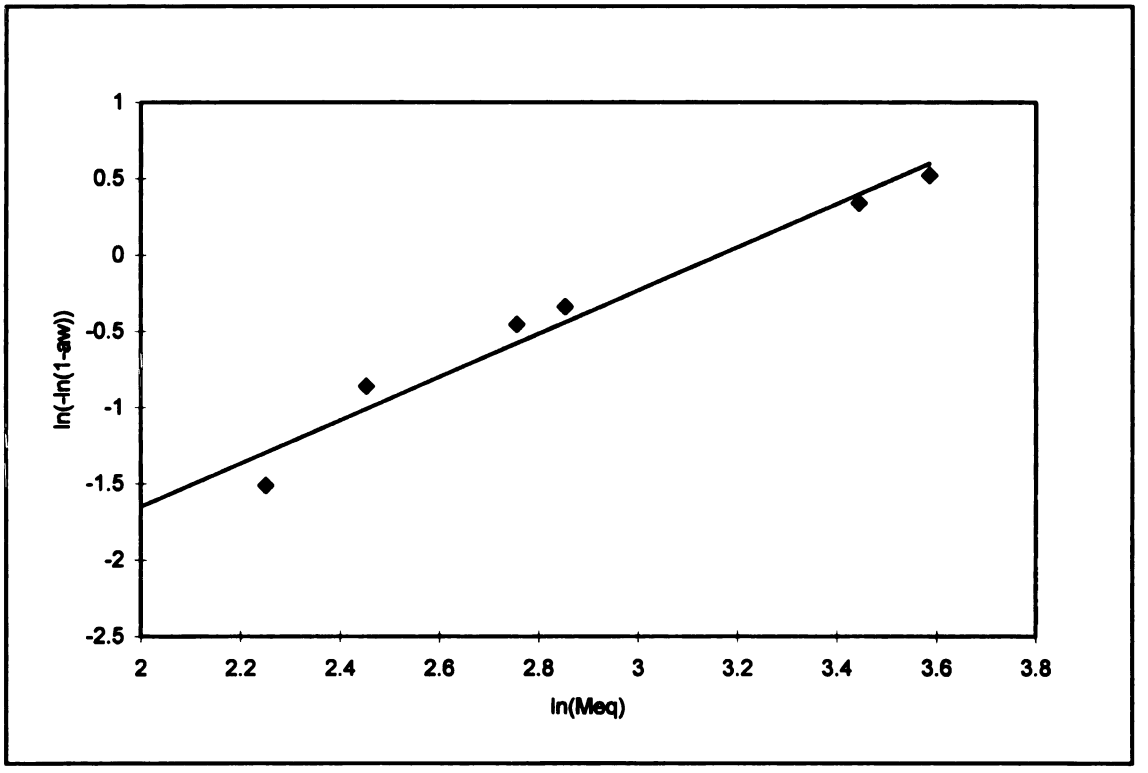

Figure 30. The plot of linear regression of Henderson equation for model product (B) at 38°C.

Brunauer, Emmett and Teller (B.E.T.) Monolayer Value

Estimation of the B.E.T. monolayer value has been used to determine the water activity value which could provide the maximum shelf life for the dried model product. Also, the Aw levels generated to obtain the monolayer values from the B.E.T. equation expression are derived from the actual isotherm data in the water activity range below Aw=0.35 (C. van den berg, 1985). Below the B.E.T. monolayer value, the rate of lipid oxidation generally increases. Above the monolayer value, the rate of lipid oxidation is again accelerated, according to increasing water activity (Leung, 1987).

The B.E.T. equation shows a linear relationship between Aw and the equilibrium moisture content of the model product. From the equilibrium sorption isotherm values, a straight line relationship was obtained from a plot of Aw/[m (1-Aw)] against Aw.

Using the slope and y-intercept values for the B.E.T. regression equation, the monolayer moisture content was determined by substitution into the following equation:

$$\text{Monolayer value} = 1 / (\text{y-intercept} + \text{slope}) \qquad \text{-------} (16)$$

The monolayer values calculated for the freeze-dried product model at 18, 28, and 38°C, respectively are summarized in Tables 40, 41, and 42. The corresponding water activity values were also estimated and compared to the water activity values determined from the Halsey equation and the Henderson equation (38°C, model product B), which best described the product sorption isotherm data.

Table 40. The monolayer values of high (A) and low (B) linoleic acid containing freeze-dried model product according to Sorption Isotherm at 18°C.

At 18°C temperature	Model Product (A)	Model Product (B)
Moisture Content ($gH_20/100g$) of the B.E.T. monolayer value	8.57	9.88
The Aw of the sorption isotherm at the B.E.T. monolayer value	0.11	0.14

Table 41. The monolayer values of high (A) and low (B) linoleic acid containing freeze-dried model product according to Sorption Isotherm at 28°C.

At 28°C temperature	Model Product (A)	Model Product (B)
Moisture Content ($gH_20/100g$) of the B.E.T. monolayer value	9.04	9.84
The Aw of the sorption isotherm at the B.E.T. monolayer value	0.16	0.25

Table 42. The monolayer values of high (A) and low (B) linoleic acid containing freeze-dried model product according to Sorption Isotherm at 38°C.

At 38°C temperature	Model Product (A)	Model Product (B)
Moisture Content ($gH_20/100g$) of the B.E.T. monolayer value	8.38	9.23
The Aw of the sorption isotherm at the B.E.T. monolayer value	0.08	0.18

The monolayer values for model product (A), at each temperature, were 8.57 (18°C), 9.04 (28°C), and 8.38 (38°C) $gH_20/100g$ dry product, respectively. The monolayer values for model product (B), at each temperature, were calculated to be 9.88 (18°C), 9.84 (28°C), and 9.23 (38°C) $gH_20/100g$ dry product, respectively. The Aw levels corresponding to the monolayer value of the model product (A) were 0.11 (18°C), 0.16 (28°C), and 0.08 (38°C), respectively. The Aw levels corresponding to the monolayer value of the model product (B) were calculated to be 0.14 (18°C), 0.25 (28°C), and 0.18 (38°C), respectively. The regression plots of the B.E.T. equation for monolayer values, using the data for the low moisture range of the sorption isotherm at each temperature, are shown in Figures 31-36, and the numerical data summarized in Tables 43-48, respectively.

Table 43. The data of model product (A) for B.E.T. monolayer value at 18°C (64°F).

	x axis	y axis
Aw	(aw)	aw/(Meq(1-aw))
0.096	0.096	0.0130
0.214	0.214	0.0250
0.355	0.352	0.0416
0.46	0.46	0.0549

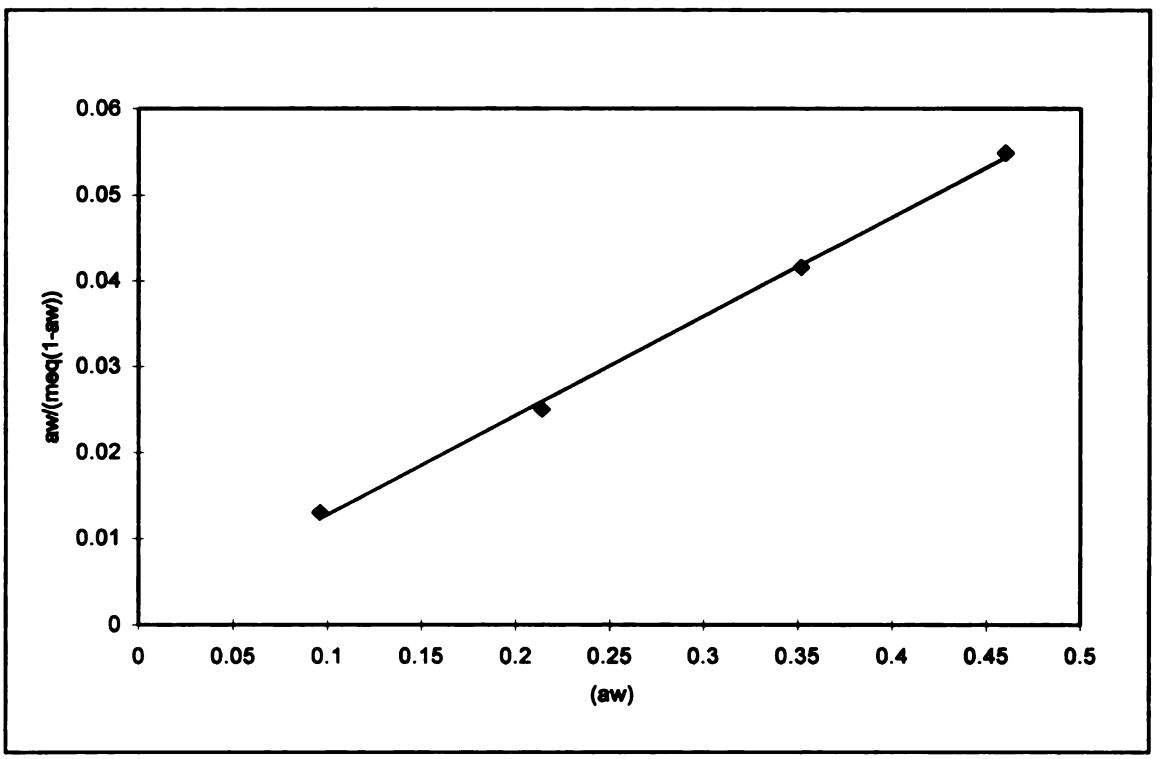

Figure 31. The linear regression plot of B.E.T. equation for the monolayer value of model product (A) at 18°C.

Table 44. The data of model product (A) for B.E.T. monolayer value at 28°C (84°F).

	x axis	y axis
Aw	(aw)	aw/(Meq(1-aw))
0.14	0.14	0.0191
0.25	0.25	0.0316
0.38	0.38	0.0453
0.455	0.455	0.0524

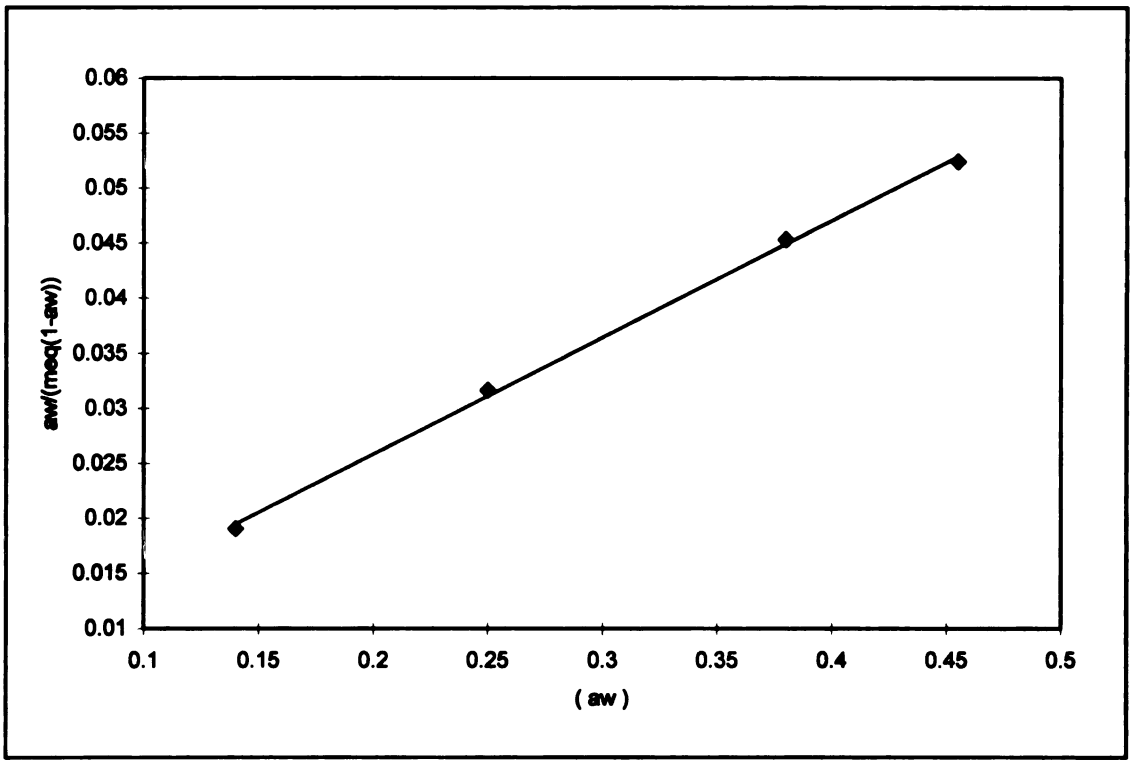

Figure 32. The linear regression plot of B.E.T. equation for the monolayer value of model product (A) at 28°C.

Table 45. The data of model product (A) for B.E.T. monolayer value at 38°C (100°F).

	x axis	y axis
Aw	(aw)	aw/(Meq(1-aw))
0.116	0.116	0.0150
0.2	0.2	0.0243
0.345	0.345	0.0417
0.445	0.445	0.0538

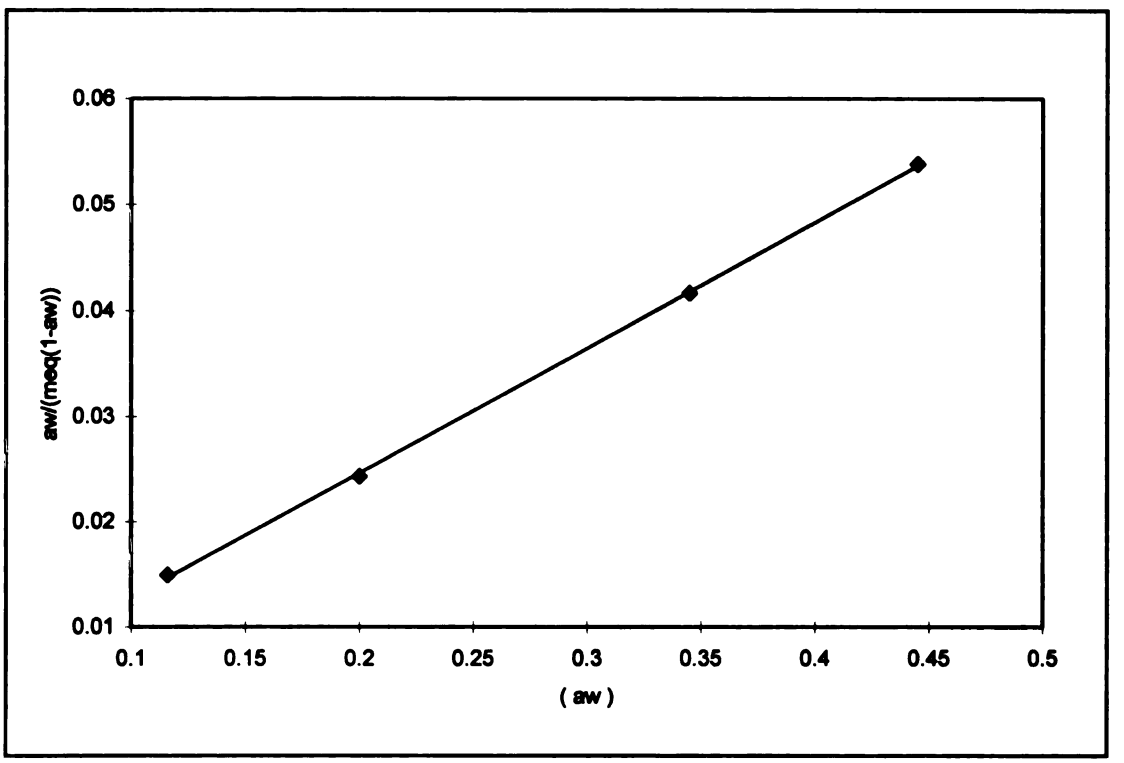

Figure 33. The linear regression plot of B.E.T. equation for the monolayer value of model product (A) at 38°C.

Table 46. The data of model product (B) for B.E.T. monolayer value at 18°C (64°F).

	x axis	y axis
Aw	(aw)	aw/(Meq(1-aw))
0.094	0.096	0.0132
0.215	0.214	0.0255
0.35	0.352	0.0383
0.46	0.46	0.0487

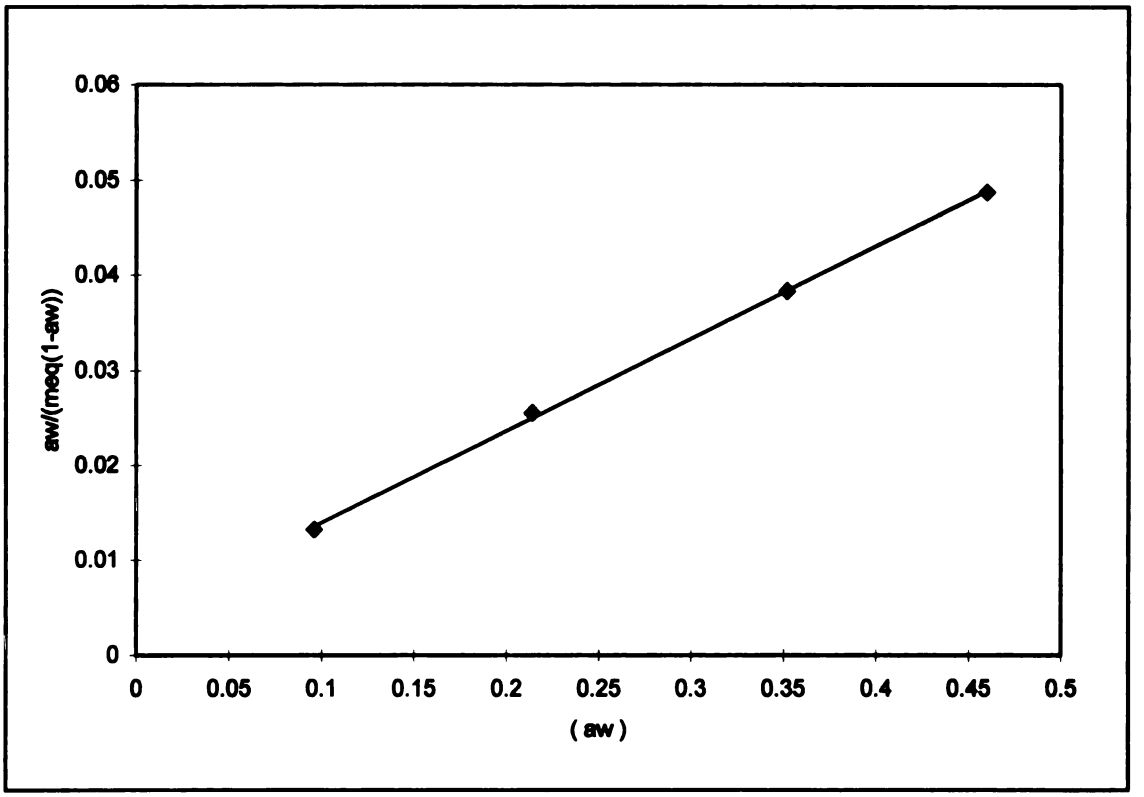

Figure 34. The linear regression plot of B.E.T. equation for the monolayer value of model product (B) at 18°C.

Table 47. The data of model product (B) for B.E.T. monolayer value at 28°C (84°F).

	x axis	y axis
Aw	(aw)	aw/(Meq(1-aw))
0.11	0.11	0.0185
0.235	0.235	0.0330
0.345	0.345	0.0416
0.455	0.455	0.0507

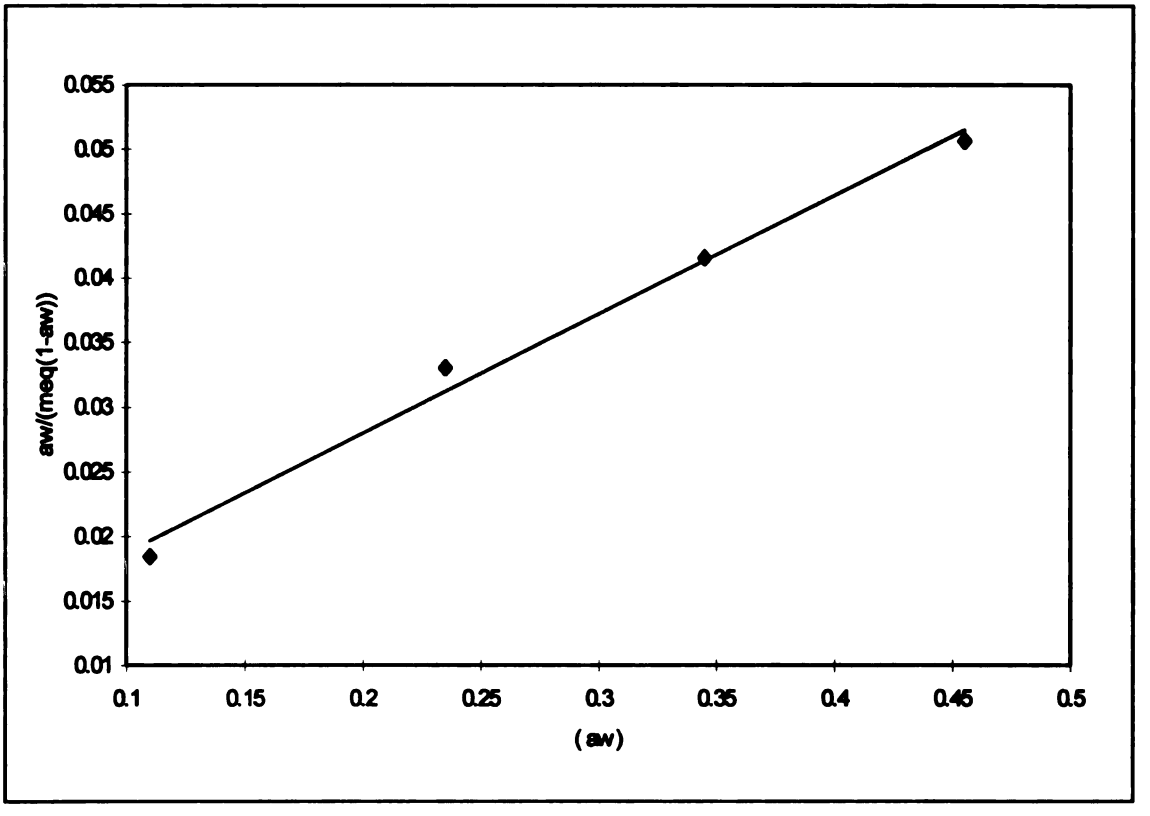

Figure 35. The linear regression plot of B.E.T. equation for the monolayer value of model product (B) at 28°C.

Table 48. The data of model product (B) for B.E.T. monolayer value at 38°C (100°F).

	x axis	y axis
Aw	(aw)	aw/(Meq(1-aw))
0.114	0.114	0.0237
0.198	0.198	0.0260
0.345	0.345	0.0453
0.47	0.47	0.0563

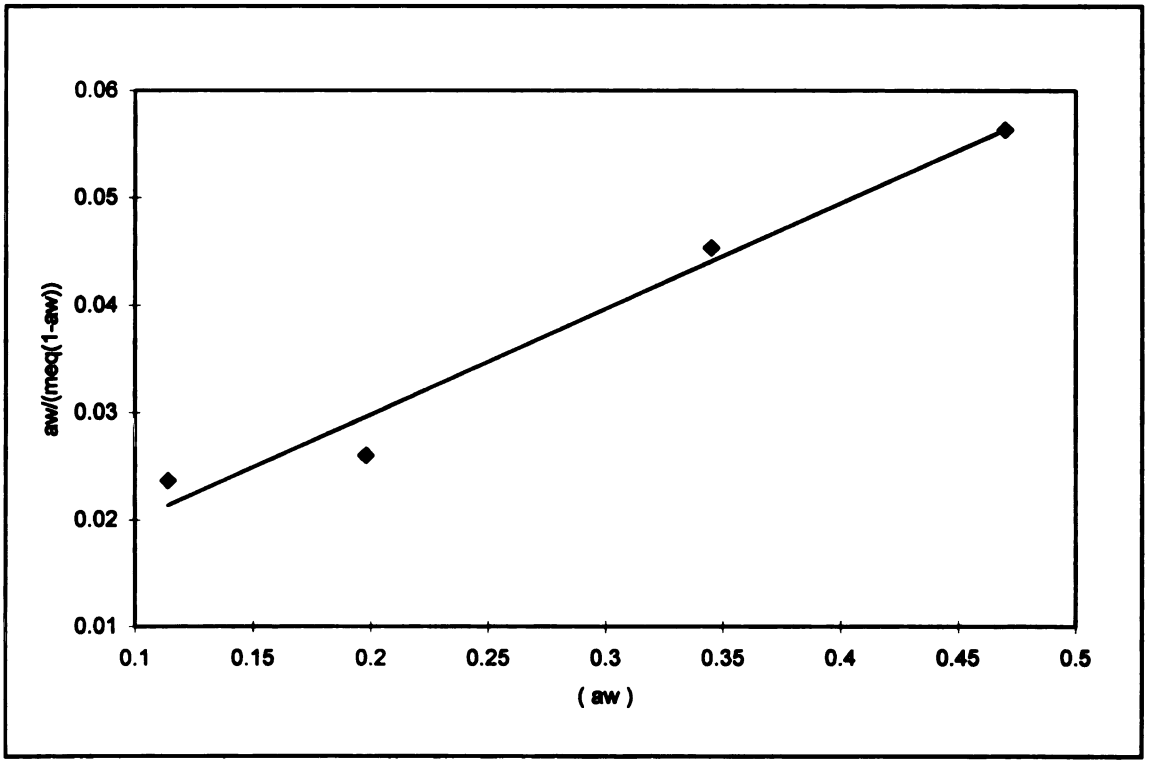

Figure 36. The linear regression plot of B.E.T. equation for the monolayer value of model product (B) at 38°C.

Statistical Selection of Best Fit Model

Correlation coefficient values for the x-y components of the linearized forms of the respective isotherm expressions were calculated from the isotherm data using the Minitab Statistic Program (Minitab Inc., PA). Results for the respective isotherm models are summarized in Tables 48-49, and formed the basis for selecting the best fit isotherm equation.

The best-fit model was based on the best correlation between the components of the x-y axis, and the lowest sums of squares at each temperature condition. Here, the Halsey model showed a consistently low sum of squares and a correlation coefficient very close to 1 at each temperature, and was selected to describe the equilibrium sorption isotherm for the product model. As indicated above, for model product B at 38°C, the Henderson model was found to give the best fit.

Table 49. The Correlation Coefficient and Sums of Squares from the isotherm data and the respective isotherm models for product model A at different temperatures (18°C, 28°C, 38°C).

Model	Sum of Squares for Error			Correlation Coefficient (ρ)		
(A)	18°C	28°C	38°C	18°C	28°C	38°C
Henderson	26.52	16.89	113.7	0.973	0.981	0.950
Chen	34.95	18.81	187.6	0.974	0.983	0.949
Halsey	0.89	4.92	9.8	0.999	0.996	0.997
G.A.B.	70.20	49.80	199.50	0.919	0.934	0.870
B.E.T.	35.49	97.64	1426.2	0.973	0.991	0.671

Table 50. The Correlation Coefficient and Sums of Squares from the isotherm data and the respective isotherm models for product model B at different temperatures (18°C, 28°C, 38°C).

Model	Sum of Squares for Error			Correlation Coefficient (ρ)		
(B)	18°C	28°C	38°C	18°C	28°C	38°C
Henderson	36.83	21.40	8.97	0.977	0.984	0.993
Chen	61.1	37.73	17.90	0.973	0.978	0.989
Halsey	1.8	5.7	15.22	0.999	0.997	0.992
G.A.B.	91.26	51.42	33.56	0.932	0.955	0.971
B.E.T.	21.3	15.82	33.11	0.990	0.991	0.981

APPENDIX C

Table 51. The mathematical model for equilibrium moisture content from the experimental data of the model product A at 18 °C (64 °F).

Henderson Equation model

	x axis	y axis	ln(-ln(1-aw))=1.7775ln(Meq)-5.6458		
Aw	ln(Meq)	ln(-ln(1-aw))	Actual	Mathematical	% difference
0.096	2.098067006	-2.293368511	8.1504	6.5932	-23.6184
0.214	2.386724015	-1.423794851	10.8778	10.7537	-1.1541
0.355	2.583793758	-0.824384151	13.2473	15.0664	12.0742
0.46	2.742193946	-0.484206187	15.5210	18.2443	14.9266
0.56	2.948373335	-0.197255858	19.0749	21.4406	11.0336
0.745	3.406427017	0.312246677	30.1573	28.5577	-5.6015
0.805	3.581558685	0.491493387	35.9295	31.5877	-13.7453

Chen Equation model

	X axis	y axis	ln(-lnaw)=-0.0807(Meq)+1.2144		
Aw	(Meq)	ln(-lnaw)	Actual	Mathematical	% difference
0.096	8.1504	0.851605891	8.1504	4.4956	-81.2977
0.214	10.8778	0.432937116	10.8778	9.6836	-12.3327
0.355	13.2473	0.035017169	13.2473	14.6144	9.3545
0.46	15.521	-0.252921561	15.5210	18.1824	14.6373
0.56	19.0749	-0.545040164	19.0749	21.8022	12.5094
0.745	30.1573	-1.222914197	30.1573	30.2022	0.1485
0.805	35.9295	-1.52825892	35.9295	33.9859	-5.7190

G.A.B Equation model

	x axis	y axis	(aw/Meq)=0.013aw+0.0175		
Aw	(aw)	(aw/Meq)	Actual	Mathematical	% difference
0.096	0.096	0.011778563	8.1504	5.1205	-59.1705
0.214	0.214	0.019673096	10.8778	10.5512	-3.0951
0.355	0.352	0.026797914	13.2473	16.0525	17.4749
0.46	0.46	0.029637266	15.5210	19.5911	20.7754
0.56	0.559	0.029357952	19.0749	22.5989	15.5936
0.745	0.745	0.024703803	30.1573	27.4048	-10.0438
0.805	0.805	0.022404988	35.9295	28.7860	-24.8160

B.E.T. Equation model

	x axis	y axis	Aw/(Meq(1-aw))=0.1394aw-0.0054		
Aw	(aw)	aw/(Meq(1-aw))	Actual	Mathematical	% difference
0.096	0.096	0.013029384	8.1504	13.3036	38.7354
0.214	0.214	0.025029384	10.8778	11.1440	2.3883
0.355	0.352	0.041547153	13.2473	12.4841	-6.1132
0.46	0.46	0.054883825	15.5210	14.5060	-6.9969
0.56	0.559	0.066722618	19.0749	17.5152	-8.9046
0.745	0.745	0.096877659	30.1573	29.6748	-1.6261
0.805	0.805	0.114897372	35.9295	38.6475	7.0327

Table 52. The mathematical model for equilibrium moisture content from the experimental data of the model product A at 28 °C (84 °F).

Henderson Equation model

	x axis	y axis	ln(-ln(1-aw))=1.7523ln(Meq)-5.5129		
Aw	ln(Meq)	ln(-ln(1-aw))	Actual	Mathematical	% difference
0.14	2.144679	-1.891649046	8.5393	7.8977	-8.1240
0.25	2.3550447	-1.245899324	10.5386	11.4168	7.6921
0.38	2.6046655	-0.738069652	13.5267	15.2548	11.3281
0.455	2.7683422	-0.499276762	15.9322	17.4819	8.8647
0.55	2.8975625	-0.225010673	18.1299	20.4439	11.3188
0.63	3.0893592	-0.005764308	21.9630	23.1687	5.2042
0.735	3.3790165	0.283693217	29.3419	27.3302	-7.3608
0.815	3.5333391	0.523188559	34.2381	31.3328	-9.2723

Chen Equation model

	X axis	y axis	ln(-lnaw)=-0.086(Meq)+1.2497		
Aw	(Meq)	ln(-lnaw)	Actual	Mathematical	% difference
0.14	8.5393	0.676058424	8.5393	6.6703	-28.0207
0.25	10.5386	0.32663426	10.5386	10.7333	1.8142
0.38	13.5267	-0.032953009	13.5267	14.9146	9.3055
0.455	15.9322	-0.238945421	15.9322	17.3098	7.9587
0.55	18.1299	-0.514437136	18.1299	20.5132	11.6185
0.63	21.963	-0.772113638	21.9630	23.5095	6.5780
0.735	29.3419	-1.178029658	29.3419	28.2294	-3.9409
0.815	34.2381	-1.586858919	34.2381	32.9832	-3.8045

G.A.B Equation model

	x axis	y axis	(aw/Meq)=0.0117aw+0.0191		
Aw	(aw)	(aw/Meq)	Actual	Mathematical	% difference
0.14	0.14	0.016394786	8.5393	6.7509	-26.4914
0.25	0.25	0.023722316	10.5386	11.3507	7.1549
0.38	0.38	0.028092587	13.5267	16.1386	16.1843
0.455	0.455	0.028558517	15.9322	18.6296	14.4791
0.55	0.55	0.030336626	18.1299	21.5391	15.8278
0.63	0.63	0.028684606	21.9630	23.7996	7.7171
0.735	0.735	0.025049503	29.3419	26.5348	-10.5790
0.815	0.815	0.023803891	34.2381	28.4612	-20.2976

B.E.T. Equation model

	x axis	y axis	Aw/(Meq(1-aw))=0.1526aw-0.0118		
Aw	(aw)	aw/(Meq(1-aw))	Actual	Mathematical	% difference
0.14	0.14	0.019063705	8.5393	17.0212	49.8314
0.25	0.25	0.031629755	10.5386	12.6502	16.6924
0.38	0.38	0.045310625	13.5267	13.2698	-1.9364
0.455	0.455	0.052400948	15.9322	14.4858	-9.9847
0.55	0.55	0.067414725	18.1299	16.9447	-6.9944
0.63	0.63	0.077525962	21.9630	20.1890	-8.7868
0.735	0.735	0.094526425	29.3419	27.6361	-6.1724
0.815	0.815	0.128669681	34.2381	39.1352	12.5132

Table 53. The mathematical model for equilibrium moisture content from the experimental data of the model product A at 38 °C (100 °F).

Henderson Equation model

	x axis	y axis	ln(-ln(1-aw))=1.5425ln(Meq)-4.9409		
Aw	ln(Meq)	ln(-ln(1-aw))	Actual	Mathematical	% difference
0.116	2.1723853	-2.093149335	9.2381	6.3356	-45.8109
0.2	2.330317	-1.499939987	10.7463	9.3070	-15.4648
0.345	2.5369613	-0.86009935	13.1163	14.0916	6.9209
0.445	2.7016431	-0.52969051	15.3889	17.4577	11.8505
0.535	2.7891815	-0.266941489	16.7582	20.6997	19.0416
0.755	3.3239743	0.341102265	28.3094	30.7015	7.7915
0.815	3.4743828	0.523188559	32.8359	34.5483	4.9567
0.905	4.009019	0.856064345	55.5797	42.8695	-29.6485

Chen Equation model

	X axis	y axis	ln(-lnaw)=-0.0646(Meq)+0.8703		
Aw	(Meq)	ln(-lnaw)	Actual	Mathematical	% difference
0.116	8.7792	0.767403218	9.2381	1.5928	-479.9782
0.2	10.2812	0.475884995	10.7463	6.1055	-76.0106
0.345	12.6412	0.06223355	13.1163	12.5088	-4.8568
0.445	14.9042	-0.21111494	15.3889	16.7402	8.0723
0.535	16.2677	-0.469222283	16.7582	20.7356	19.1819
0.755	27.7705	-1.269267061	28.3094	33.1202	14.5253
0.815	32.2779	-1.586858919	32.8359	38.0365	13.6728
0.905	55.0928	-2.304383356	55.5797	49.1437	-13.0963

G.A.B Equation model

	x axis	y axis	(aw/Meq)=0.0053aw+0.0212		
Aw	(aw)	(aw/Meq)	Actual	Mathematical	% difference
0.116	0.116	0.013213049	9.2381	5.3175	-73.7298
0.2	0.2	0.019452982	10.7463	8.9847	-19.6065
0.345	0.345	0.027291713	13.1163	14.9814	12.4496
0.445	0.445	0.029857356	15.3889	18.8891	18.5307
0.535	0.535	0.032887255	16.7582	22.2587	24.7121
0.755	0.755	0.027187123	28.3094	29.9585	5.5047
0.815	0.815	0.025249474	32.8359	31.9364	-2.8165
0.905	0.905	0.016426829	55.5797	34.8124	-59.6550

B.E.T. Equation model

	x axis	y axis	Aw/(Meq(1-aw))=0.1895aw-0.0193		
Aw	(aw)	aw/(Meq(1-aw))	Actual	Mathematical	% difference
0.116	0.116	0.014946888	9.2381	48.9268	81.1186
0.2	0.2	0.024316228	10.7463	13.4409	20.0474
0.345	0.345	0.041666737	13.1163	11.4311	-14.7420
0.445	0.445	0.053797037	15.3889	12.3302	-24.8062
0.535	0.535	0.07072528	16.7582	14.0168	-19.5572
0.755	0.755	0.110967849	28.3094	24.8976	-13.7036
0.815	0.815	0.136483644	32.8359	32.5982	-0.7290
0.905	0.905	0.172913989	55.5797	62.5918	11.2029

Table 54. The mathematical model for equilibrium moisture content from the experimental data of the model product B at 18 °C (64 °F).

Henderson Equation model

	x axis	y axis	Ln(-ln(1-aw))=1.5833ln(Meq)-5.236		
Aw	ln(Meq)	ln(-ln(1-aw))	Actual	Mathematical	% difference
0.094	2.085149443	-2.315508512	8.045794	6.3253	-27.199899
0.215	2.367161688	-1.418521889	10.66707	11.1461	4.29770234
0.35	2.664524768	-0.842150991	14.36112	16.0406	10.4699791
0.46	2.861461895	-0.484206187	17.48707	20.1096	13.0410678
0.58	3.065979049	-0.142139113	21.45546	24.9592	14.0379253
0.756	3.592437467	0.344005968	36.3225	33.9296	-7.0524779
0.815	3.773752144	0.523188559	43.54314	37.9952	-14.601799

Chen Equation model

	X axis	y axis	ln(-lnaw)=-0.0644(Meq)+1.0565		
Aw	(Meq)	ln(-lnaw)	Actual	Mathematical	% difference
0.094	8.045793782	0.860549876	8.045794	3.0427	-164.42908
0.215	10.66707279	0.429908747	10.66707	9.7297	-9.6343884
0.35	14.36112306	0.048620745	14.36112	15.6503	8.23738857
0.46	17.48707253	-0.252921561	17.48707	20.3326	13.9950414
0.58	21.45545766	-0.607470205	21.45546	25.8380	16.961766
0.756	36.32250302	-1.273987974	36.3225	36.1877	-0.3725066
0.815	43.54313884	-1.586858919	43.54314	41.0459	-6.0838966

G.A.B Equation model

	x axis	y axis	(aw/Meq)=0.0072aw+0.018		
Aw	(aw)	(aw/Meq)	Actual	Mathematical	% difference
0.094	0.094	0.011683123	8.045794	5.0330	-59.861363
0.215	0.215	0.020155483	10.66707	10.9986	3.01398187
0.35	0.35	0.024371353	14.36112	17.0565	15.8027871
0.46	0.46	0.026305146	17.48707	21.5841	18.9816327
0.58	0.58	0.027032749	21.45546	26.1544	17.9661674
0.756	0.756	0.020813544	36.3225	32.2482	-12.634352
0.815	0.815	0.018717071	43.54314	34.1461	-27.519956

B.E.T. Equation model

	x axis	y axis	Aw/(Meq(1-aw))=0.1204aw-0.0019		
Aw	(aw)	aw/(Meq(1-aw))	Actual	Mathematical	% difference
0.094	0.094	0.012895279	8.045794	11.0169	26.9686243
0.215	0.215	0.025675774	10.66707	11.4186	6.58119986
0.35	0.35	0.037494389	14.36112	13.3813	-7.3227242
0.46	0.46	0.048713234	17.48707	15.9272	-9.7935733
0.58	0.58	0.064363688	21.45546	20.3285	-5.5439833
0.756	0.756	0.085301408	36.3225	34.7652	-4.4794007
0.815	0.815	0.101173354	43.54314	45.7819	4.88997738

Table 55. The mathematical model for equilibrium moisture content from the experimental data of the model product B at 28 °C (84 °F).

Henderson Equation model

	x axis	y axis	ln(-ln(1-aw))=1.4626ln(Meq)-4.6786		
Aw	ln(Meq)	ln(-ln(1-aw))	Actual	Mathematical	% difference
0.11	1.9015788	-2.14957378	6.696459	5.6358	-18.821047
0.235	2.2305698	-1.317218231	9.305167	9.9565	6.5415964
0.345	2.5393259	-0.86009935	12.67113	13.6094	6.89443584
0.455	2.8021453	-0.499276762	16.47996	17.4173	5.3814109
0.545	2.9351401	-0.238945421	18.82414	20.8104	9.54462711
0.75	3.4051634	0.32663426	30.11922	30.6352	1.68416215
0.805	3.674155	0.491493387	39.41534	34.2904	-14.94575

Chen Equation model

	X axis	y axis	Ln(-lnaw)=-0.0696(Meq)+1.0006		
Aw	(Meq)	ln(-lnaw)	Actual	Mathematical	% difference
0.11	6.6964587	0.791758684	6.696459	3.0006	-123.17113
0.235	9.3051669	0.370300528	9.305167	9.0560	-2.7510958
0.345	12.671126	0.06223355	12.67113	13.4823	6.01642128
0.455	16.479963	-0.238945421	16.47996	17.8096	7.46563734
0.545	18.824141	-0.499276762	18.82414	21.5500	12.6488107
0.75	30.119215	-1.245899324	30.11922	32.2773	6.68604402
0.805	39.415336	-1.52825892	39.41534	36.3342	-8.4800488

G.A.B Equation model

	x axis	y axis	(aw/Meq)=0.0036aw+0.0227		
Aw	(aw)	(aw/Meq)	Actual	Mathematical	% difference
0.11	0.11	0.016426593	6.696459	4.7627	-40.601281
0.235	0.235	0.025254786	9.305167	9.9805	6.76618762
0.345	0.345	0.027227257	12.67113	14.4098	12.0660582
0.455	0.455	0.027609285	16.47996	18.6950	11.8484945
0.545	0.545	0.028952185	18.82414	22.0988	14.818173
0.75	0.75	0.024901047	30.11922	29.5276	-2.0037427
0.805	0.805	0.020423522	39.41534	31.4478	-25.335872

B.E.T. Equation model

	x axis	y axis	Aw/(Meq(1-aw))=0.1262aw-0.0003		
Aw	(aw)	aw/(Meq(1-aw))	Actual	Mathematical	% difference
0.11	0.11	0.018456846	6.696459	9.0999	26.4121286
0.235	0.235	0.033012792	9.305167	10.4639	11.0738661
0.345	0.345	0.041568331	12.67113	12.1815	-4.0190916
0.455	0.455	0.050659238	16.47996	14.6157	-12.755348
0.545	0.545	0.063631175	18.82414	17.4915	-7.6186311
0.75	0.75	0.099604188	30.11922	31.7965	5.27506765
0.805	0.805	0.104736012	39.41534	40.7559	3.28923392

Table 56. The mathematical model for equilibrium moisture content from the experimental data of the model product B at 38 °C (100 °F).

Chen Equation model

	X axis	y axis	ln(-lnaw)=-0.0751(Meq)+1.0469		
Aw	(Meq)	ln(-lnaw)	Actual	Mathematical	% difference
0.114	5.4358275	0.775444344	5.435828	3.6146	-50.385759
0.198	9.4891382	0.482110203	9.489138	7.5205	-26.176904
0.345	11.621493	0.06223355	11.62149	13.1114	11.3634758
0.47	15.738987	-0.281007617	15.73899	17.6819	10.9879427
0.51	17.335143	-0.395498114	17.33514	19.2064	9.74272588
0.755	31.30162	-1.269267061	31.30162	30.8411	-1.4931811
0.815	36.069276	-1.586858919	36.06928	35.0700	-2.8493017

Halsey Equation model

	X axis	y axis	Ln(-ln(aw))=-1.2871ln(Meq)+3.1837		
Aw	Ln(Meq)	ln(-ln(aw))	Actual	Mathematical	% difference
0.114	1.6930118	0.775444344	5.435828	6.4952	16.3107258
0.198	2.2501478	0.482110203	9.489138	8.1578	-16.319848
0.345	2.4528562	0.06223355	11.62149	11.3044	-2.8048968
0.47	2.7561409	-0.281007617	15.73899	14.7593	-6.637975
0.51	2.8527358	-0.395498114	17.33514	16.1323	-7.4560959
0.755	3.4436698	-1.269267061	31.30162	31.8071	1.5892567
0.815	3.5854414	-1.586858919	36.06928	40.7086	11.3964767

G.A.B Equation model

	x axis	y axis	(aw/Meq)=0.0026aw+0.0242		
Aw	(aw)	(aw/Meq)	Actual	Mathematical	% difference
0.114	0.114	0.020971968	5.435828	4.6537	-16.805444
0.198	0.198	0.020865962	9.489138	8.0114	-18.445532
0.345	0.345	0.029686375	11.62149	13.7467	15.4595342
0.47	0.47	0.029862151	15.73899	18.4879	14.8688265
0.51	0.51	0.029420006	17.33514	19.9796	13.2359111
0.755	0.755	0.024120158	31.30162	28.8575	-8.4694401
0.815	0.815	0.022595408	36.06928	30.9662	-16.479421

B.E.T. Equation model

	x axis	y axis	Aw/(Meq(1-aw))=0.1355aw-0.0004		
Aw	(aw)	aw/(Meq(1-aw))	Actual	Mathematical	% difference
0.114	0.114	0.023670392	5.435828	8.5511	36.4311343
0.198	0.198	0.026017409	9.489138	9.3414	-1.5819819
0.345	0.345	0.04532271	11.62149	11.3645	-2.2610951
0.47	0.47	0.056343682	15.73899	14.0127	-12.319603
0.51	0.51	0.060040828	17.33514	15.1491	-14.430467
0.755	0.755	0.098449623	31.30162	30.2410	-3.5072524
0.815	0.815	0.122137338	36.06928	40.0373	9.91084162

APPENDIX D

Table 57. Experimental data for retained antioxidant levels in pouch structures as a function of storage time at 23 °C, 50 % RH.

Storage (Weeks)	Pouch number	Type	Sample weight (g)	Area Response	Injected volume(ml)	Antioxidants Level Average
0	1	Vit. E 1		25445	0.02	
		Vit. E 2	1.0641	25025	0.02	
		Vit. E 3		24773	0.02	73 ppm
	2	Vit. E 1		24231	0.02	(7.019)*
		Vit. E 2	1.0457	24835	0.02	
		Vit. E 3		24489	0.02	
0	3	BHT 1		641805	0.02	
		BHT 2	1.0356	648445	0.02	
		BHT 3		647065	0.02	1137 ppm
	4	BHT 1		656513	0.02	(3.646)*
		BHT 2	1.0486	650126	0.02	
		BHT 3		654936	0.02	
2	5	Vit. E 1		13433	0.02	
		Vit. E 2	0.7635	12511	0.02	
		Vit. E 3		14710	0.02	63.5 ppm
	6	Vit. E 1		12736	0.02	(6.836)*
		Vit. E 2	0.6809	12536	0.02	
		Vit. E 3		12824	0.02	
2	7	BHT 1		279284	0.02	
		BHT 2	0.8519	278473	0.02	
		BHT 3		279546	0.02	608 ppm
	8	BHT 1		289245	0.02	(3.836)*
		BHT 2	0.8678	288077	0.02	
		BHT 3		289925	0.02	
4	9	Vit. E 1		10179	0.02	
		Vit. E 2	0.6898	12048	0.02	
		Vit. E 3		14222	0.02	62 ppm
	10	Vit. E 1		13207	0.02	(6.83)*
		Vit. E 2	0.7019	13446	0.02	

		Vit. E 3		13007	0.02	
4	11	BHT 1		96393	0.01	
		BHT 2	0.7871	94345	0.01	
		BHT 3		98122	0.01	446.5 ppm
	12	BHT 1		128865	0.01	(3.29)*
		BHT 2	0.9354	128634	0.01	
		BHT 3		126018	0.01	
6	13	Vit. E 1		14035	0.02	
		Vit. E 2	0.8191	15017	0.02	
		Vit. E 3		15871	0.02	61.5 ppm
	14	Vit. E 1		12875	0.02	(6.83)*
		Vit. E 2	0.706	12461	0.02	
		Vit. E 3		12470	0.02	
6	15	BHT 1		188052	0.02	
		BHT 2	0.9542	186209	0.02	
		BHT 3		186475	0.02	279 ppm
	16	BHT 1		148028	0.02	(3.09)*
		BHT 2	0.8803	143680	0.02	
		BHT 3		144687	0.02	
8	17	Vit. E 1		8525	0.02	
		Vit. E 2	0.5001	8379	0.02	
		Vit. E 3		8355	0.02	60 ppm
	18	Vit. E 1		11517	0.02	(6.88)*
		Vit. E 2	0.6214	11114	0.02	
		Vit. E 3		11370	0.02	
8	19	BHT 1		110723	0.02	
		BHT 2	0.7768	110146	0.02	
		BHT 3		109976	0.02	211 ppm
	20	BHT 1		91421	0.02	(3.06)*
		BHT 2	0.7011	91412	0.02	
		BHT 3		94181	0.02	
10	21	Vit. E 1		11054	0.02	
		Vit. E 2	0.7018	10484	0.02	
		Vit. E 3		12120	0.02	45 ppm
	22	Vit. E 1		7539	0.02	(6.63)*
		Vit. E 2	0.6592	7756	0.02	
		Vit. E 3		6578	0.02	

10	23	BHT 1		78223	0.02	
		BHT 2	0.8008	78299	0.02	
		BHT 3		77509	0.02	149 ppm
	24	BHT 1		73716	0.02	(2.98)*
		BHT 2	0.7151	72383	0.02	
		BHT 3		74857	0.02	
12	25	Vit. E 1		4464	0.02	
		Vit. E 2	0.5718	4807	0.02	
		Vit. E 3		4041	0.02	40.5 ppm
	26	Vit. E 1		12224	0.02	(6.85)*
		Vit. E 2	0.7251	10337	0.02	
		Vit. E 3		11749	0.02	
12	27	BHT 1		40743	0.02	
		BHT 2	0.7255	39951	0.02	
		BHT 3		39642	0.02	112 ppm
	28	BHT 1		66554	0.02	(3.37)*
		BHT 2	0.8454	64777	0.02	
		BHT 3		65252	0.02	
14	29	Vit. E 1		24190	0.01	
		Vit. E 2	0.7462	24037	0.01	
		Vit. E 3		23599	0.01	29 ppm
	30	Vit. E 1		9660	0.01	(6.24)*
		Vit. E 2	0.6513	9290	0.01	
		Vit. E 3		8684	0.01	
14	31	BHT 1		36321	0.02	
		BHT 2	0.8373	34572	0.02	
		BHT 3		32443	0.02	79.5 ppm
	32	BHT 1		48733	0.02	(3.31)*
		BHT 2	0.8513	45573	0.02	
		BHT 3		46045	0.02	
16	33	Vit. E 1		11719	0.01	
		Vit. E 2	0.7261	11078	0.01	
		Vit. E 3		10082	0.01	27 ppm
	34	Vit. E 1		16397	0.01	(6.24)*
		Vit. E 2	0.6734	16727	0.01	
		Vit. E 3		15682	0.01	
16	35	BHT 1		18942	0.02	

		BHT 2	0.8401	18051	0.02	
		BHT 3		16568	0.02	36.5 ppm
	36	BHT 1		18068	0.02	(3.30)*
		BHT 2	0.7898	17988	0.02	
		BHT 3		18459	0.02	
18	37	Vit. E 1		27220	0.02	
		Vit. E 2	0.7086	33612	0.02	
		Vit. E 3		33215	0.02	26 ppm
	38	Vit. E 1		20536	0.02	(6.55)*
		Vit. E 2	0.7154	23469	0.02	
		Vit. E 3		21031	0.02	
18	39	BHT 1		24496	0.02	
		BHT 2	0.8957	23463	0.02	
		BHT 3		23328	0.02	32 ppm
	40	BHT 1		7880	0.02	(3.26)*
		BHT 2	0.8058	11526	0.02	
		BHT 3		9918	0.02	

( )* = x 10^{-13} calibration factor

Table 58. Experimental data for retained antioxidant levels in pouch structures as a function of storage time at 45 °C, 50 % RH.

Storage (Days)	Type	Sample weight (g)	Area Response	Injected volume(ml)	Antioxidants (ppm)	Antioxidants level Average
0	Vit. E 1	1.3591	16553	0.01	82	
			13910	0.01	69	
			13813	0.01	69	73 ppm
	Vit. E 2	1.3658	14222	0.01	70	
			16230	0.01	80	
			13808	0.01	68	
	BHT 1	1.4165	537600	0.01	1142	
			550836	0.01	1171	
			545862	0.01	1160	1168 ppm
	BHT 2	1.6847	679814	0.01	1215	
			645585	0.01	1153	
			652225	0.01	1165	

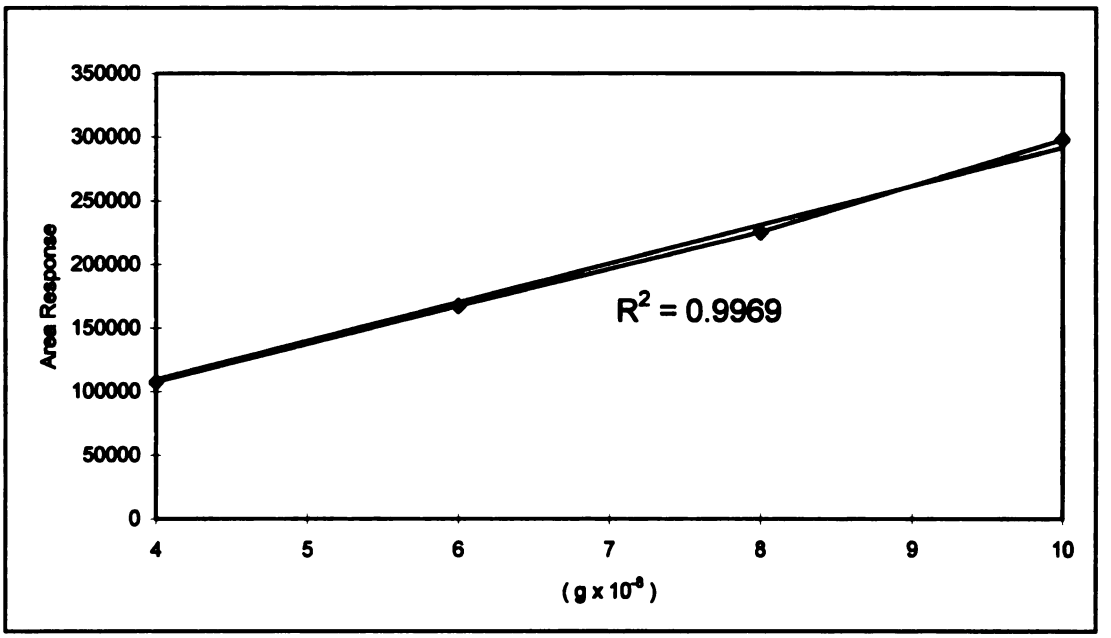

Figure 37. Standard Calibration Curve for BHT using HPLC.

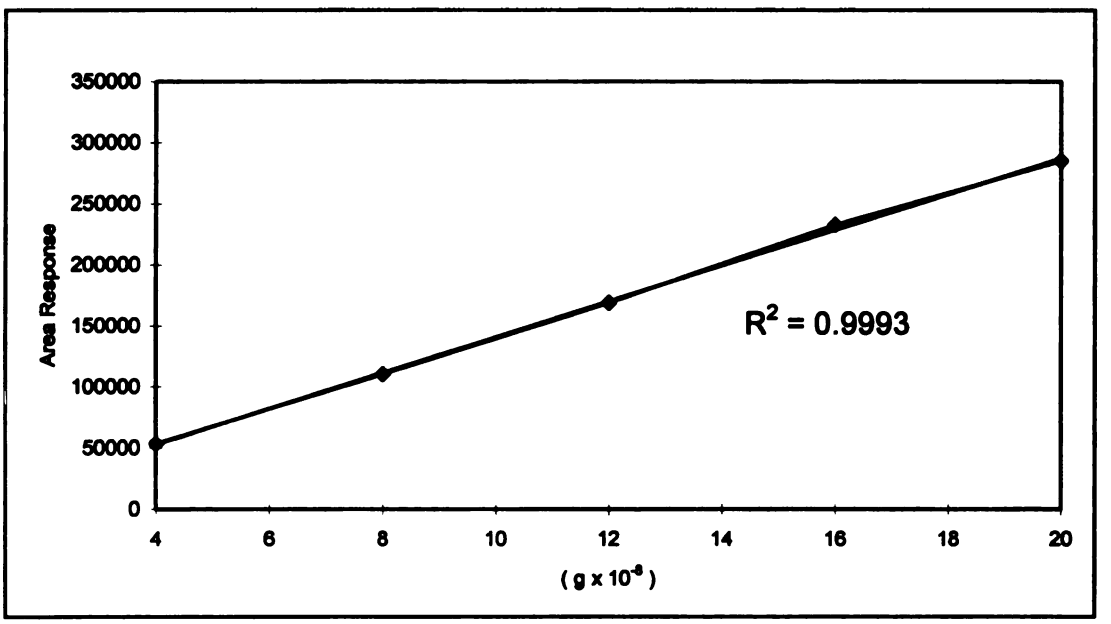

Figure 38. Standard Calibration Curve for α-tocopherol using HPLC.

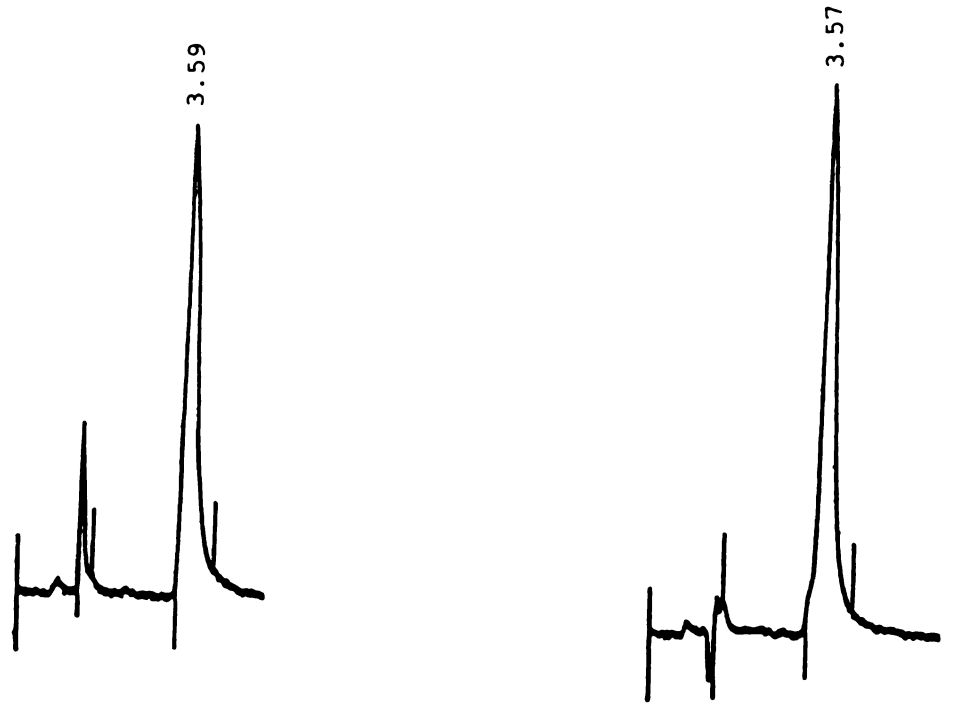

Figure 39. HPLC-chromatogram of an extracted BHT from the laminated film.

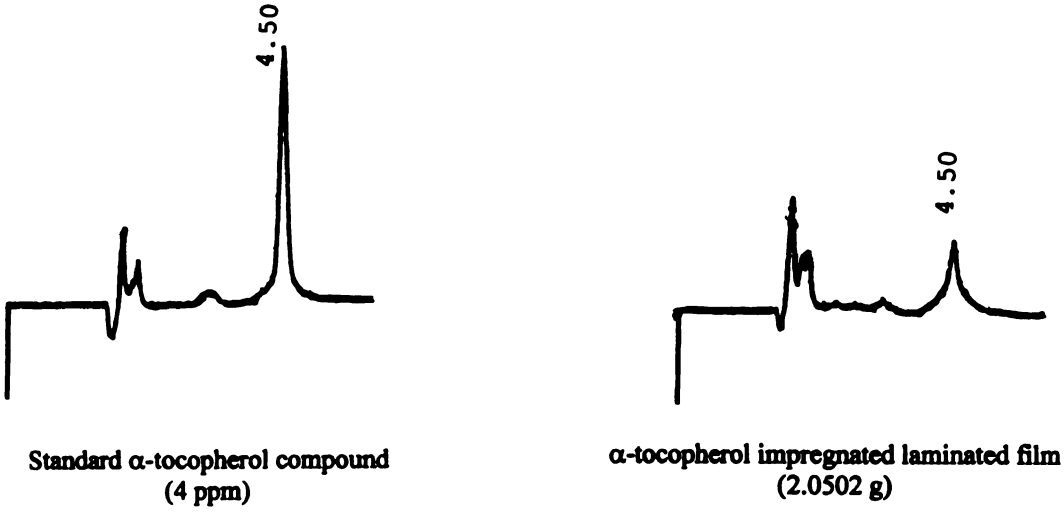

Figure 40. HPLC-chromatogram of an extracted α-tocopherol from the laminated film.

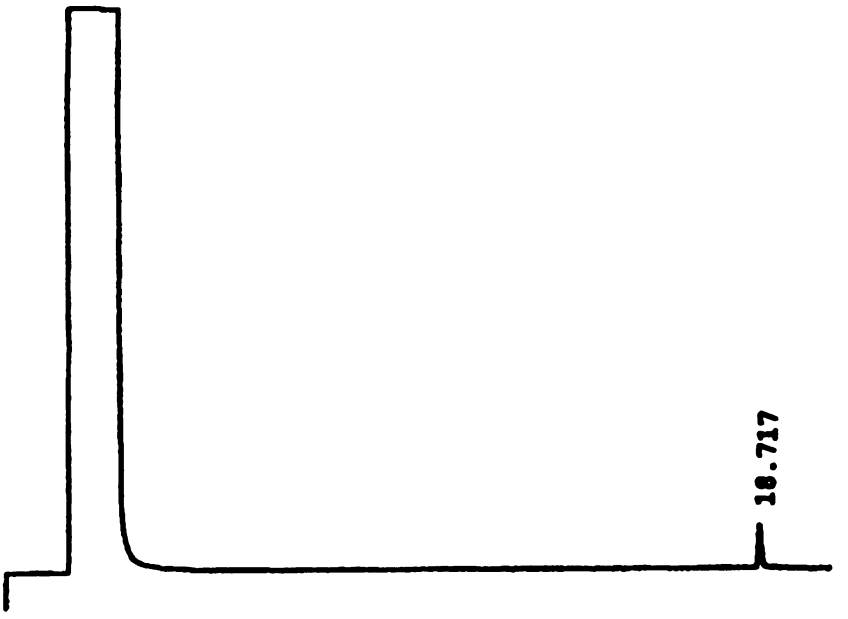

Standard linoleic acid (6 ppm)

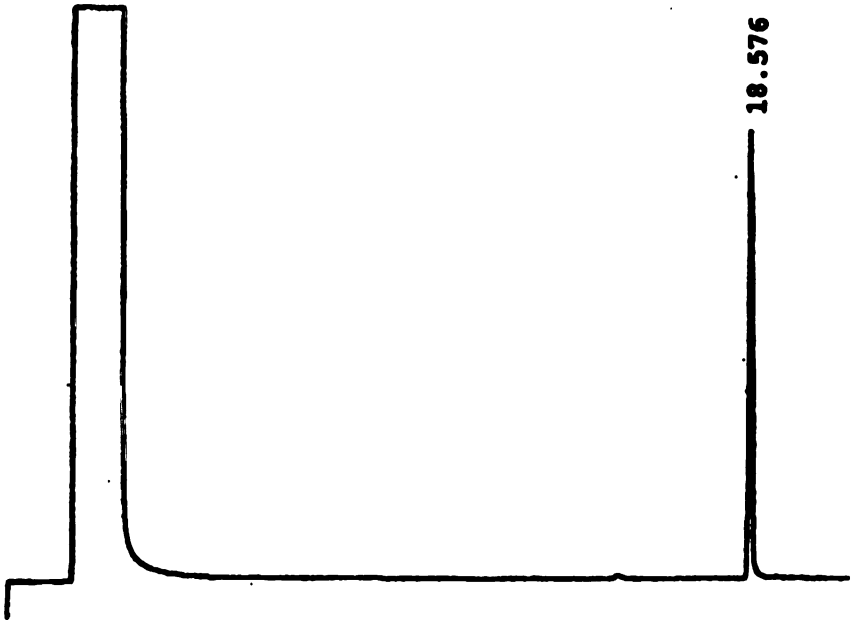

Linoleic acid in model product (4 days, BHT)

Figure 41. GC chromatogram of the methyl ester extracted from the model product.

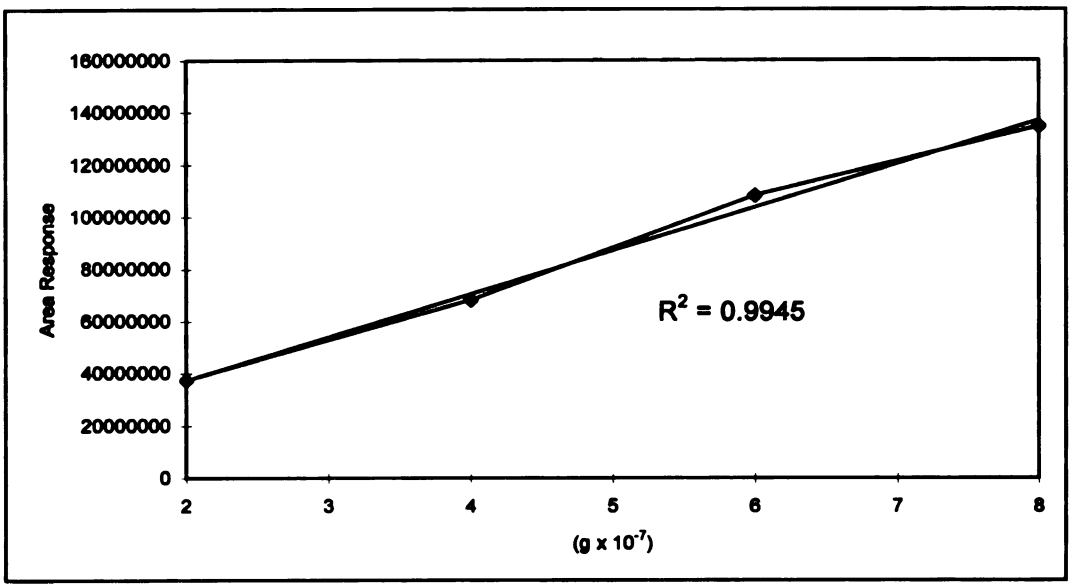

Figure 42. Standard Calibration Curve of trans- 9-12-octadecadienoic methyl ester.

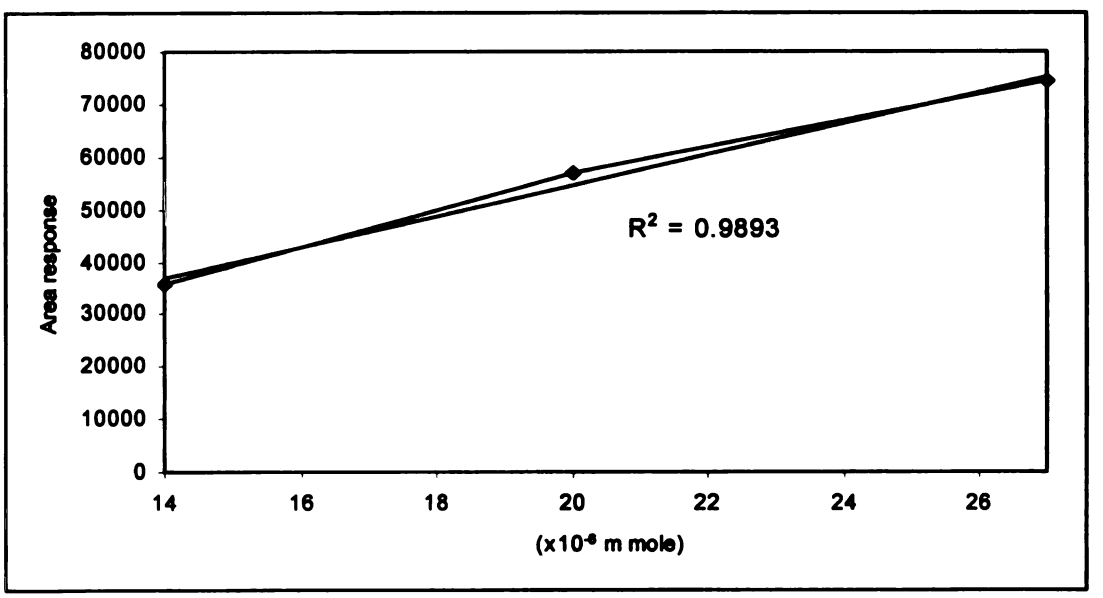

Figure 43. Standard Calibration Curve for Hexanal using GC/MS.

		Vit. E 3		13007	0.02	
4	11	BHT 1		96393	0.01	
		BHT 2	0.7871	94345	0.01	
		BHT 3		98122	0.01	446.5 ppm
	12	BHT 1		128865	0.01	(3.29)*
		BHT 2	0.9354	128634	0.01	
		BHT 3		126018	0.01	
6	13	Vit. E 1		14035	0.02	
		Vit. E 2	0.8191	15017	0.02	
		Vit. E 3		15871	0.02	61.5 ppm
	14	Vit. E 1		12875	0.02	(6.83)*
		Vit. E 2	0.706	12461	0.02	
		Vit. E 3		12470	0.02	
6	15	BHT 1		188052	0.02	
		BHT 2	0.9542	186209	0.02	
		BHT 3		186475	0.02	279 ppm
	16	BHT 1		148028	0.02	(3.09)*
		BHT 2	0.8803	143680	0.02	
		BHT 3		144687	0.02	
8	17	Vit. E 1		8525	0.02	
		Vit. E 2	0.5001	8379	0.02	
		Vit. E 3		8355	0.02	60 ppm
	18	Vit. E 1		11517	0.02	(6.88)*
		Vit. E 2	0.6214	11114	0.02	
		Vit. E 3		11370	0.02	
8	19	BHT 1		110723	0.02	
		BHT 2	0.7768	110146	0.02	
		BHT 3		109976	0.02	211 ppm
	20	BHT 1		91421	0.02	(3.06)*
		BHT 2	0.7011	91412	0.02	
		BHT 3		94181	0.02	
10	21	Vit. E 1		11054	0.02	
		Vit. E 2	0.7018	10484	0.02	
		Vit. E 3		12120	0.02	45 ppm
	22	Vit. E 1		7539	0.02	(6.63)*
		Vit. E 2	0.6592	7756	0.02	
		Vit. E 3		6578	0.02	

10	23	BHT 1		78223	0.02	
		BHT 2	0.8008	78299	0.02	
		BHT 3		77509	0.02	149 ppm
	24	BHT 1		73716	0.02	(2.98)*
		BHT 2	0.7151	72383	0.02	
		BHT 3		74857	0.02	
12	25	Vit. E 1		4464	0.02	
		Vit. E 2	0.5718	4807	0.02	
		Vit. E 3		4041	0.02	40.5 ppm
	26	Vit. E 1		12224	0.02	(6.85)*
		Vit. E 2	0.7251	10337	0.02	
		Vit. E 3		11749	0.02	
12	27	BHT 1		40743	0.02	
		BHT 2	0.7255	39951	0.02	
		BHT 3		39642	0.02	112 ppm
	28	BHT 1		66554	0.02	(3.37)*
		BHT 2	0.8454	64777	0.02	
		BHT 3		65252	0.02	
14	29	Vit. E 1		24190	0.01	
		Vit. E 2	0.7462	24037	0.01	
		Vit. E 3		23599	0.01	29 ppm
	30	Vit. E 1		9660	0.01	(6.24)*
		Vit. E 2	0.6513	9290	0.01	
		Vit. E 3		8684	0.01	
14	31	BHT 1		36321	0.02	
		BHT 2	0.8373	34572	0.02	
		BHT 3		32443	0.02	79.5 ppm
	32	BHT 1		48733	0.02	(3.31)*
		BHT 2	0.8513	45573	0.02	
		BHT 3		46045	0.02	
16	33	Vit. E 1		11719	0.01	
		Vit. E 2	0.7261	11078	0.01	
		Vit. E 3		10082	0.01	27 ppm
	34	Vit. E 1		16397	0.01	(6.24)*
		Vit. E 2	0.6734	16727	0.01	
		Vit. E 3		15682	0.01	
16	35	BHT 1		18942	0.02	

		BHT 2	0.8401	18051	0.02	
		BHT 3		16568	0.02	36.5 ppm
	36	BHT 1		18068	0.02	(3.30)*
		BHT 2	0.7898	17988	0.02	
		BHT 3		18459	0.02	
18	37	Vit. E 1		27220	0.02	
		Vit. E 2	0.7086	33612	0.02	
		Vit. E 3		33215	0.02	26 ppm
	38	Vit. E 1		20536	0.02	(6.55)*
		Vit. E 2	0.7154	23469	0.02	
		Vit. E 3		21031	0.02	
18	39	BHT 1		24496	0.02	
		BHT 2	0.8957	23463	0.02	
		BHT 3		23328	0.02	32 ppm
	40	BHT 1		7880	0.02	(3.26)*
		BHT 2	0.8058	11526	0.02	
		BHT 3		9918	0.02	

( )* = x 10^{-13} calibration factor

Table 58. Experimental data for retained antioxidant levels in pouch structures as a function of storage time at 45 °C, 50 % RH.

Storage (Days)	Type	Sample weight (g)	Area Response	Injected volume(ml)	Antioxidants (ppm)	Antioxidants level Average
0	Vit. E 1	1.3591	16553	0.01	82	
			13910	0.01	69	
			13813	0.01	69	73 ppm
	Vit. E 2	1.3658	14222	0.01	70	
			16230	0.01	80	
			13808	0.01	68	
	BHT 1	1.4165	537600	0.01	1142	
			550836	0.01	1171	
			545862	0.01	1160	1168 ppm
	BHT 2	1.6847	679814	0.01	1215	
			645585	0.01	1153	
			652225	0.01	1165	

2	Vit. E 1	0.8055	34588	0.01	73	
			34465	0.01	72	
			35577	0.01	75	72.5 ppm
	Vit. E 2	0.8458	34016	0.01	68	
			37106	0.01	74	
			36484	0.01	73	
	BHT 1	0.8405	186051	0.01	167	
			174310	0.01	156	
			171047	0.01	153	185 ppm
	BHT 2	0.8993	248335	0.01	208	
			253494	0.01	212	
			249700	0.01	209	
4	Vit. E 1	1.1996	51035	0.01	72	
			50591	0.01	71	
			51975	0.01	73	72 ppm
	Vit. E 2	1.0331	40811	0.01	67	
			44750	0.01	73	
			45414	0.01	74	
	BHT 1	0.8892	51275	0.01	43	
			50579	0.01	43	
			51671	0.01	44	40 ppm
	BHT 2	0.9422	46120	0.01	37	
			47807	0.01	38	
			45992	0.01	37	
6	Vit. E 1	0.7184	23460	0.01	55	
			23069	0.01	54	
			23439	0.01	55	55.5 ppm
	Vit. E 2	0.9165	29913	0.01	55	
			30710	0.01	57	
			29612	0.01	55	
	BHT 1	0.8887	N/A	0.01	N/A	
			N/A	0.01	N/A	
			N/A	0.01	N/A	N/A
	BHT 2	0.951	N/A	0.01	N/A	
			N/A	0.01	N/A	
			N/A	0.01	N/A	

Vit. E = calibration factor (6.77×10^{-13} (g/Area Response))
BHT = calibration factor (3.01×10^{-13} (g/Area Response))

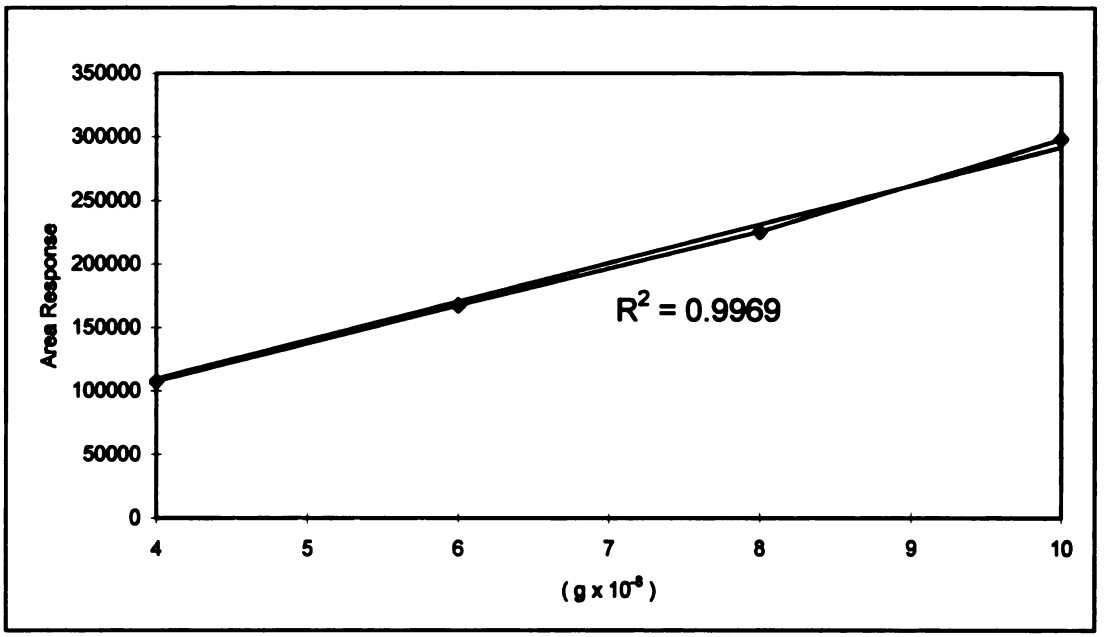

Figure 37. Standard Calibration Curve for BHT using HPLC.

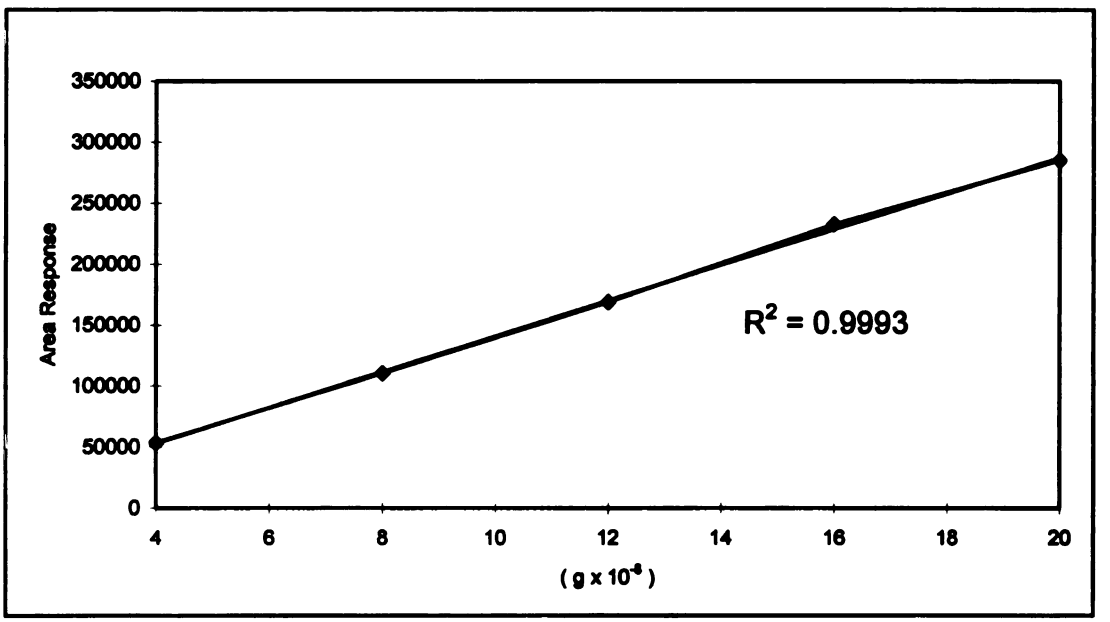

Figure 38. Standard Calibration Curve for α-tocopherol using HPLC.

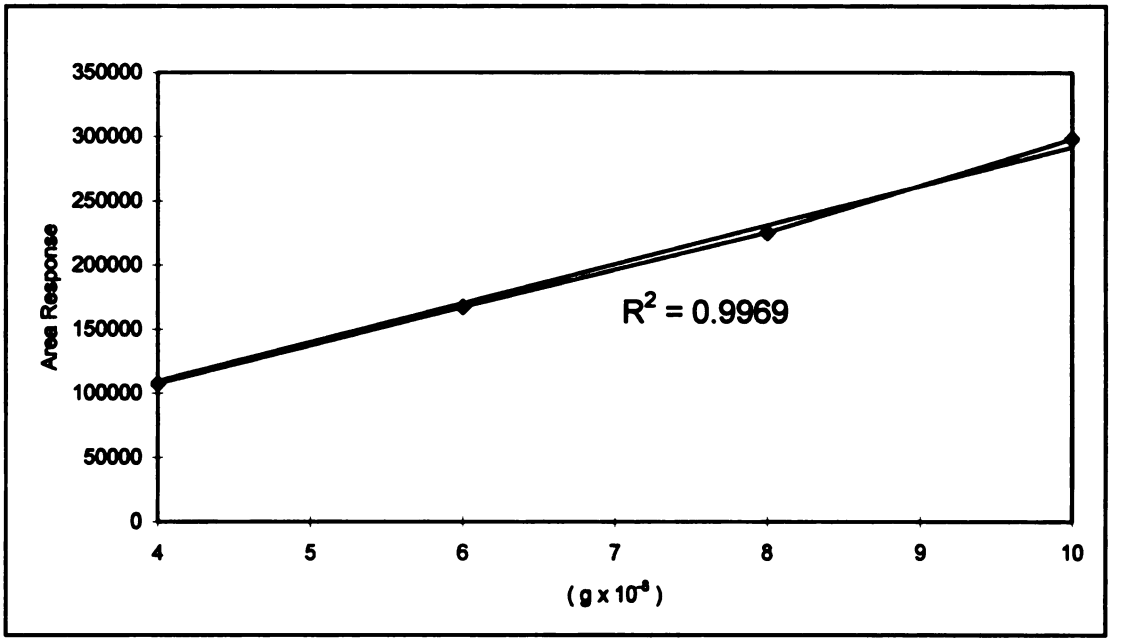

Figure 37. Standard Calibration Curve for BHT using HPLC.

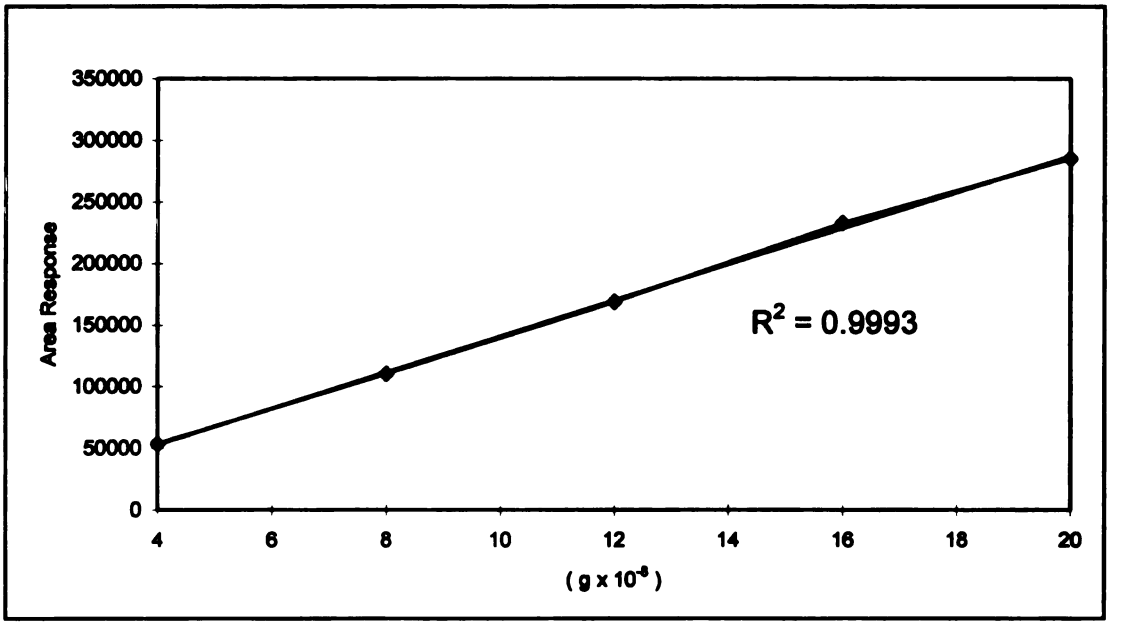

Figure 38. Standard Calibration Curve for α-tocopherol using HPLC.

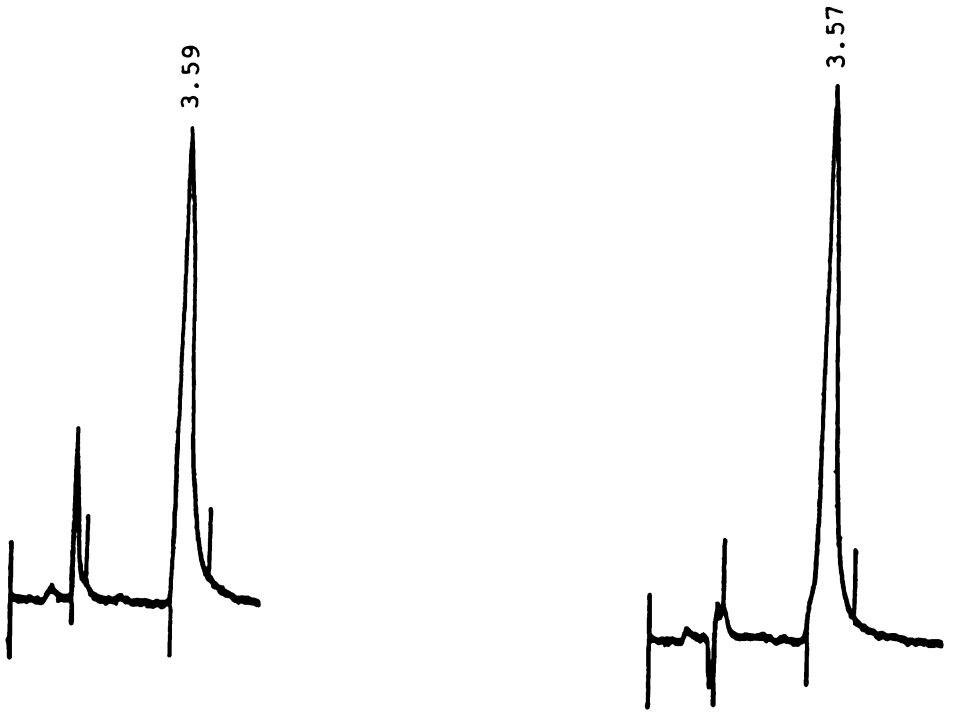

Figure 39. HPLC-chromatogram of an extracted BHT from the laminated film.

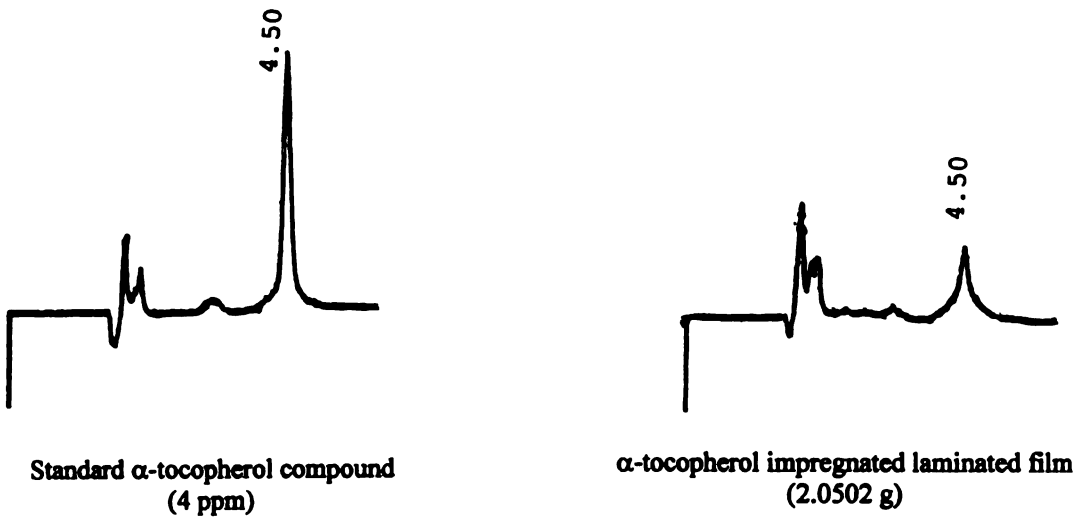

Figure 40. HPLC-chromatogram of an extracted α-tocopherol from the laminated film.

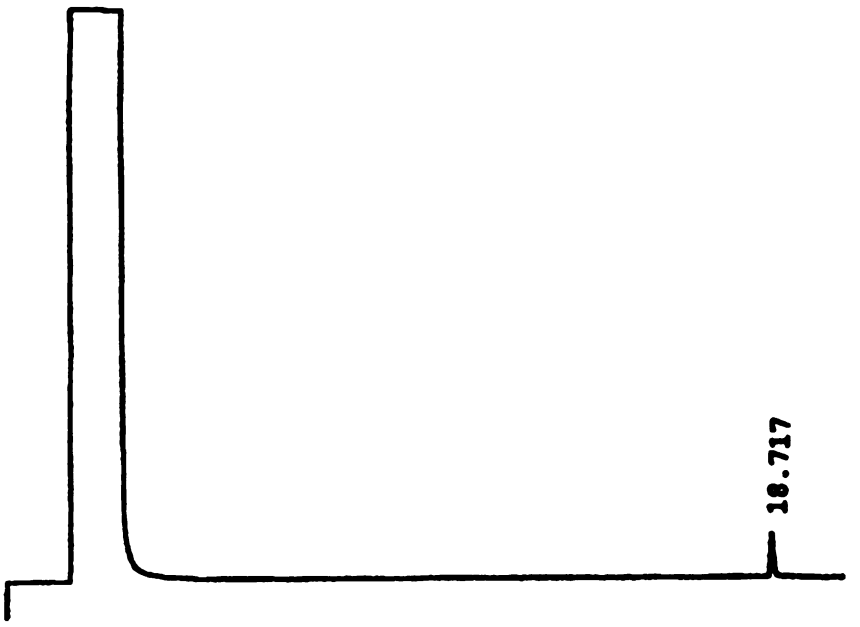

Standard linoleic acid (6 ppm)

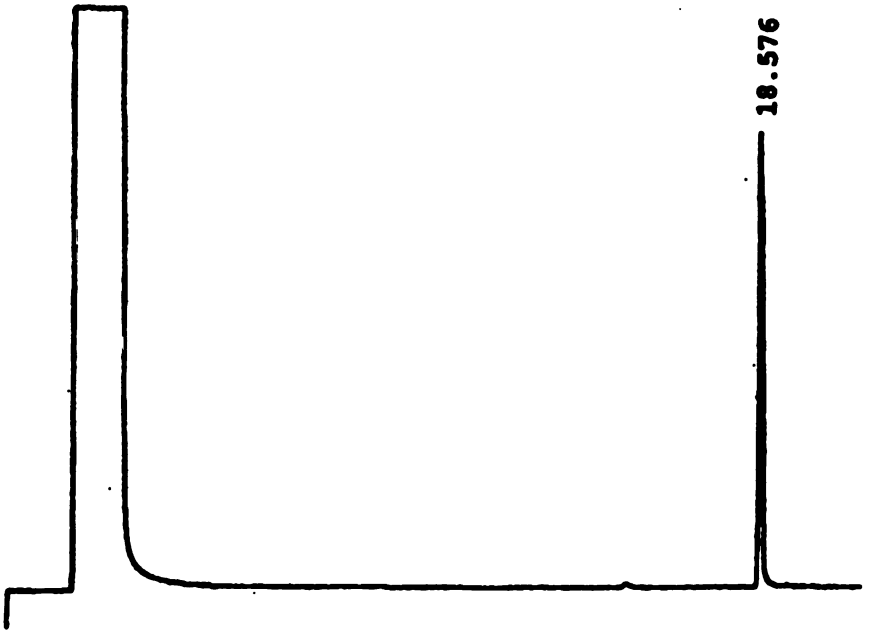

Linoleic acid in model product (4 days, BHT)

Figure 41. GC chromatogram of the methyl ester extracted from the model product.

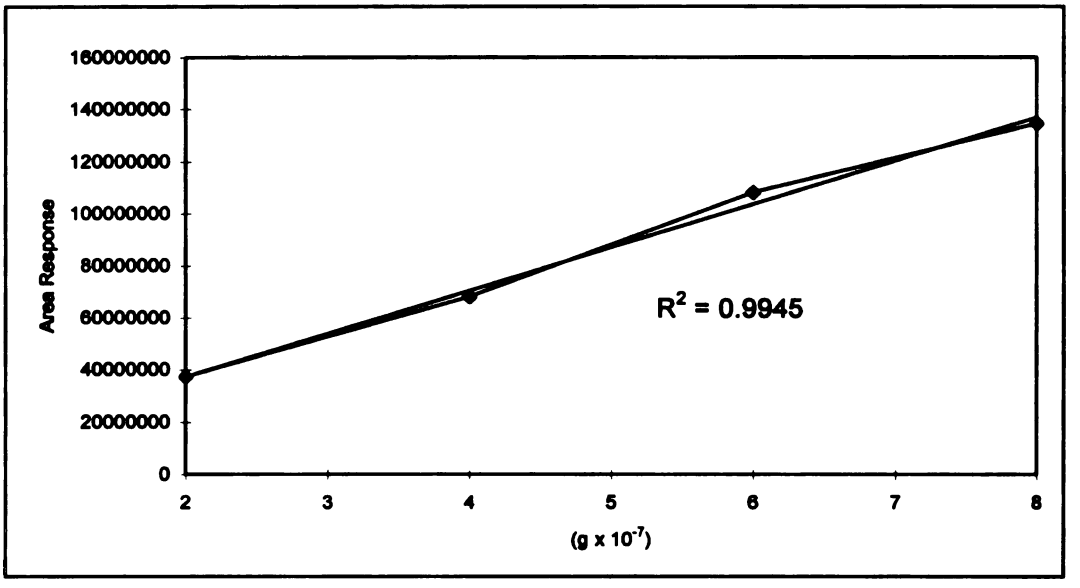

Figure 42. Standard Calibration Curve of trans- 9-12-octadecadienoic methyl ester.

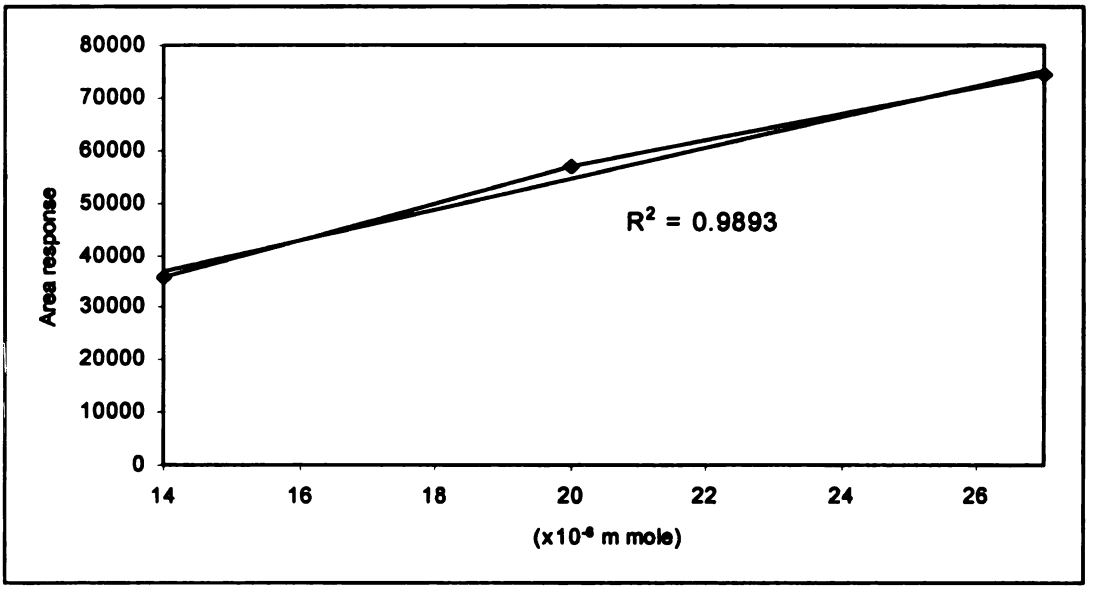

Figure 43. Standard Calibration Curve for Hexanal using GC/MS.

Hexanal
Formula: $C_6H_{12}O$
MW: 100 CAS#: 66-25-1 NIST#: 63070 ID#: 6367 DB: mainlib
Other DBs: Fine, TSCA, RTECS, HODOC, NIH, EINECS, IRDB
Contributor: D.HENNEBERG, MAX-PLANCK INSTITUTE, MULHEIM, WEST GERMANY
53 Masses and Abundances

26	32	38	2	45	196	55	147	66	3	73	10	83	15	96	3
27	330	39	126	46	6	56	816	67	88	74	1	84	2	99	3
28	82	40	32	50	1	57	441	68	7	77	1	85	4	100	9
29	382	41	655	51	3	58	94	69	16	79	4	86	Tr	101	1
30	16	42	113	52	1	59	8	70	10	80	1	94	1		
31	25	43	531	53	25	60	1	71	80	81	14	95	2		
37	Tr	44	999	54	25	65	5	72	197	82	141	97	2		

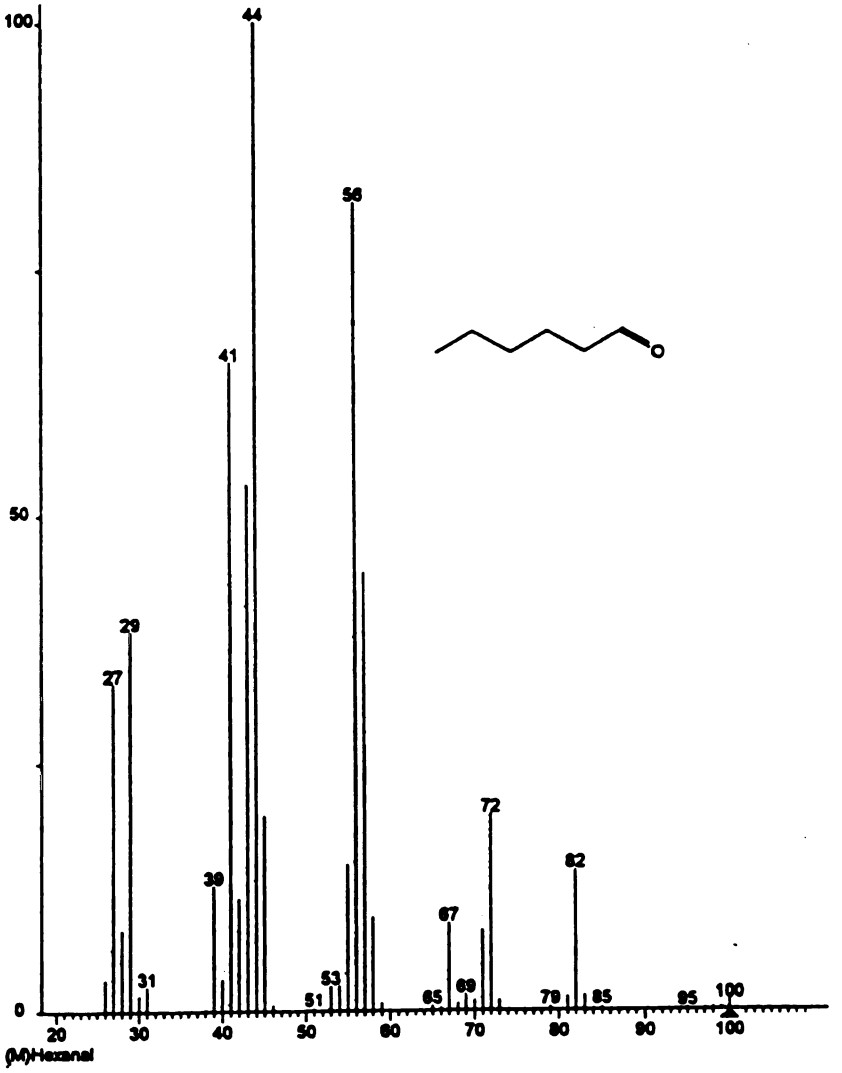

Figure 44. Standard Mass Spectrum of Hexanal.

The total ion currents selected at m/z 29, 44, 56, 72, and 100 in SIM mode for hexanal

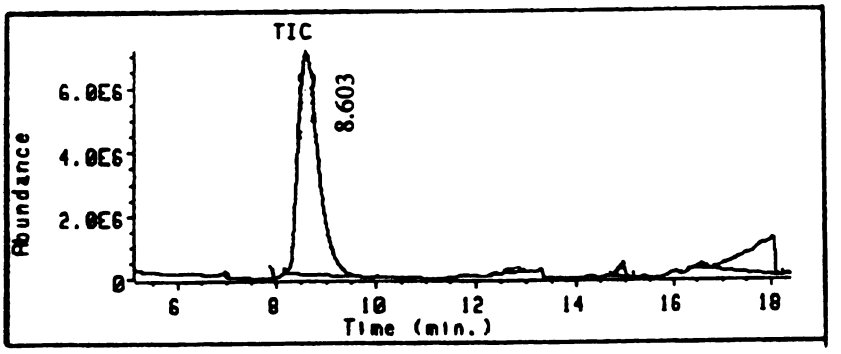

Figure 45. The model product (B) after freezing-dry (0.1645 g) using SIM of Mass spectrum.

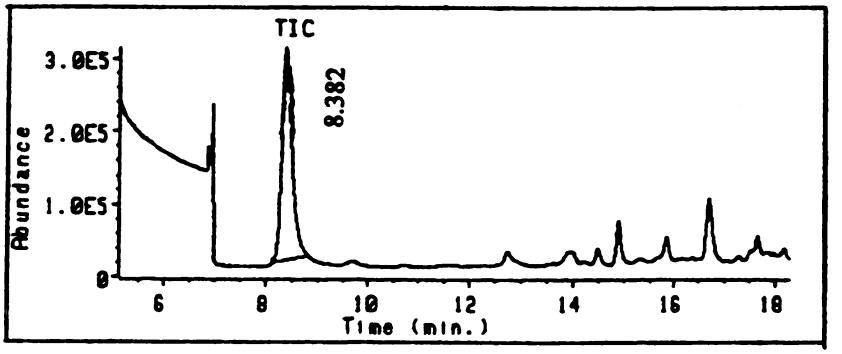

Figure 46. The linoleic acid (0.0241 g), (99%, Acros Organics) using SIM of Mass spectrum.

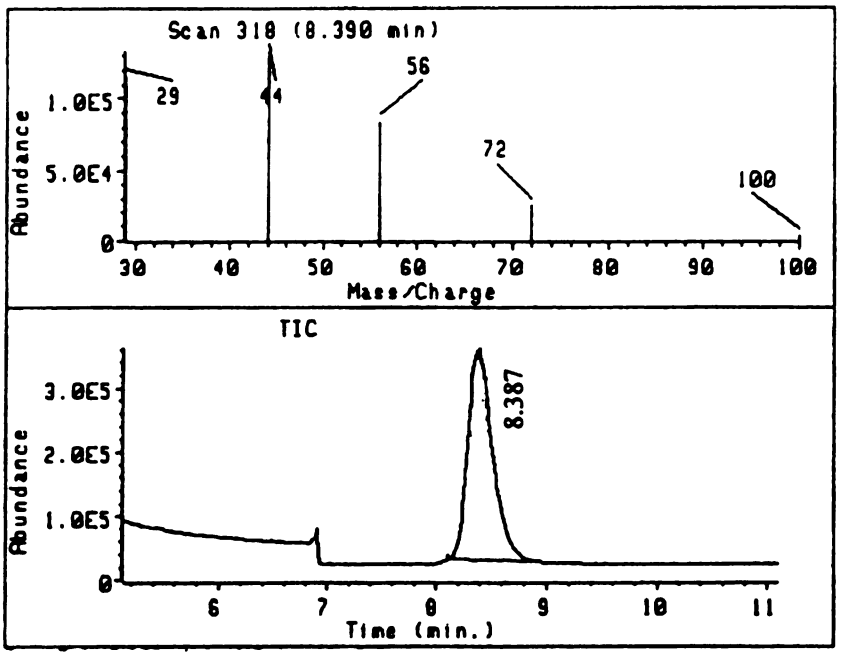

Figure 47. The hexanal standard compound using SIM of Mass spectrum.

The profile of the selected ion current range in SIM mode for hexanal

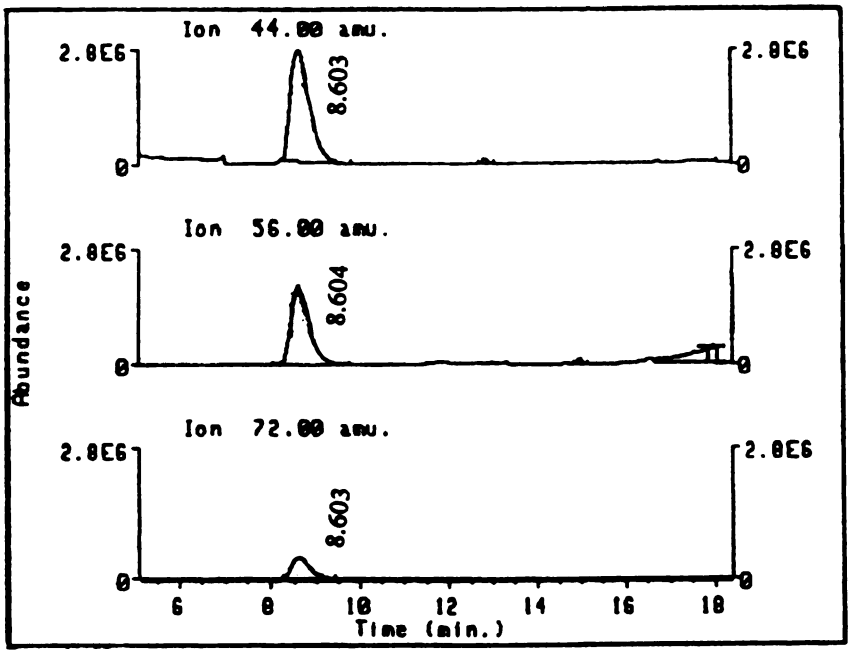

Figure 48. The model product (B) after freezing-dry (0.1645 g) using SIM of Mass spectrum.

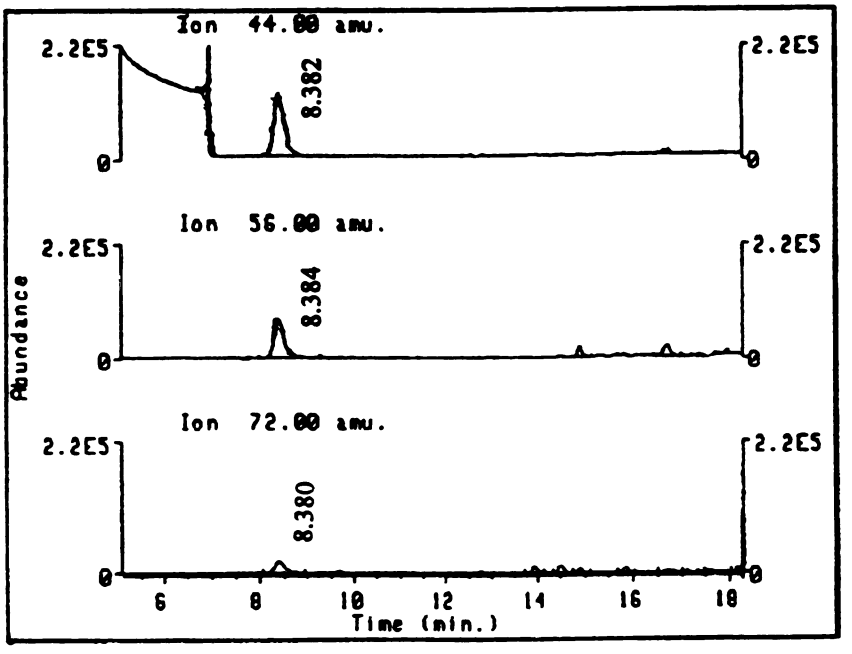

Figure 49. The linoleic acid (0.0241 g), (99%, Acros Organics) using SIM of Mass spectrum.

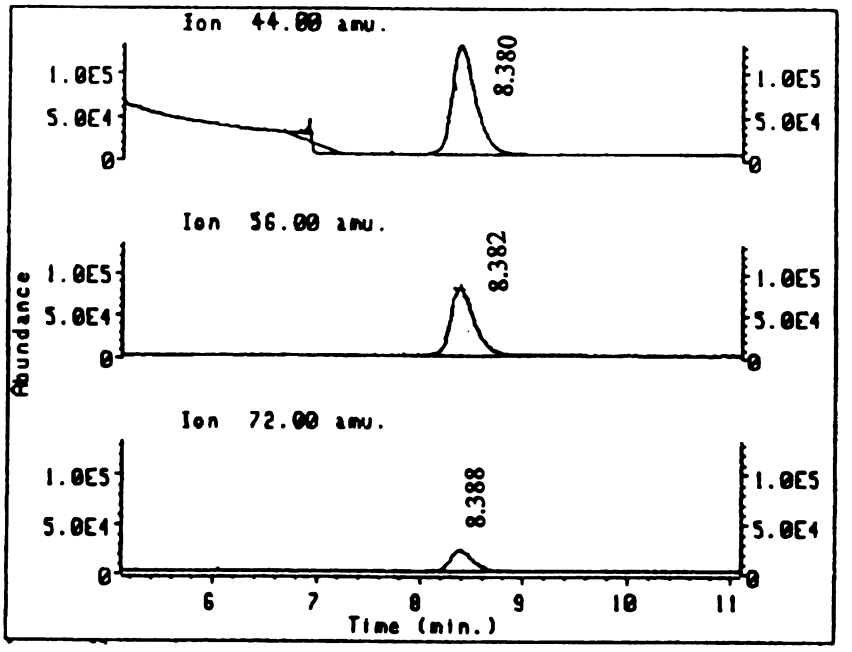

Figure 50. The hexanal standard compound using SIM of Mass spectrum.

Table 59. The ratio of the selected ion profiles at m/z 44, 56, and 72 for hexanal.

(1) Hexanal standard

Hexanal Standard	Total ions	Ion 44	Ion 56	Ion 72	At m/z (44/44)	At m/z (56/44)	At m/z (72/44)
(ppm)		Area Response				Ratio of each ion	
200	13103931	5539125	3624348	889171	1	0.65	0.16
400	28108899	12317988	7729692	1986165	1	0.63	0.16
600	52183827	20944542	13377271	3275147	1	0.64	0.16
800	75446973	28780401	18051896	4818452	1	0.63	0.17

(2) Sample product

	Total ions	Ion 44	Ion 56	Ion 72	At m/z 44/44	At m/z 56/44	At m/z 72/44
		Area Response				Ratio of each ion	
Linoleic acid	39577467	18109765	11098908	2682988	1	0.61	0.15
Model product (B)	1976506482	778529724	502088472	122492128	1	0.65	0.16

Table 60. Experimental hexanal data for model products from each package structure as a function of storage time at 23 °C, 50 % RH.

Storage (Weeks)	Pouch Number	Types	Tested weight(g)	Area Response	Hexanal (ppm)	Average
0	1	Initial	0.2268	11992503	0.26	
	2	Initial	0.1556	7482111	0.39	0.33 ppm
	3	Initial	0.1729	8777682	0.35	
2	4	Control1	0.1865	25825613	0.69	0.55 ppm
	5	Control2	0.1883	15431150	0.41	
	6	Vit. E 1	0.1622	17274000	0.53	0.58 ppm
	7	Vit. E 2	0.1737	21900202	0.63	
	8	BHT 1	0.1805	15124836	0.42	0.48 ppm
	9	BHT 2	0.1682	17879940	0.53	
4	10	Control1	0.1621	20828770	0.64	0.60 ppm
	11	Control2	0.1878	22033331	0.59	
	12	Vit. E 1	0.1686	24701755	0.73	0.67 ppm

	13	Vit. E 2	0.1519	18495483	0.61	
	14	BHT 1	0.1625	22386569	0.69	0.55 ppm
	15	BHT 2	0.1522	12082418	0.40	
6	16	Control1	0.2253	22537950	0.50	0.64 ppm
	17	Control2	0.2478	38220047	0.77	
	18	Vit. E 1	0.1599	11086964	0.35	0.46 ppm
	19	Vit. E 2	0.1713	19183524	0.56	
	20	BHT 1	0.1658	17265890	0.52	0.62 ppm
	21	BHT 2	0.2059	29171667	0.71	
8	22	Control1	0.1674	12648215	0.38	0.44 ppm
	23	Control2	0.1762	17155443	0.49	
	24	Vit. E 1	0.1729	11571040	0.33	0.43 ppm
	25	Vit. E 2	0.1801	18694963	0.52	
	26	BHT 1	0.1763	18795256	0.53	0.40 ppm
	27	BHT 2	0.1788	9445895	0.26	
10	28	Control1	0.1821	12662707	0.35	0.42 ppm
	29	Control2	0.1746	17042780	0.49	
	30	Vit. E 1	0.1817	26437902	0.73	0.64 ppm
	31	Vit. E 2	0.1772	19536651	0.55	
	32	BHT 1	0.1793	11456329	0.32	0.7 ppm
	33	BHT 2	0.1769	38019835	1.08	
12	34	Control1	0.1841	21136465	0.38	0.52 ppm[a]
	35	Control2	0.1852	36391982	0.65	
	36	Vit. E 1	0.1784	16072924	0.30	0.44 ppm[a]
	37	Vit. E 2	0.1913	32419547	0.56	
	38	BHT 1	0.2174	42550000	0.65	0.71 ppm[a]
	39	BHT 2	0.2295	53094528	0.77	
14	40	Control1	0.8075	29777419	0.18	0.38 ppm
	41	Control2	0.8124	93680026	0.58	
	42	Vit. E 1	0.8854	92114231	0.45	0.42 ppm
	43	Vit. E 2	0.9942	76628027	0.38	
	44	BHT 1	1.0282	169819986	0.83	0.72 ppm
	45	BHT 2	1.0109	122427781	0.61	
16	46	Control1	1.0413	252051564	0.48	0.59 ppm[b]
	47	Control2	1.002	346646748	0.69	
	48	Vit. E 1	1.0149	146532180	0.29	0.49 ppm[b]
	49	Vit. E 2	1.0039	341457224	0.68	

	50	BHT 1	1.0018	309377090	0.62	0.52 ppm[b]
	51	BHT 2	1.0776	226938539	0.42	
18	52	Control1	0.9841	77107701	0.39	0.51 ppm
	53	Control2	0.9166	115926387	0.63	
	54	Vit. E 1	1.3075	117382865	0.45	0.28 ppm
	55	Vit. E 2	1.0902	91209532	0.42	
	56	BHT 1	1.0162	134801322	0.66	0.56 ppm
	57	BHT 2	1.0251	92546647	0.45	
20	58	Control1	1.0738	435213710	2.03	1.66ppm[c]
	59	Control2	1.0446	269770596	1.29	
	60	Vit. E 1	1.0606	222323283	1.05	1.34ppm[c]
	61	Vit. E 2	1.0931	354066478	1.62	
	62	BHT 1	1.0781	443459227	2.06	1.46ppm[c]
	63	BHT 2	1.0834	187198975	0.86	
22	64	Control1	1.1088	289834916	1.31	1.12ppm[c]
	65	Control2	1.0903	265470681	1.22	
	66	Vit. E 1	1.1671	314271198	1.35	0.98ppm[c]
	67	Vit. E 2	1.0737	153559103	0.72	
	68	BHT 1	1.1071	299580586	1.35	1.03ppm[c]
	69	BHT 2	1.0021	140132819	0.70	
24	70	Control1	1.0784	139299955	0.65	0.81 ppm
	71	Control2	1.0486	201706738	0.96	
	72	Vit. E 1	1.0309	125905960	0.61	0.59 ppm
	73	Vit. E 2	1.0474	120299053	0.57	
	74	BHT 1	1.131	242582484	1.07	0.79 ppm
	75	BHT 2	1.0628	105930847	0.50	
26	76	Control1	1.2749	453182673	0.89	0.78 ppm
	77	Control2	1.5641	413138287	0.66	
	78	Vit. E 1	1.4418	395655627	0.69	0.74 ppm
	79	Vit. E 2	1.5807	499550769	0.79	
	80	BHT 1	1.7554	582417498	0.83	0.87 ppm
	81	BHT 2	1.5921	573383583	0.90	
28	82	Control1	1.088	133139751	0.61	0.58 ppm
	83	Control2	1.0043	108451346	0.54	
	84	Vit. E 1	1.0355	131729587	0.64	0.67 ppm
	85	Vit. E 2	1.0125	196982761	0.97	
	86	BHT 1	1.0156	222915897	1.10	0.94 ppm

	87	BHT 2	1.0358	158806077	0.77

Calibration factor = 5×10^{-15} (g/A.U)
(a) = 3.33×10^{-15} (g/A.U) C.F.
(b) = 2×10^{-15} (g/A.U) C.F.
(c) = multiplier : 3000 in mass spectrum

Table 61. Experimental hexanal data for model products from each package structure as a function of the storage time at 45 °C, 50 % RH.

Storage (days)	Pouch Number	Types	Tested weight(g)	Area Response	Hexanal (ppm)	Average
0	1	Control	1.0861	40297132	0.19	
	2	Control	1.1917	46175336	0.19	0.21 ppm
	3	Control	1.0325	51060730	0.25	
2	4	Control1	1.0071	1440785559	7.2	7.1 ppm
	5	Control2	1.0375	1451991086	7.0	
	6	Vit. E 1	1.0298	2363682208	12	13 ppm
	7	Vit. E 2	1.0277	2815748133	14	
	8	BHT 1	1.0638	56125009	0.26	0.23 ppm
	9	BHT 2	1.0118	39574553	0.20	
4	10	Control1	1.0469	513358678	2.5	2.5 ppm
	11	Control2	1.0841	542953058	2.5	
	12	Vit. E 1	1.0891	575261315	2.6	2.6 ppm
	13	Vit. E 2	1.0146	504732764	2.5	
	14	BHT 1	1.0145	42771370	0.21	0.27 ppm
	15	BHT 2	1.0084	64890482	0.32	
6	16	Control1	1.0475	270144442	1.29	1.64 ppm
	17	Control2	1.0015	397307843	1.98	
	18	Vit. E 1	1.0574	408603505	1.93	1.91 ppm
	19	Vit. E 2	1.0132	381085947	1.88	
	20	BHT 1	1.0131	41022760	0.20	0.19 ppm
	21	BHT 2	1.0027	32993965	0.17	

Calibration factor = 5×10^{-15} (g/A.U)

Table 62. Experimental methyl ester data of model products as a function of the storage time at 45 °C, 50 % RH.

Storage (days)	Types	Tested weight(g)	Injection	Area Response	linoleic acid % (wt/wt)	Average % (g/g)
0	Control		1	770029	0.7260	
	Control	2.5253	2	758612	0.7152	0.72
	Control		3	752789	0.7097	
2	Control		1	42378	0.0258	
	Control	3.1262	2	39735	0.0242	0.03
	Control		3	43615	0.0266	
	BHT		1	691275	0.5383	
	BHT	3.0071	2	786271	0.6123	0.57
	BHT		3	718910	0.5599	
	Vit. E		1	42378	0.0248	
	Vit. E	3.2527	2	39735	0.0233	0.02
	Vit. E		3	43615	0.0255	
4	Control		1	28746	0.0200	
	Control	2.7337	2	30656	0.0214	0.02
	Control		3	29013	0.0202	
	BHT		1	658786	0.5771	
	BHT	2.7175	2	655984	0.5747	0.57
	BHT		3	641332	0.5619	
	Vit. E		1	13135	0.0109	
	Vit. E	2.2947	2	15490	0.0129	0.01
	Vit. E		3	19143	0.0159	
6	Control		1	20954	0.0140	
	Control	2.8417	2	27389	0.0184	0.02
	Control		3	23633	0.0158	
	BHT		1	688227	0.5735	
	BHT	2.8568	2	670899	0.5591	0.56
	BHT		3	685829	0.5715	
	Vit. E		1	45552	0.0308	
	Vit. E	2.8155	2	42683	0.0289	0.03
	Vit. E		3	44196	0.0299	

Calibration factor = 1×10^{-13} (g/A.U)

APPENDIX E

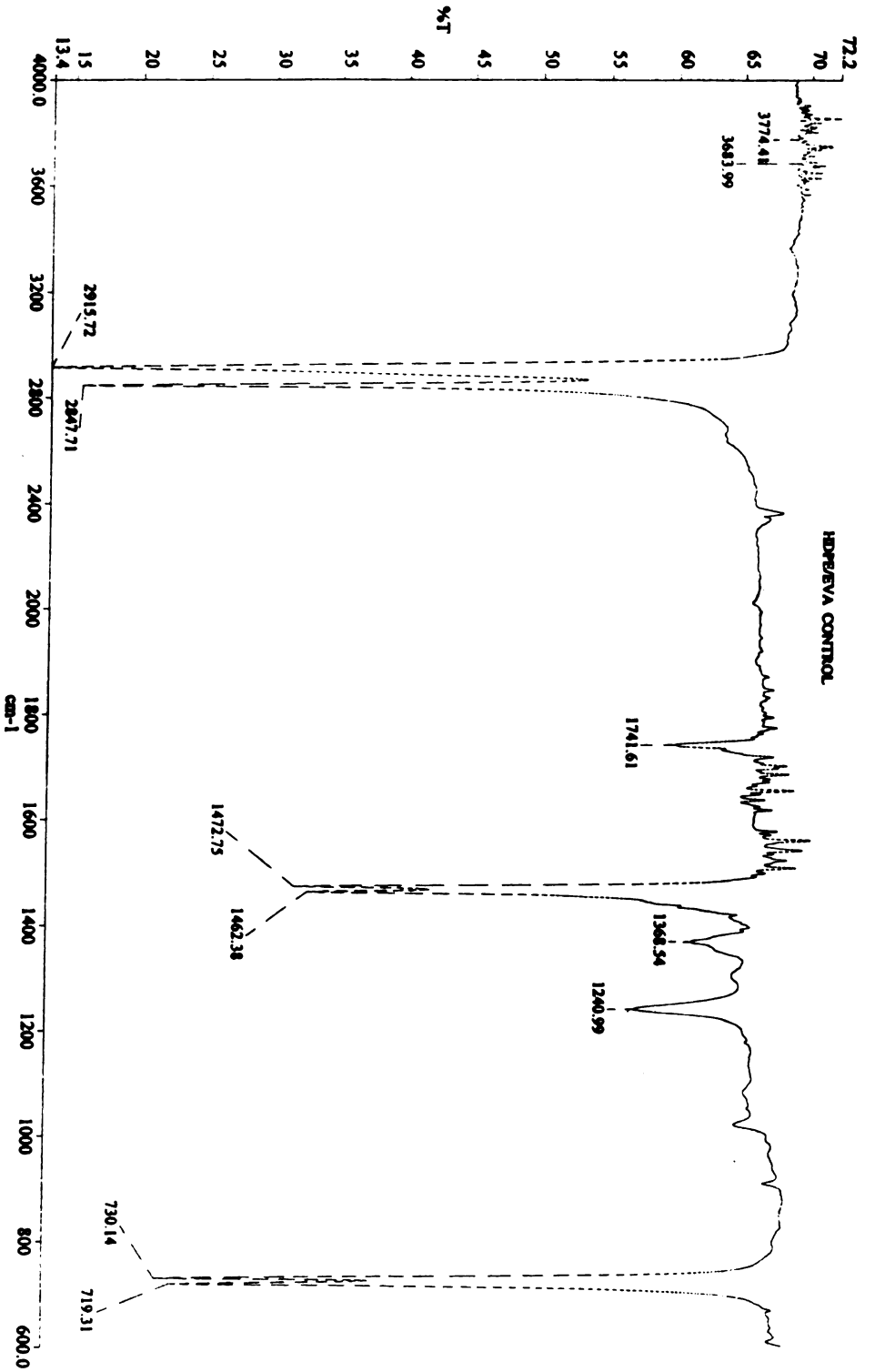

Figure 51. High density polyethylene side of HDPE/Suryln-EVA laminate film structure with no antioxidants.

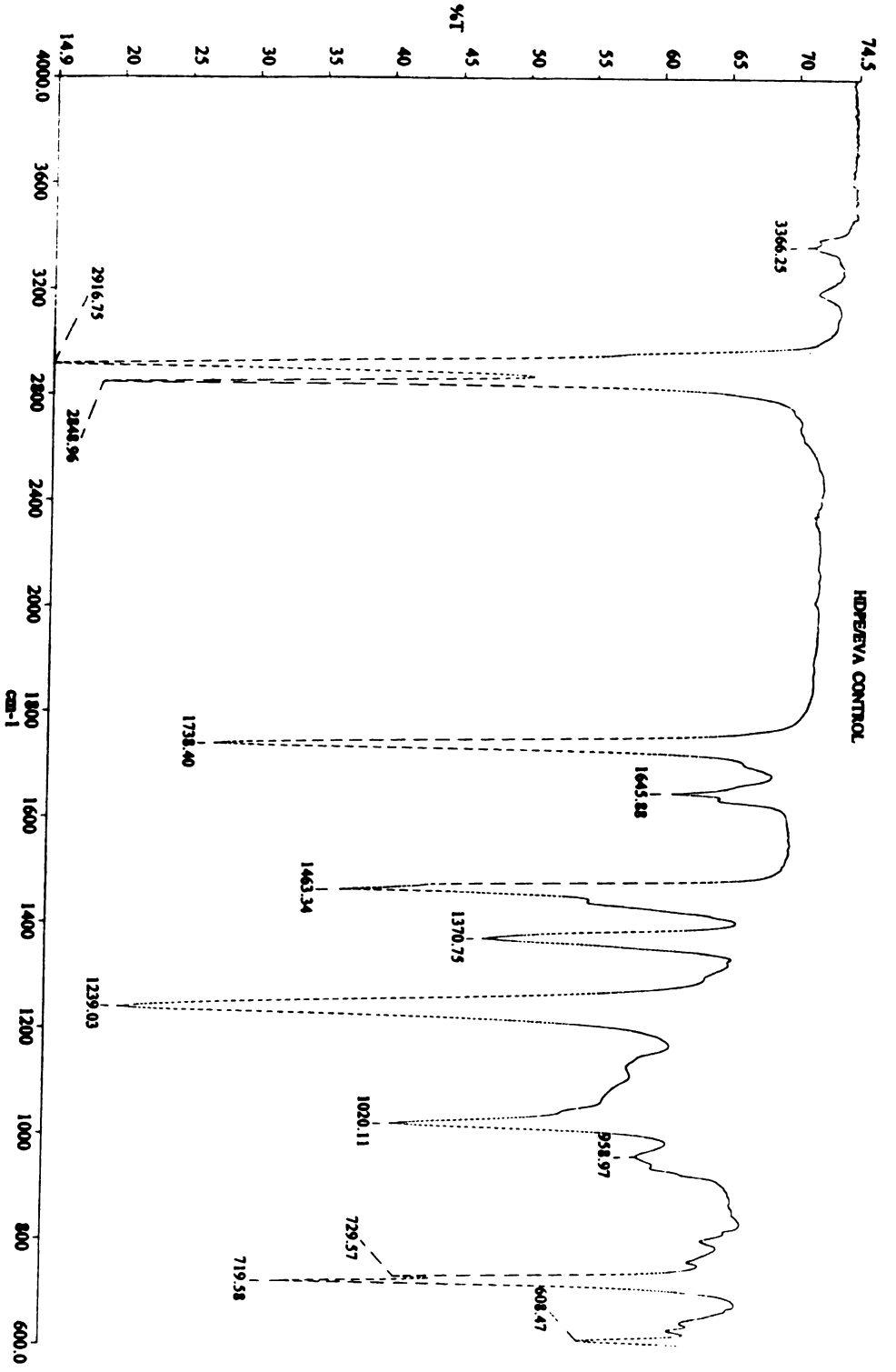

Figure 52. Heat seal layer (Suryln-EVA) side of HDPE/Suryln-EVA laminate film structure with no antioxidants.

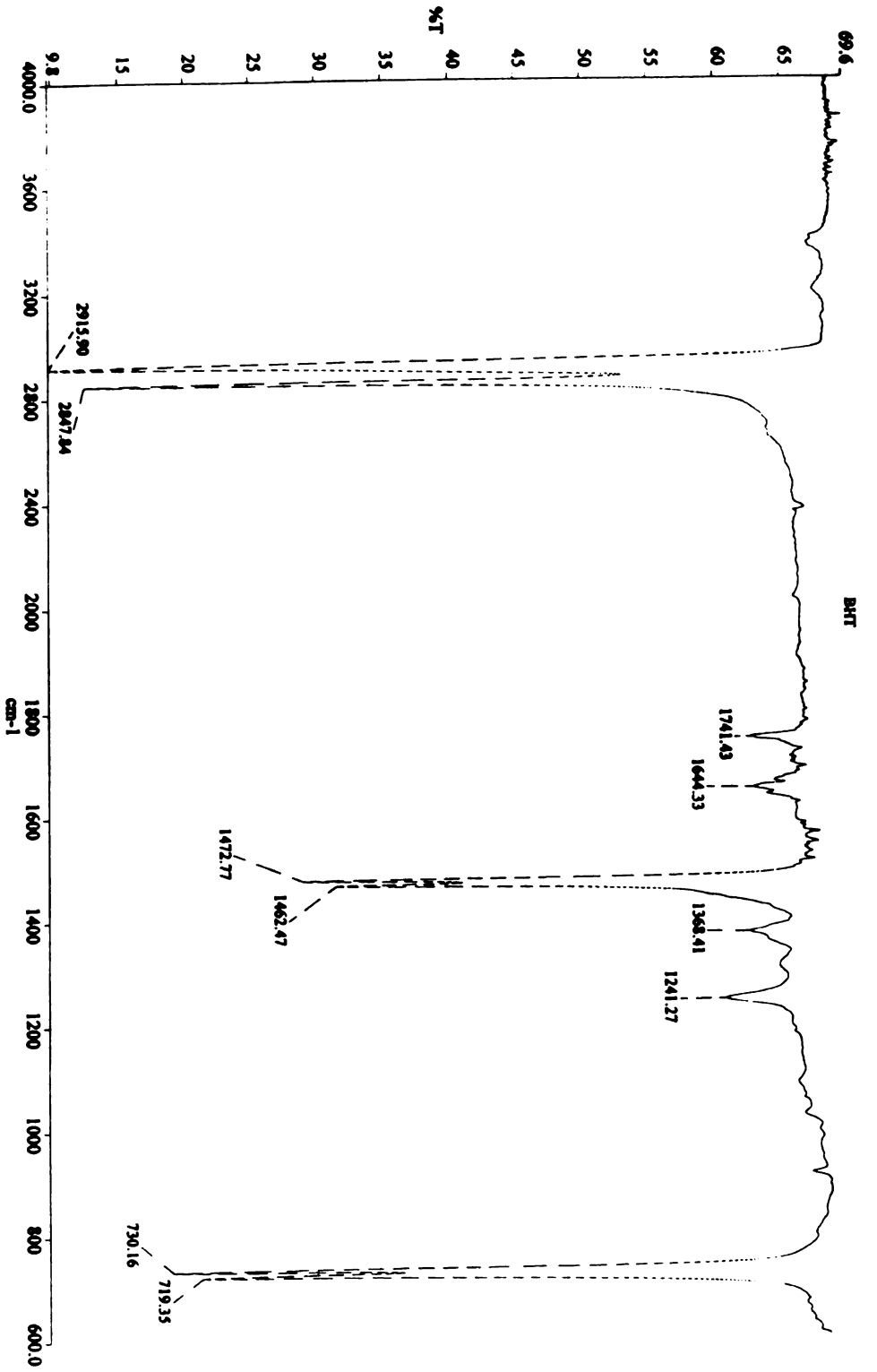

Figure 53. High density polyethylene side of BHT impregnated HDPE/Suryln-EVA laminate film structure.

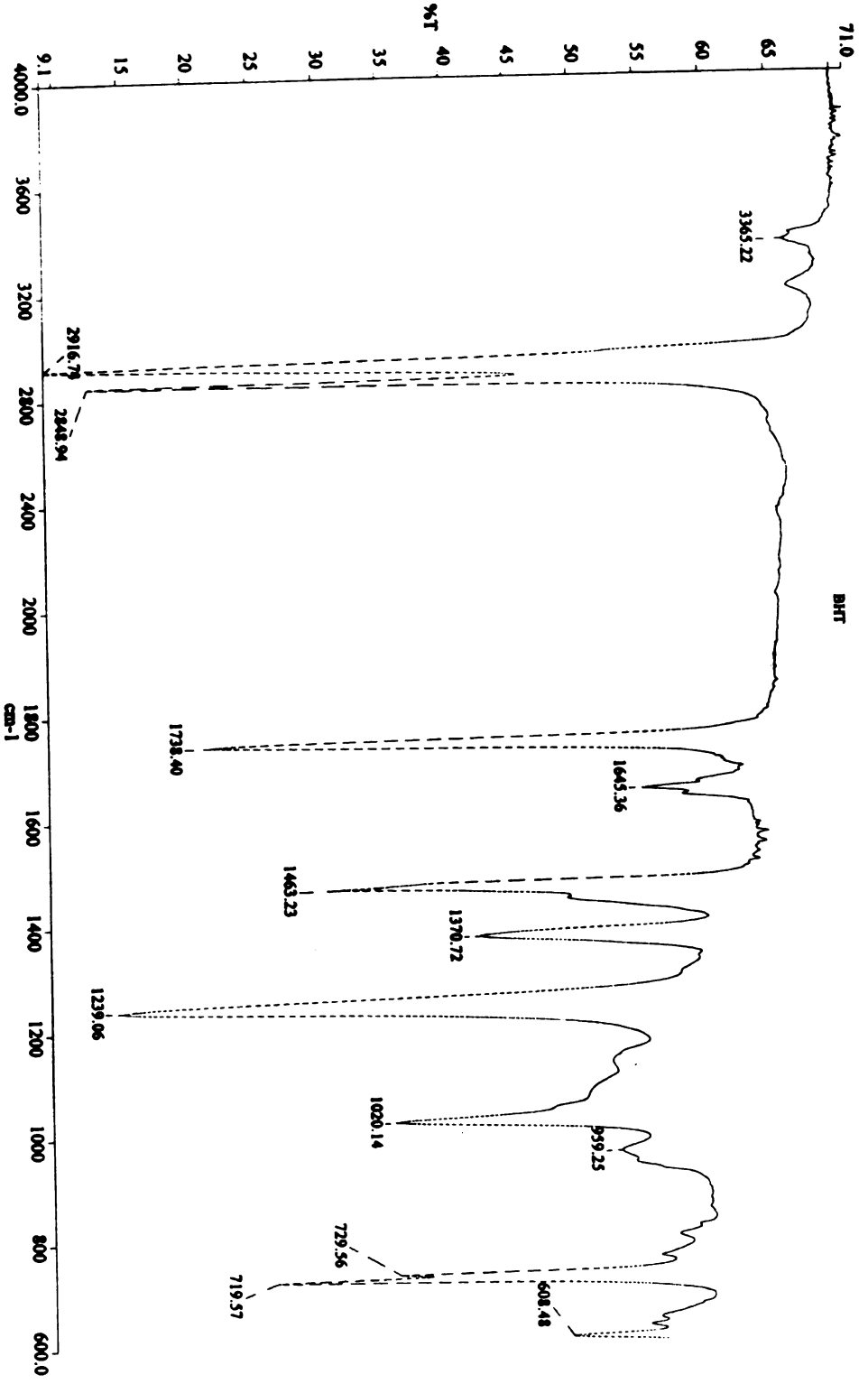

Figure 54. Heat seal layer (Suryln-EVA) side of BHT impregnated HDPE/Suryln-EVA laminate film structure.

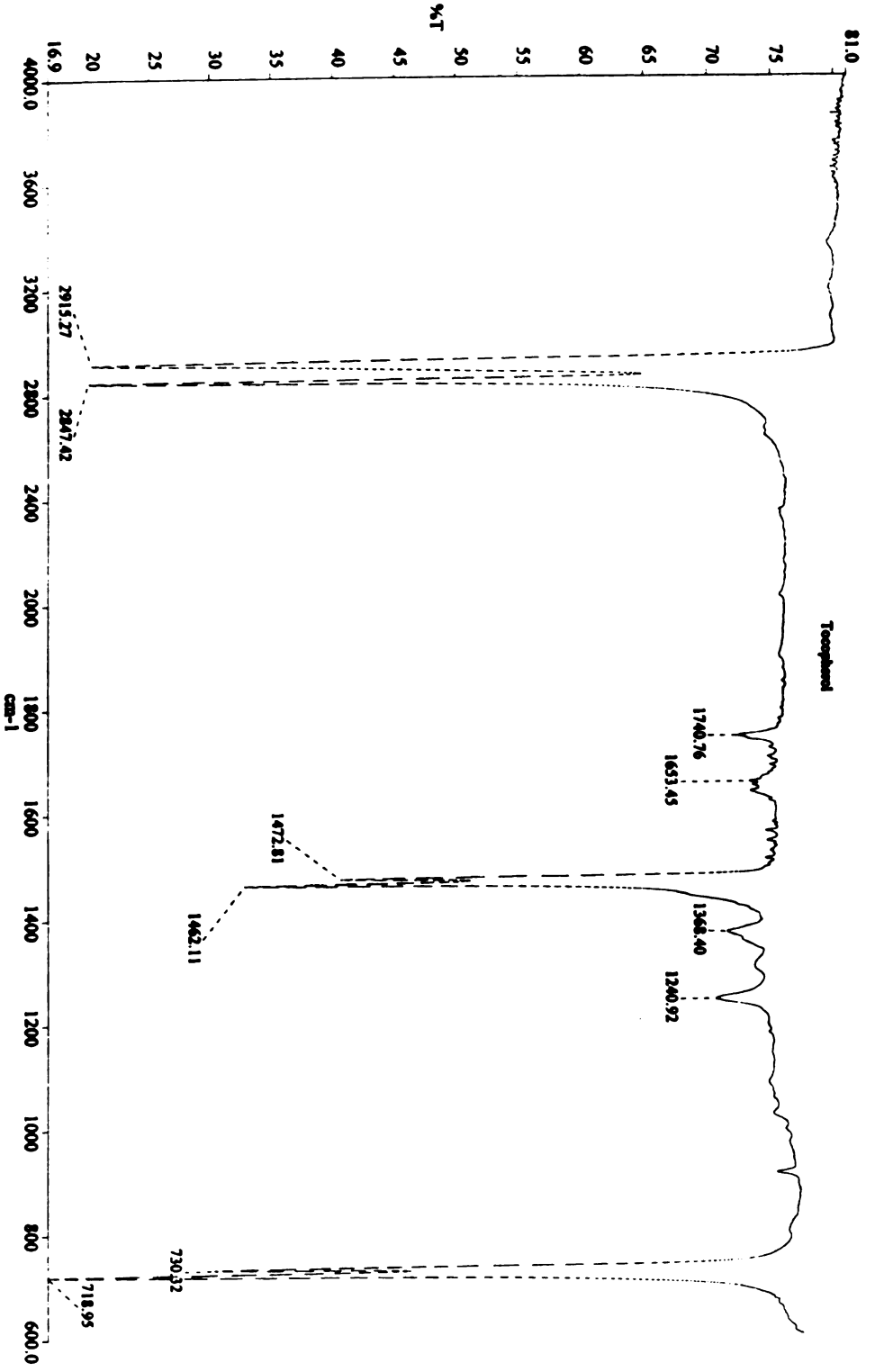

Figure 55. High density polyethylene side of α-tocopherol impregnated HDPE/Suryln-EVA laminate film structure.

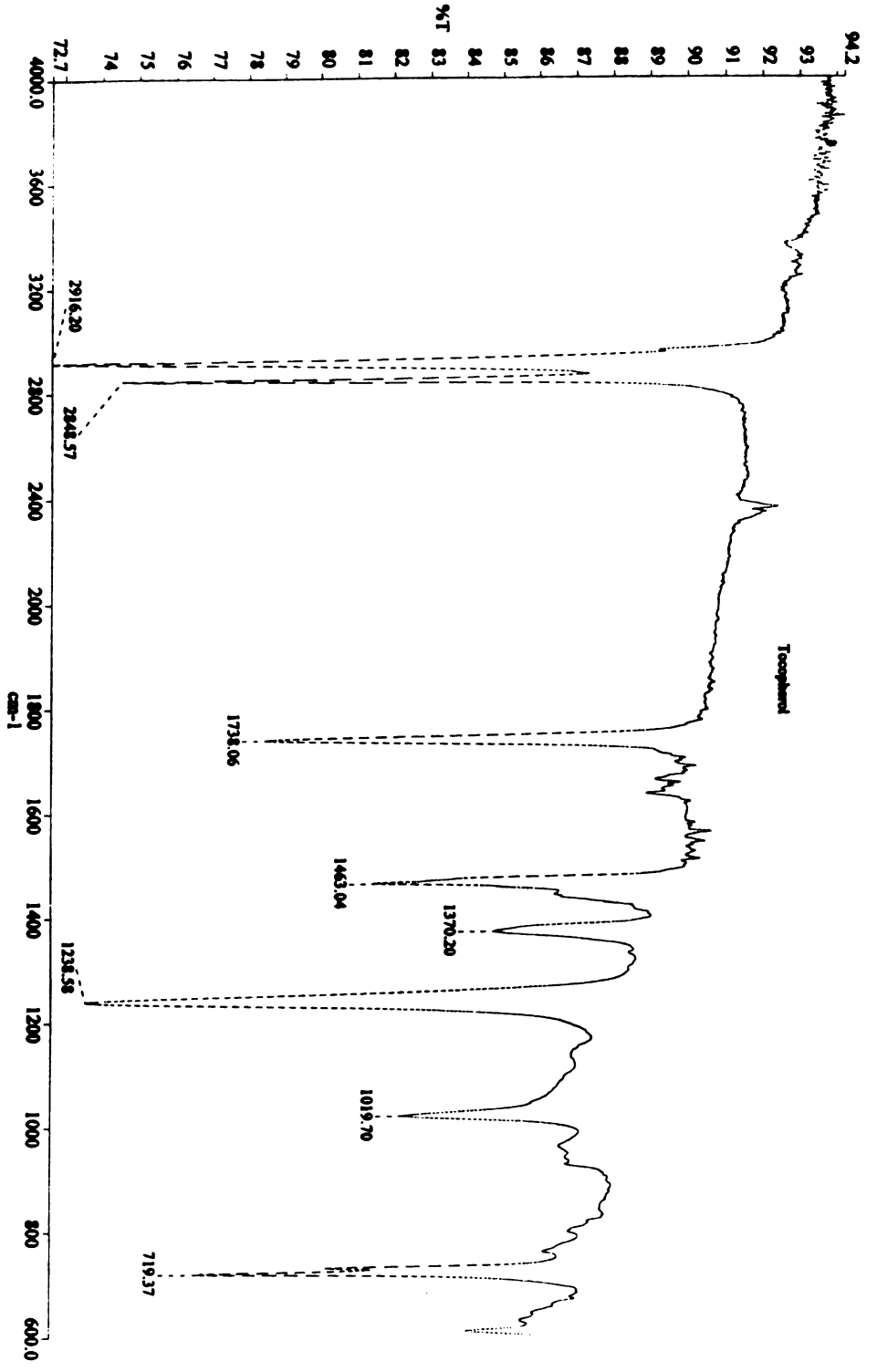

Figure 56. Heat seal layer (Suryln-EVA) side of α-tocopherol impregnated HDPE/Suryln-EVA laminate film structure.

REFERENCES

Allen, J. C. and Hamilton, R. J. 1994. Rancidity in Foods. Third edition. Blackie Academic & Professional.

AOAC. 1975. *Official Methods of Analysis*, 12th ed. Association of Official Analytical Chemists, Washington, DC.

Bailey, L. A. 1995. Mass Transfer of BHT from a Multi-Layer Lamination. M.S. Thesis, Michigan State University, East Lansing.

Beal, Andrew D. and Mottram, Donald S. 1994. Compounds of Contributing to the Characteristic Aroma of Malted Barley. Journal of Agricultural Food Chemistry. 42: 2880-2884.

Berends, C. L. 1993. Measure of the Effect of Water Activity on the Rate of Lipid Oxidation at Constant Oxygen Concentration. M.S. Thesis, Michigan State University, East Lansing.

Bidlack, W. R. and Tappel, A. L., 1973. Fluorescent Products of phospholipids during Lipid Peroxidation. Lipid, 8:203-207.

Birley, A. W., Haworth, B., Batchelor, J. 1991. Physics of Plastics: Processing, Properties, and Materials Engineering. Oxford University Press, New York.

Bradly, D. and Min, D. B. 1992, Singlet Oxygen Oxidation of Foods. Crit. Rev. in Food Science and Nutrition, 31: 211.

Brunauer, S., Emmett, H. P. and Teller, E. 1938. Adsorption of Gases in Multimolecular Layers. J. Amer. Chem. Soc. 60: 309 - 319.

Buttery, R. G. and Ling, L. C. 1995. Volatile Flavor Components of Corn Tortillas and Related Products. Journal of Agricultural and Food Chemistry. 43: 1878-1882.

Burton, G. W., Hughes, L., Foster, D. O., Pietrzak, E., Goss-Sampson, M. A., and Muller, David P. R. 1993. Free Radicals: From Basic Science to Medicine. G. Poli, E. Albano & M.U. Dianzani (eds.), Birkhauser Verlag Basel, Switzerland, 388-399.

Calvert, P. D. and Billingham, N. C. 1979. Loss of Additives from Polymers: A Theroetical Model, Journal of Applied Polymer Science, vol. 24, 357-370.

Chan, H. W.-S. 1987. The Mechanism of Autoxidation, *In Autoxidation of Unsaturated Lipids* (Chan, H.W.-S., edited) Academic Press, London: 1-16.

Charalambous, George 1992. Off-flavors in Foods and Beverages. (Developments in Food Sciences; 28). Elsevier Science Publishers, Amsterdam, The Netherlands.

Chung, H. Y. and Cadwallader, K. R. 1994. Aroma Extract Dilution Analysis of Blue Crab Claw Meat Volatiles. Journal of Agricultural Food Chemistry. 42: 2867-2870.

Cort, W. M. 1974. Antioxidant Activity of Tocopherols, Ascorbyl Palmitate, and Ascorbic Acid and their mode of action. Journal of American Oil Chemist's Society. 51:321- 325.

Coulter, Roberta Buford 1988. Extending Shelf Life by Using Traditional Phenolic Antioxidants. Cereal Foods World. February, vol. 33, No.2 :207-210.

Crank, J. 1975. The mathematics of diffusion, 2nd edition, Clarendon Press, Oxford, England.

Crosby, N. T. 1981. Food Packaging Materials, Applied Science Publishers, London, England.

C. van den berg. 1985. Development of B.E.T. - Like Models for Sorption of Water on Foods, Theory and Relevance. *In Properties of Water in Foods* (edited by D. Simatos and J.L.Multon, Martinus Nijhoff Publishers, Dordrecht/Boston/Lancaster, NATO ASI Series, No. 90), 119-131.

Dawson, P. L., Sheldon, B. W., Larick, D. K., and Turner, B. E. 1991. Role of Glycerophophorylcholine and Glycerophosphorylethanolamine in Linoleic Acid Oxidation. Journal of Agricultural Food Chemistry, 39, 12-16.

Dougherty, Marion E. Jr. 1988. Tocopherols as Food Antioxidants. Cereal Foods World. February, vol. 33, No.2:222-223.

Dziezak, J. D. 1986. Antioxidants: The Ultimate Answer to Oxidation. Food Technology. September: 94-102.

Dreher, M. L. 1987. Handbook of Dietary Fiber. Dietary Fiber Ingredients and Food Uses. Marcel Dekker Inc., New York, Chapter 11: 381-441.

Eitenmiller, R. R. 1997. Vitamin E Content of Fats and Oils-Nutritional Implications. Food Technology. May, vol.51, No.5 : 78-81.

Esterbauer, H., Zollner, H., and Schaur, R. J. 1990. Aldehydes Formed by Lipid Peroxidation: Mechanism of Formation, Occurrence, and Determination, *In Membrane Lipid Oxidation* (edited by Carmen Vigo-Pelfrey, CRC press, Inc., Boca Raton, Florida) Chapter 11: 239-252.

Fennema, O. R. 1996. Water and Ice. *In Food Chemistry* (edited by Owen R. Fennema), Third edition, Marcel Dekker, Inc., New York, Chapter 2: 17-94.

Frankel, E. N. 1984. Lipid oxidation: Mechanisms, Products and Biological Significance. Journal of American Oil Chemist's Society, 61 (12): 1908 - 1915.

Frankel, E. N.1991. Recent Advances in Lipid Oxidation. Review. Journal of the Science of Food and Agriculture, 54: 495-511.

Frankel, E. N., Hu, M. -L., and Tappel, A. L. 1989. Rapid Headspace Gas Chromatopgraphy of Hexanal as a Measure of Lipid Peroxidation in Biological Samples. Lipids, 24: 976-981.

Fritsch, C. W. and Gale, J. A. 1977. Hexanal as a Measure of Rancidity in Low-Fat Foods. Journal of American Oil Chemist's Society, 54: 225 - 228.

Fujii, Hamano, and Yuasa, 1995. Inhibition of the Autoxidation of Methyl Linoleate by Protein and Highly Concentrated Dextrin in an Emulsion System. Bioscience-Biotechnology-and-Biochemistry, 59 (9) 1761-1763.

Gardner, H. W. 1985. Oxidation of Lipids in Biological Tissue and Its Significance. *In Chemical Changes in Food during Processing,* edited by T.R. Richardson and J.W. Finley, Van Nostrand Reinhold/AVI, New York.

Giese, James 1996. Antioxidants: Tools for Preventing Lipid Oxidation, Food Technology. November: 73-81.

Gloria, M. B. A., Grulke, E. A., Gray, J. I. 1993. Effect of Type of Oxidation on Beta-Carotene Loss and Volatile Products Formation in Model Systems. Food Chemistry, 46 (4) 401-406.

Gopala, G. and Prabhakar, V. 1995. Retarding Autoxidation in Raw Peanut Oil by Addition of Water. Journal of American Oil Chemists' Society. 72 (10) 1219-1221.

Gray, J. I. 1978 Measurement of Lipid Oxidation: A Review. Journal of the American Oil Chemists' Society, June, vol. 55, 539-546.

Han, J. K., Miltz, J., Harte, B. R., Giacin, J. R. 1987. Loss of 2-Tertiary-Burtyl-4-Methoxy Phenol (BHA) from High-Density Polyethylene Film. Polymer Engineering and Science, July, vol. 27, No. 13, 934-938.

Hall, Gunnar; Andersson, Jonas; Lingnert, Hans; Olofsson, Bertil. 1985. Flavor Changes in Whole Milk Power during Storage (II. The Kinetics of the Formation of Volatile Fat Oxidation Products and Other Volatile Compounds). Journal of Food Quality. 7: 153-190.

Hallberg, Marianne Lilja and Lingnert, Hans. 1991. Lipid Oxidation in Potato Slices under Conditions Simulating the Production of Potato Granules. Journal of American Oil Chemist's Society, vol. 68, no. 3: 167-170.

Henderson, S. K., Witchwoot, A. and Nawar, W.W. 1980. The Autoxidation of Linoleates at Elevated Temperatures. Journal of American Oil Chemist's Society, 57: 409-413.

Ho, Y. C. and Yam, K. L. 1994. Comparison of Vitamin E , Irganox 1010 and BHT as Antioxidants on Release of Off-Flavor from HDPE bottles. Journal of Plastic Film & Sheeting, 10: 194 - 212.

Hoojjat, P., Harte, B. R., Hernandez, R. J. and Giacin, J. R. 1987. Mass Transfer of BHT from HDPE Film and Its Influence on Product Stability. Journal of Packaging Technology.1(3) : 78.

Jadhav, S. J., Nimbalkar,S. S., Kulkarni, A. D. ,and Madhavi,D. L. 1996. Lipid oxidation in biological and food systems., *In Food antioxidants* (Madhavi, D. L. *et al.*, ed.) Chapter 2: 5-63.

Jeon, I. J. and Bassette, R. 1984. Analysis of n-Pentanal and n-Hexanal as Indices of Potato Chip Shelf-Life. Journal of Food Quality, 7: 97-105.

Johnson, Mary, and Fischer, J. G. 1994. Role of Minerals in Protection Against Free Radicals. Food Technology. May: 112-120

Karmas, Endel 1980. Techniques for Measurement of Moisture Content of Foods. Food Technology. April: 52-58.

King, D. L., Hahm, Tae S., Min, Davis B. 1993. Chemistry of Antioxidants in Relation to Shelf Life of Foods. *In Shelf-Life Studies of Foods and Beverages*. Charalambous, G. (Ed.) Elsevier Science Publishers: 629-705.

Kishida, E., Tokumaru, S., Ishitani, Y., Yamamoto, M., Oribe, M., Iguchi, H., Kojo, S.1993. Comparison of the Formation of Malondialdehyde and Thiobarbituric Acid-Reactive Substances from Autoxidized Fatty Acids Based on Oxygen Consumption. Journal of Agricultural and Food Chemistry. 41(10): 1598-1600.

Kochhar, S. P. 1993. Oxidative Pathways to the Formation of Off-Flavors. *In Food Taints and Off-Flavors*. (edited by Saxby, M.J.), Blackie Academic & Professional, Glasgow, UK.

Koelsch, C. M. 1989. A System for the Measurement of the Rate of Lipid Oxidation at Concentration at Constant Oxygen Concentrations and Relative Humidity. M.S. Thesis, Michigan State University. East Lansing.

Kumor, E. A. 1986. The Characterization and Stability of the Lipids in Oat Cereal. M.S. Thesis, Michgan State University, East Lansing.

Labuza, T. P. 1971. Kinetics of Lipid Oxidation in Foods. CRC Critical Reviews in Food Technology. October: 355-405.

Laermer, S. F. & Nabholtz, F. 1990. Use of Biological Antioxidants as Polypropylene Stabilizers. Plastics and Rubber Processing and Applications. 14: 235 - 239.

Laermer, S. F., Young, S. S., and Zambetti, P. F. 1994. Could Your Packaging Use A Dose of Vitamin E ?. Food Processing. June. Vol. 55: 35 - 36.

Laermer, S. F., Young, S. S., and Zambetti, P. F. 1993. Vitamin E: New Developments in Polyolefin Antioxidant Technology. Proc. in SPO '93, pp. 541-585.

Laermer, S. F. and Zambetti, P. F. 1992. Alpha-Tocopherol (Vitamin E)-The Natural Antioxidant for Polyolefins. Journal of Plastic & Sheeting. 8: 228 - 248.

Landvik, S. V., Diplock, A. T., and Packer L. 1996. Efficacy of Vitamin E in Human Health and Disease. *In Handbook of Antioxidants* (edited by Cadenas and Packer), Marcel Dekker, Inc., New York, Chapter 4, 463-87

Leino, M. E. 1992. Effect of Freezing, Freeze-Drying, and Air-Drying on Odor of Chive Characterized by Headspace Gas Chromatography and Sensory analyses. Journal of Agricultural Food Chemistry, 40: 1379-1384.

Leung, Henry K. 1987. Influence of Water Activity on Chemical Reactivity. *In Water Activity: Theory and Applications to Food.* (edited by Rockland, Louis B. and Beuchat, Larry R.), IFT Basic Symposium Series, Chicago, Illinois, 27-54.

Likens, S. T. and Nickerson, G. B. 1964. Detection of Certain Hop Oil Constituents in Brewing Products. Am. Soc. Brewing Chemists Proc., 5-15.

Lin, J. F. 1996. Mass Transfer of α-Tocoherol (Vitamin E) from a Multi-Layer Laminate Structure and Its Influence on Product Stability. M.S. Thesis, Michigan State University, East Lansing.

Luddy, F. E., Barford, R. A., Herb, S. F., and Magidman, P. 1968. A Rapid and Quantitative Procedure for the Preparation of Methyl Esters of Butter Oil and Other Fats. Journal of the American Oil Chemists' Society. 45. 549-552.

Luning, P. A., Rijk, T. D., Wichers, H. J., and Roozen, J. P. 1994. Gas Chromatography, Mass Chromatography, and Sniffing Port Analyses of Volatile Compounds of Fresh Bell Peppers (*Capsicum annuum*) at Different Ripening Stages. Journal of Agricultural Food Chemistry. vol. 42, no. 4, 977-983.

Machlin, L. J. 1984. Vitamin E. *In Handbook of Vitamins*. Marcel Decker, Inc., New York, Chapter 3, 99- 145.

Madhavi, D. L. and Salunkhe, D. K. 1996. Toxicological Aspects of Food Antioxidants. *In Food antioxidants*. Marcel Dekker, Inc., New York, 267-359.

Marion E. Dougherty, Jr. 1988. Tocopherols as Food Antioxidants. Cereal Foods World, 33: 222 - 223.

Marshell, W. E. 1974. Health Foods, Organic Foods, Natural Foods (*what they are and what makes them attractive to consumers*), Food Technology. February, 28: 50-56

Martin, R. A.; Richard, C.; and Rousseau-Richard, C. 1990. Oxidation of Linoleic Acid and Related or Similar Compounds. *In Membrane Lipid Oxidation* (edited by Carmen Vigo-Pelfrey), Chaper 4, 63-99.

Maskan, M., Oner, M.D., and Kaya, A. 1993. Storage Stability and Accelerated Shelf-Life Testing of Margarine Samples. Journal of Food Quality. 16: 175 -186.

Mate, J. I., Saltveit, M. E., and Krochta, J. M. 1996. Peanut and Walnut Rancidity: Effects of Oxygen Concentration and Relative Humidity. Journal of Food Science 61 (2): 465-467.

Mathluothi, M. 1986. The influence of Light Transmittance and Gas Permeability of Various Packing Materials on the Quality of Whole Natural Yoghurt during Storage. *In Food Packaging and Preservation* (edited by J.O.Bosset, etc.), Elsevier Applied Science Publishing Co. Inc., New York.

McCord, Joe M. 1994. Free Radicals and Prooxidants in Health and Nutrition. Food Technology. May, 106-111.

Moran, D. P. J., Rajah, K. K. 1994. Fats in Food Products. First edition. Blackie Academic & Professional, Glasgow, UK.

Moreau, D. L. and Rosenberg, M. 1996. Oxidation Stability of Anhydrous Milkfat Microencapsulated in Whey Proteins. Journal of Food Science, Vol. 61, No. 1, 39-43.

Morrison, William R. and Smith, Lloyd M. 1964. Preparation of Fatty Acid Methyl Esters and Dimethylacetals from Lipid with Boron Fluride-Methanol. Journal of Lipid Research, Vol. 5, 600-608.

Nelson, Gary J. 1991. Isolation and Purification of Lipids from Biological Matrices. *In Analyses of Fats, Oils and Lipoproteins* (edited by Edward G. Perkins), the American Oil Chemist's Society, Champaign, Illinois.

Nelson, Katherine A. and Labuza, Theodore P. 1992. Relationship Between Water and Lipid Oxidation Rates (Water Activity and Glass Transition Theory). *In Lipid Oxidation in Food* (edited by Allen J. St. Angelo), the American Oil Chemist's Society, Champaign, Illinois.

Noormarji, H. (Sheiler) 1990. Effect of Lipid Oxidation on Functional and Nutritional Properties of Chicken Myofibrillar Proteins Stored at Different Water Activities. Ph.D. Thesis, Michigan State University, East Lansing.

Packer, L. 1992. New Horizons in Vitamin E Research – the Vitamin E Cycle, Biochemistry, and Clinical Applications. *Lipid-Soluble Antioxidants: Biochemistry and Clinical Applications* (edited by A.S.H. Ong and L. Packer), 1 –16.

Pershern, A. S., Breene, W. M., and Lulai, E. C. 1995. Analysis of Factors Influencing Lipid Oxidation in Hazelnuts (*CORYLUS SPP.*). Journal of Food Processing and Preservation. 19: 2-26.

Porter, W. L., Levasseur, L. A., Henick, A. S. 1977. Evaluation of Some Natural and Synthetic Phenolic Antioxidants in Linoleic Acid Monolayers on Silica. Journal of Food Science. vol. 42 (6): 1533-1535.

Pokorny, Jan. 1971. Stability of Fats by Phenolic Antioxidant. Can.Inst. Food Technol. J. 4 (2): 68 - 74.

Quast, D. and Karel, M., 1972. Effects of Environmental Factors on the Oxidation of Potato Chips. Journal of Food Science. 37: 584-588.

Quast, D. and Karel, M., 1971. Effects of Oxygen Diffusion on Oxidation of Some Dry Foods. Journal of Food Technology, 6: 95-106.

Ragnarsson, J. O. and Labuza, T. P. 1977. Accelerated Shelf-life Testing for Oxidative Rancidity in Foods- A Review. Food Chemistry. 2: 291 - 308.

Ragnhild Reinton and Astri Rogstad. 1981. Antioxidant Activity of Tocopherols and Ascorbic Acid. Journal of Food Science. 46: 970 – 973.

Raws, H. R. and Vansanten, P. J., 1970, A Possible Role of Singlet Oxygen Oxidation in the Initiation of Fatty Acid Autoxidation. Journal of American Oil Chemistry's Society, 47: 121-125.

Reineccius, G. A.1984. Determination of Flavor Compounds. *In Modern Methods of Food Analysis* (edited by Stewart, Kent K and Whitaker, John R.), AVI Publishing company, Westport, Connecticut.

Reineccius, G. A.1993. Biases in Analytical Flavor Profiles Introduced by Isolation Method. *In Flavor Measurement* (edited by Ho, Chi-Tang and Manley, C. H.), Marcel Dekker, Inc., New York.

Rho, K. L., Selb, P. A., Chung, O. K. and Chung, D. S. 1986. Retardation of Rancidity in Deep-Fried Instant Noodles (Ramyon). Journal of American Oil Chemists' Society. 63 (2): 251 - 256.

Roberta B. C. 1988. Extending Shelf Life by Using Traditional Phenolic Antioxidants. Cereal Foods World. 33: 207 - 210.

Robertson, Gordon L. 1993. Food Packaging: Principles and Practice, Marcel Dekker, Inc. New York.

Rockland, L. B. and Nishi, S. K. 1980. Influence of Water activity on Food Product Quality and Stability. Food Technology. April, 42-51.

Roozen, J. P., Frankel, E. N. and Kinsella, J. E. 1994. Enzymic and Autoxidation of Lipids in Low Fat Foods: Model of Linoleic Acid in Emulsified Hexadecane. Food Chemistry. 50: 33-38.

Roozen, J. P., Frankel, E. N. and Kinsella, J. E. 1994. Enzymic and autoxidation of Lipids in Low Fat Foods: Model of Linoleic Acid in Emulsified Triolein and Vegetable Oils. Food Chemistry. 50: 39-43.

Roseiers, C. D., Rivest, M.-J., Boily, M.-J., Jette, M., Carrobe-Cohen, A., Kumar, A. 1993. Gas Chromatographic-Mass Spectrometric Assay of Tissue Malondialdehyde, 4-Hydroxynonenal, and Other Aldehydes after Their Reduction to Stable Alcohols. Analytical Biochemistry. 208, 161-170.

Rossell, J. B. 1994. Measurement of Rancidity. *In Rancidity in Foods* (edited by Allen, J.C. and Hamilton, R.J.) Third edition. Blackie Academic & Professional, Glasgow, UK, Chapter 2, 22-53.

Sakakibara, H., Yanai, T., Yajima, I., and Hayashi, K. 1988. Changes in Volatile Flavor Compounds of Powered Dried Bonito (Katsuobushi) during Storage. Agric. Biol. Chem., 52 (11): 2731-2739.

Schieberle, P. and Grosch, W. 1981. Model Experiments about the Formation of Volatile Carbonyl Compounds. Journal of American Oil Chemist's Society. 58: 602-607.

Schuler, Peter 1990. Natural Antioxidants Exploited Commercially. *In Food Antioxidants* (edited by Hudson, B.J.F.), Chapter 4. Elsevier Applied Science, New York.

Scott, W. J. 1957. Water Relations of Food Spoilage Microorganisms. Adv. Fd Res., 7: 83-127.

Shahidi, F. and Wanasundara, U. 1995. Effect of natural antioxidants on the stability of canola oil. *In Food Flavors: Generation, analysis and Process Influence* (edited by Charalambous, G.), Elsevier Science, Amsterdam, The Netherlands.

Slover, H. T. and Lanza, E. 1979. Quantitative analysis of food fatty acids by capillary gas chromatography. Journal of the American Oil Chemists' Society. 56. 933-943.

Thomas, D. B. 1994. Rate of Lipid Oxidation at Various Initial Oxygen Concentrations using Absorbing Sachets in the Packages. M.S. Thesis, Michigan State University, East Lansing.

Till, D. E., Ehntholt, D. J., Reid, R. C., Schwartz, P. S., Sideman, K. R., Schwope, A. D. and Whelan, R. H. 1982. Migration of BHT Antioxidant from High Density Polyethylene to Foods and Food Simulants. Ind. Eng. Chem. Prod. Res. Dev., 21: 106-113.

Tjhio, K. H. and Karel, M. 1969. Autoxidation of Methyl Linoleate in Freeze-Dried Model Systems. 4. Effects of Metals and of Histidine in the Absence of Water. Journal of Food Science, 34: 540 - 543.

Troller, John A. 1989. Water Activity and Food Quality. *In Water and Food Quality* (edited by Thelma M. Hardman), Chapter1: 1-31.

Troller, J. A. and Christian, J. H. B. 1978. Water Activity Methods. *In Water Activity and Food*, Academic Press, New York, Chapter 2: 15-28.

Young, L.G. ; Lun, A.; J. Pos ; Forshaw, R. P. ; Edmeades, D. 1975. Vitamin E Stability in Corn and Mixed Feed. Journal of Animal Science, 40: 497 - 499.

Warner, K. J. H., Dimick, P. S., Ziegler, G. R., Mumma, R. O., and Hollender, R. 1996. 'Flavor-Fade' and Off-Flavors in Ground Roasted Peanuts as Related to Selected Pyrazines and Aldehydes. Journal of Food Science. 61(2): 469-472.

Watson, J. T. 1985. Introduction to Mass Spectrometry. Raven Press, New York.

Watson, J. T. and Sparkman, O. D. 1996. Mass Spectrometry: Principles and Practice. American Chemical Society Short Course, Michigan State University, East Lansing.

Widicus, W. A. and Kirk, J. R. 1981. Storage Stability of Alpha-Tocopherol in a Dehydrated Model Food System containing Methylene Linoleate. Journal of Food Science. 46: 813 - 816.

Wolf, J. C., Thompson, D. R., Warthesen, J. J., and Reineccius, G. A. 1981. Relative Importance of Food Composition in Free Lysine and Methionine Losses during Elevated Temperature Processing. Journal of Food Science. 46: 1074.

Zambetti, P. F. 1995. Vitamin E: Effective Antioxidant for Extrusion Coating Polymers. Packaging Technology & Engineering. September: 56-59.